ALFRED-WEGENER-INSTITUT
HELMHOLTZ-ZENTRUM FÜR POLAR- UND MEERESFORSCHUNG

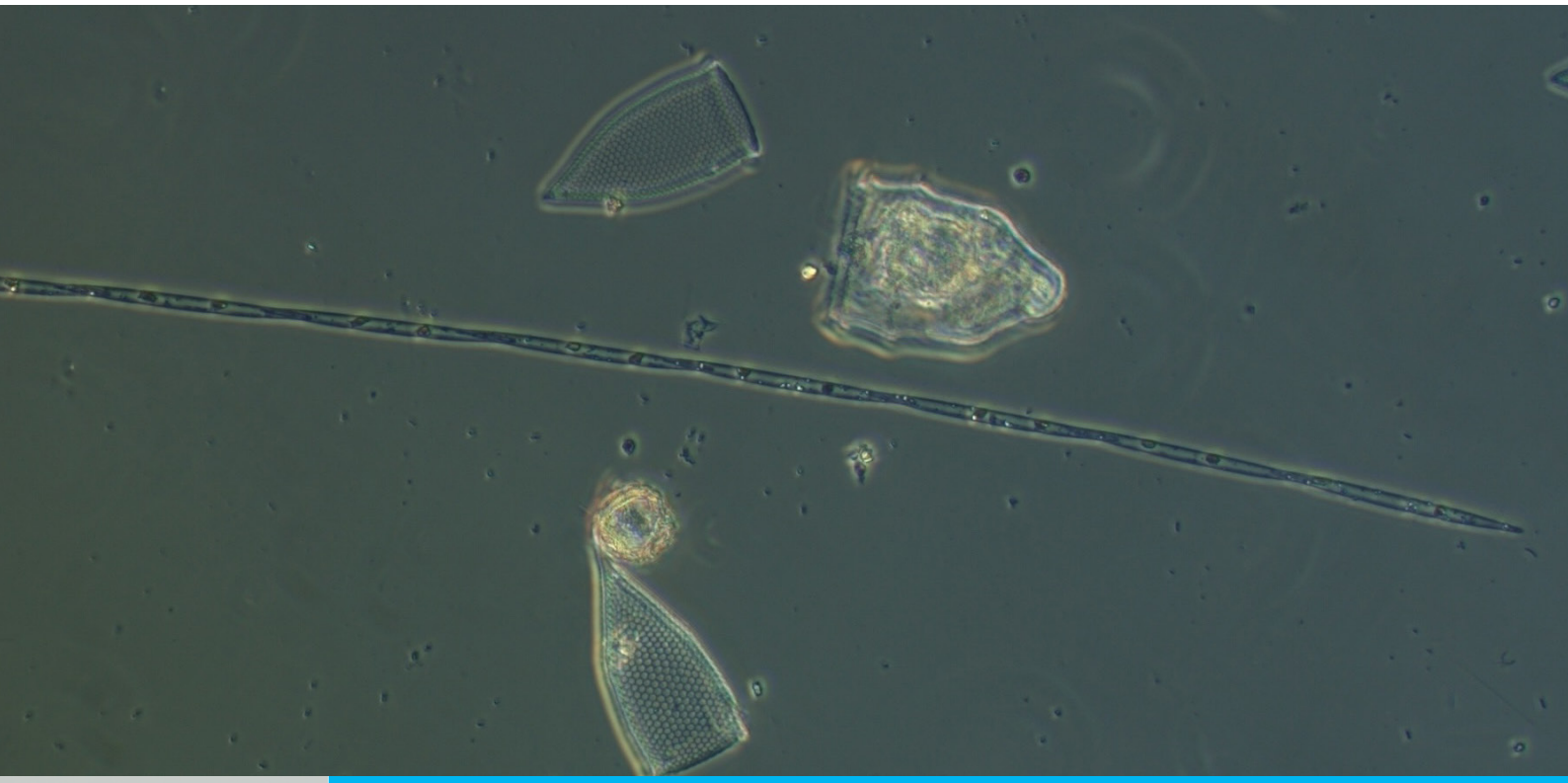

801
2025

Berichte
zur Polar- und Meeresforschung
Reports on Polar and Marine Research

The Expedition PS143/2 of the Research Vessel POLARSTERN to the Arctic Ocean in 2024

Edited by

Katja Metfies
with contributions of the participants

HELMHOLTZ

Die Berichte zur Polar- und Meeresforschung werden vom Alfred-Wegener-Institut, Helmholtz-Zentrum für Polar- und Meeresforschung (AWI) in Bremerhaven, Deutschland, in Fortsetzung der vormaligen Berichte zur Polarforschung herausgegeben. Sie erscheinen in unregelmäßiger Abfolge.

Die Berichte zur Polar- und Meeresforschung enthalten Darstellungen und Ergebnisse der vom AWI selbst oder mit seiner Unterstützung durchgeführten Forschungsarbeiten in den Polargebieten und in den Meeren.

Die Publikationen umfassen Expeditionsberichte der vom AWI betriebenen Schiffe, Flugzeuge und Stationen, Forschungsergebnisse (inkl. Dissertationen) des Instituts und des Archivs für deutsche Polarforschung, sowie Abstracts und Proceedings von nationalen und internationalen Tagungen und Workshops des AWI.

Die Beiträge geben nicht notwendigerweise die Auffassung des AWI wider.

Herausgeber
Dr. Horst Bornemann

Redaktionelle Bearbeitung und Layout
Susan Amir Sawadkuhi

Alfred-Wegener-Institut
Helmholtz-Zentrum für Polar- und Meeresforschung
Am Handelshafen 12
27570 Bremerhaven
Germany

www.awi.de
www.awi.de/reports

Erstautor:innen bzw. herausgebende Autor:innen eines Bandes der Berichte zur Polar- und Meeresforschung versichern, dass sie über alle Rechte am Werk verfügen und übertragen sämtliche Rechte auch im Namen der Koautor:innen an das AWI. Ein einfaches Nutzungsrecht verbleibt, wenn nicht anders angegeben, bei den Autor:innen. Das AWI beansprucht die Publikation der eingereichten Manuskripte über sein Repositorium ePIC (electronic Publication Information Center, s. Innenseite am Rückdeckel) mit optionalem print-on-demand.

The Reports on Polar and Marine Research are issued by the Alfred Wegener Institute, Helmholtz Centre for Polar and Marine Research (AWI) in Bremerhaven, Germany, succeeding the former Reports on Polar Research. They are published at irregular intervals.

The Reports on Polar and Marine Research contain presentations and results of research activities in polar regions and in the seas either carried out by the AWI or with its support.

Publications comprise expedition reports of the ships, aircrafts, and stations operated by the AWI, research results (incl. dissertations) of the Institute and the Archiv für deutsche Polarforschung, as well as abstracts and proceedings of national and international conferences and workshops of the AWI.

The papers contained in the Reports do not necessarily reflect the opinion of the AWI.

Editor
Dr. Horst Bornemann

Editorial editing and layout
Susan Amir Sawadkuhi

Alfred-Wegener-Institut
Helmholtz-Zentrum für Polar- und Meeresforschung
Am Handelshafen 12
27570 Bremerhaven
Germany

www.awi.de
www.awi.de/en/reports

The first or editing author of an issue of Reports on Polar and Marine Research ensures that he possesses all rights of the opus, and transfers all rights to the AWI, including those associated with the co-authors. The non-exclusive right of use (einfaches Nutzungsrecht) remains with the author unless stated otherwise. The AWI reserves the right to publish the submitted articles in its repository ePIC (electronic Publication Information Center, see inside page of verso) with the option to "print-on-demand".

Titel: Die pennate Diatomee Pseudo-nitzschia (lange Kette) und Tintinniden der Gattungen Parafavella (links) und Ptychocylis (rechts) unter dem Mikroskop (Foto: Sebastian Schroeder & Tabea Galonska, AWI)

Cover: The pennate Diatomee Pseudo-nitzschia (long chain) and Tintinnids of the genus Parafavella (left) and Ptychocylis (right) under the microscope (Photo: Sebastian Schroeder & Tabea Galonska, AWI)

The Expedition PS143/2 of the Research Vessel POLARSTERN to the Arctic Ocean in 2024

Edited by

Katja Metfies
with contributions of the participants

Please cite or link this publication using the identifiers

https://epic.awi.de/id/eprint/60428
https://doi.org/10.57738/BzPM_0801_2025

ISSN 1866-3192

PS143/2 FRAM2024

12 July 2024 – 06 August 2024

Tromsø – Tromsø

Chief scientist
Katja Metfies

Coordinator
Ingo Schewe

Contents

ÜBERBLICK UND EXPEDITIONSVERLAUF

Katja Metfies DE.AWI

Expedition PS143/2 des Forschungsschiffes *Polarstern* startete am 12. Juli 2024 mit dem Auslaufen in Tromsö. Das Expeditionsprogramm begann in den frühen Morgenstunden des 15.07.2024 in der Fram Strasse, dem Untersuchungsgebiet zwischen Spitzbergen und Grönland, wo sich auch das Lanzeitobservatorium HAUSGARTEN (LTER HAUSGARTEN) befindet.

Ziel der Expedition war es, einen Beitrag zum besseren Verständnis der marinen Biodiversität und klimarelevanter Prozesse des arktischen Ozeans vor dem Hintergrund des Klimawandels zu leisten. Ein Großteil der durchgeführten Arbeiten dieser Expedition dienten dem Austausch von Geräten und Installationen, sowie gezielter Probennahmen an ausgewählten Stationen, um die Langzeitbeobachtungen des Langzeitobservatoriums HAUSGARTEN, sowie der Helmholtz Infrastruktur Initiative FRAM (Frontiers in Arctic Marine Monitoring) fortzuführen.

Insgesamt standen die Ziele dieser Expedition in unmittelbarem Zusammenhang mit der Umsetzung des Forschungsprogramms „Changing Earth – Sustaining our Future“ des Forschungsbereichs „Erde und Umwelt“ der Helmholtz-Gemeinschaft, an dem das AWI zusammen mit sechs weiteren Helmholtz-Zentren beteiligt ist. Hier trägt die Expedition direkt zur Umsetzung der Forschungsziele von Topic 2 „Ocean and cryosphere in climate“ und Topic 6 “Marine and Polar Life: Sustaining Biodiversity, Biotic Interactions and Biogeochemical Functions” bei. In Topic 6 (Subtopics 6.1 “Future ecosystem functionality” und 6.3 “The future biological carbon pump”) werden die mit steigenden Wassertemperaturen und dem Rückgang des Meereises verbundenen Veränderungen im Ökosystem im Pelagial und im tiefen Ozean ermittelt und quantifiziert, sowie Rückkopplungsprozesse auf ozeanographische Prozesse untersucht. Vor diesem Hintergrund umfassten die Untersuchungen dieser Expedition die Identifizierung räumlicher und zeitlicher Entwicklungen ausgewählter Plankton- und Benthos-Gemeinschaften, sowie die Erweiterung unserer Langzeitbeobachtungsdaten. Darüber hinaus leisten die Untersuchungen einen direkten Beitrag zu nationalen und internationalen Projekten wie z.B. SIOS (Svalbard Integrated Observing System) und ICOS (Integrated Carbon Observation System), sowie den EU-Projekten Arctic PASSION, AtlantEco und OBAMA_NEXT. Schwerpunkt dieser Expedition waren Untersuchungen in der Wassersäule. So wurden neben Messungen an ausgewählten Stationen des LTER HAUSGARTEN, auf zwei Transekten durch die Fram Strasse entlang 79.56°N und 78.59°N von Schelfkante zu Schelfkante hoch aufgelöste Untersuchungen physikalischer, biologischer und biogeochemischer Prozesse in der oberen Wassersäule und der Tiefsee gemacht. Hier kamen neben stationär eingesetzten Geräten auch autonome Geräte zum Einsatz. Untersuchungen der Meereisbiota haben dieses Beobachtungsprogramm ergänzt, um die Rolle der kryo-pelagischen Kopplung im Ökosystem der Framstraße zu untersuchen. Ausgewählte Stationen des LTER HAUSGARTEN wurden nach ihrer Untersuchung auf PS143/1 auf PS143/2 nochmals besucht, um die kurzfristige Entwicklung des Systems in einem multidisziplinären Ansatz von der Oberfläche zur Tiefsee zu untersuchen.

Im Rahmen dieses Ansatzes wurden Untersuchungen zur Biodiversität, Biomasse und Verteilung verschiedener Plankton-Gruppen und der zugehörigen biogeochemischen Parameter durchgeführt. Dabei wurden klassische Mikroskopie und biogeochemische Analytik parallel zu modernsten optischen und molekulargenetischen Hochdurchsatzmethoden eingesetzt. Komplementär zu den Untersuchungen in der Wassersäule wurden an

ausgewählten Stationen Untersuchungen der Biodiversität, Biomasse und Verteilung von benthischen Organismen durchgeführt. Die Messungen biologischer und biogeochemischer Parameter im Pelagial und im Benthos der Fram Straße wurden durch Messungen ozeanographischer und chemischer Parameter ergänzt.

Zusammen mit Langzeitstudien zu Mechanismen und Umfang des vertikalen Exports organischen Materials in der Wassersäule sollen die Erkenntnisse und Daten aus den pelagischen und benthischen Langzeitbeobachtungen zu einem besseren Verständnis des Kohlenstoffflusses und möglicher klimawandelbedinter Veränderungen im arktischen Ozean beitragen. Im Detail basierte die Umsetzung der wissenschaftlichen Ziele dieser Expedition auf dem Einsatz verschiedener gezielt eingesetzter optischer Beobachtungssysteme und Probennehmer für pelagische und benthische Studien, sowie die Aufnahme und das Ausbringen von Verankerungen, die mit Sedimentfallen, Sensorsystemen oder automatischen Probennehmern bestückt waren. Darüber hinaus wurde ein Autonomes Unterwasserfahrzeugs (AUV) eingesetzt. Nach Ablegen in Tromsö wurden parallel zum vorher beschriebenen Arbeitsprogramm kontinuierlich Proben aus der unteren Atmosphäre genommen um die Konzentrationen von Ammoniak- und Ammonium der Atmosphäre im Rahmen des italienischen Projekts GAIA zu bestimmen.

Die Stationsarbeiten in der Fram Strasse wurden im östlichen Teil des LTER HAUSGARTEN begonnen, um dann zunächst in der nördlichen und westlichen Fram Strasse fortgeführt. Nach abschliessenden Arbeiten in der östlichen Fram Strasse wurde die Expedition nach einem Transit von 3.5 Tagen um 8:00 Uhr am 06.08.2024 mit dem Einlaufen in Tromsö beendet.

SUMMARY AND ITINERARY

Expedition PS143/2 of the research vessel *Polarstern* departed from Tromsø on July 12, 2024. The expedition program started in the early hours of 15.07.2024 in the Fram Strait, the study area between Spitsbergen and Greenland, where the Long-term Ecological Research Site HAUSGARTEN (LTER HAUSGARTEN) is located. The aim of this expedition was to enhance our understanding of marine biodiversity and climate-relevant processes in the Arctic Ocean under the impact of climate change. A large part of the work on this expedition focussed on continuing the long-term observations at LTER HAUSGARTEN and the Helmholtz Infrastructure Initiative FRAM (Frontiers in Arctic Marine Monitoring). This involved the exchange of equipment and installations, as well as targeted sampling at selected stations in order.

Overall, the objectives of this expedition are directly related to the implementation of the research program "Changing Earth - Sustaining our Future" of the research field "Earth and Environment" of the Helmholtz Association, in which the AWI is involved together with six other Helmholtz Centres. Here, PS143/2 contributes directly to the realization of the research goals of Topic 2 "Ocean and cryosphere in climate" and Topic 6 "Marine and Polar Life: Sustaining Biodiversity, Biotic Interactions and Biogeochemical Functions". In Topic 6 (Subtopics 6.1 "Future ecosystem functionality" and 6.3 "The future biological carbon pump"), changes associated with rising water temperatures and sea ice coverage are determined and quantified

for pelgagic and deep-sea ecosystems, and feedback processes on oceanographic processes are investigated. With reference to this, the scientific work of this expedition included the identification of spatial and temporal developments of selected plankton and benthic communities, as well as the development of a comprehensive repository for observation data. In addition, the investigations make a direct contribution to national and international projects such as SIOS (Svalbard Integrated Observing System) and ICOS (Integrated Carbon Observation System), as well as the EU projects Arctic PASSION, AtlantEco and OBAMA_NEXT.

Investigations in the water column at the heart of this expedition. In addition to measurements at selected stations of LTER HAUSGARTEN, high-resolution investigations of physical, biological and biogeochemical processes in the upper water column and the deep sea were carried out on two transects through the Fram Strait along 79.56°N and 78.59°N from shelf break to shelf shelf break. Here, autonomous devices were used for continuous under way measurements in addition to station work. Studies of the sea ice biota have supplemented this observation program in order to investigate the role of cryo-pelagic coupling in the Fram Strait ecosystem. Selected stations of the LTER HAUSGARTEN were revisited on PS143/2 after their investigation on PS143/1 to address the short-term development of the system in a multidisciplinary approach from the surface to the deep sea. As this approach was applied, studies were undertaken on the biodiversity, biomass and distribution of various plankton groups and the associated biogeochemical parameters. Classical microscopy and biogeochemical analysis were used in parallel to the latest optical and molecular genetic high-throughput methods. Complementary investigations of biodiversity, biomass and distribution of benthic organisms were carried out at selected stations. The measurements of biological and biogeochemical parameters in the pelagic and benthos of the Fram Strait were complemented by measurements of oceanographic and chemical parameters. Together with long-term studies on the mechanisms and extent of the vertical export of organic material in the water column, the findings and data from the pelagic and benthic long-term observations should contribute to a better understanding of the carbon flux and possible climate change-induced changes in the Arctic Ocean.

In detail, the implementation of the scientific objectives of this expedition was based on the use of various targeted optical observation systems and samplers for pelagic and benthic studies, as well as the exchange of moorings equipped with sediment traps, sensor systems or automatic samplers. Additionally, an autonomous underwater vehicle (AUV) was deployed. After depature in Tromsö, samples were continuously measured from the lower atmosphere in parallel to the previously described work program in order to determine the concentrations of ammonia and ammonium in the atmosphere as part of the Italian GAIA project.

The station work was started in the eastern part of the LTER HAUSGARTEN and then continued in the northern and western Fram Strait before being completed after final work in the eastern Fram Strait. The expedition was completed after a transit of 3.5 days at 8:00 am on 06.08.2024 with the arrival in Tromsø.

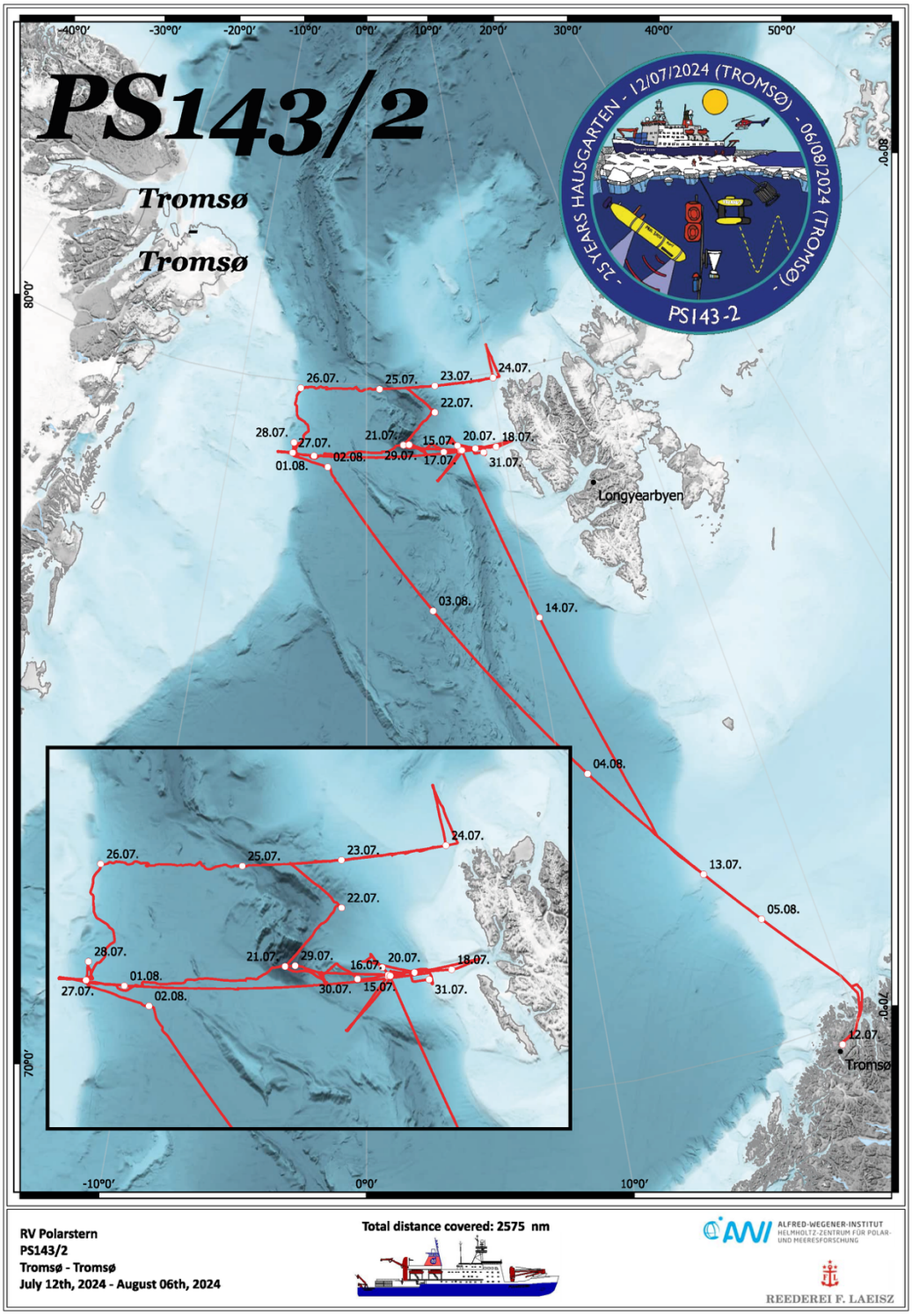

Abb. 1.1: Fahrtverlauf der Expedition PS143/2 vom Bremerhaven nach Tromsø. Siehe https://doi.pangaea.de/10.1594/PANGAEA.9726159 für eine Darstellung des Master tracks in Verbindung mit der Stationslisten für PS143/2.

Fig. 1.1: Cruise tack of expedition PS143/2 from Bremerhaven to Tromsø. See https://doi.pangaea.de/10.1594/PANGAEA.9726159 to display the master tracks in conjunction with the station list for PS143/2.

WEATHER CONDITIONS DURING PS143/2

Julia Wenzel DE.DWD

After the *Polarstern* left the start and end port of the expedition in Tromsø (Norway) on the evening of 12 July, it reached the influence area of a low-crossed Svalbard on 14 July. The significant wave height therefore rose to 2.5 m in the night to 13 July and the southwest wind temporarily increased to 7 Bft in the night to 14 July. Additionally, in the morning of 14 July fog occurred.

In the morning of 15 July, the *Polarstern* reached the research area, the Fram Strait, and stayed in the eastern part of the Fram Strait, west of Svalbard, until 20 July. Initially, the working area was at the outer area of a high-pressure system centered south of the Fram Strait, which started to move into the Barents Sea on 18 July. Thereby, mostly moderate south-westerly winds and a sea state of less than 1 m occurred. In the morning of 16 July fog dominated in the afternoon and on 17 July the sun could temporarily prevail.

On 18 July, a trough was moveing across the Fram Strait. On its back side a high-pressure system formed over the western part of the Fram Strait and also moved eastwards. Thus, the wind shifted to the north on 19 July, which led to a clearing of the clouds and plenty of sunshine until 20 July. The high was located over the Barents Sea on 20 and 21 July, with a ridge still extending to the Fram Strait.

On 21 July, the Polarstern reached the ice edge in the area of the central HAUSGARTEN stations, dominated by low stratus, which was temporarily changing to fog. At the same time, the Fram Strait was approached from the south by the warm front of a low located east of Iceland. Thus, starting in the night to 22 July advection fog occurred over the working area, which was so dense at times that the visibility was reduced to just 100 m (for example on 23 and 24 July). During the night of 23 July, the wind temporarily increased to 6 Bft within the frontal area. From 23 July, the low was moving directly off the coast of Greenland to the north while weakening. It was located over the western Fram Strait on 24 July and already at the northeast coast of Greenland on 25 July. The wind temporarily increased to 6 Bft on 25 July and it rained over the working area, so that the fog was temporarily and locally lifted. In the period from 23 to 26 July the *Polarstern* travelled a transect along 79.9° North.

With the prevailing southerly air flow between this and other lows and an initially stationary high over the Kara Sea, mild and humid air was continuously transported into the Fram Strait, so that the fog persisted almost without interruption until the end of the research work in the Fram Strait.

On 27 July, when *Polarstern* was in the area of the western stations (at 5° West), the occluded front of a low-pressure system near Iceland approached the Fram Strait from the south. The associated stratocumulus clouds moved over the fog on 27 and 28 July and led to a temporary and local reduction of the fog above the water surface during this time. However, the fog kept coming back so quickly that these very short weather windows could not be used for any helicopter flights.

During the night to 29 July, the *Polarstern* was heading back east along 79° North to the area around the central HAUSGARTEN at 79° North 4° East. Another low-pressure system just north of Iceland slowly moved north from 29 July and filled up over the Greenland Sea by 31 July. The associated occlusion reached the Polarstern on 30 July. Therefore, on this day,

instead of the fog, stratocumulus clouds and, for the first time in nine days, a relative humidity of less than 100% occurred again. Additionally, during the night to 30 July, the wind backed southeast and increased to 6 Bft.

Meanwhile, the high moved from the Kara Sea to the northwest and was located between Svalbard and Franz-Josef-Land on 31 July. Consequently, on 31 July, when the *Polarstern* was just west of Svalbard, the wind slowly turned back to the south and subsequently decreased continuously. At the same day, dense fog continued to prevail again. From 31 July in the evening to 1 August in the afternoon, the *Polarstern* again travelled west along 79° North. On 2 August, when the *Polarstern* was at the westernmost stations at 79° North 5° West, the wind had already dropped to 2 to 3 Bft and turned to the east. At the outer area of the high, the fog was temporarily very thin on this day and finally dissipated completely in the evening. That same evening, the research work in the Fram Strait was completed and the return journey to Norway began.

The sun did not last long, because during the night to 3 August, the *Polarstern* got into the area of the former occlusion front of a low-pressure system that had filled over the Greenland Sea the day before, so that fog was extending again from the south over the Greenland Sea to the Fram Strait. In the same night, the research vessel left the sea ice and reached the open waters with at begin wind from southeast with 4 to 5 Bft and a significant wave height of less than 1 m (mainly swell from the southeast). Due to a small-scale high over the Greenland Sea, which was situated just west of the route and that formed a high-pressure bridge with the high over Franz-Josef-Land, the wind veered from southwest to northwest by the morning of 3 August and dropped to 1 Bft by the evening. When traveling southeast, the fog lifted for a few hours on 3 August lying as low stratus over the route.

The high over Franz-Josef-Land moved over Novaya Zemlya (4 August) into the southern Barents Sea (5 August). The associated westward-reaching ridge, in which the small-scale Greenland Sea high was embedded, simultaneously moved clockwise (anticyclonally) around the high to the north. Therefore, from 3 August in the evening, the wind veered from north to southeast over the route and increased to 5 Bft on 4 August. In the early morning of 4 August, the *Polarstern* left the fog area of the former occlusion, but on the southern flank of the ridge another foggy air mass was brought in from the southeast to east, so that the *Polarstern* did finally leave the fog and low stratus behind only in the morning of 5 August. Thus, the last day of the return journey was characterized by sunny weather and decreasing winds. In the morning of 6 August, the *Polarstern* finally reached the harbour of Tromsø.

In summary, this trip was very foggy with 19 out of 26 days of fog occurence. In addition, the expedition was characterized by a low sea state with a significant wave height of maximally 2.5 m.

2. DEEP SEA ECOLOGY AND TECHNOLOGY

Autun Purser[1], Normen Lochthofen[1], Janine Ludszuweit[1], Christian Detsch[1], Michael Busack[1], Jonas Hagemann[1], Sascha Lehmenhecker[1], Lilian Boehringer[1], Babett Günther[2,4], Vincent Schnell[3,] Nils Handelmann[3]

not on board: Thomas Soltwedel[1], Melanie Bergmann[1], Ulrich Hoge[1], Ingo Schewe[1], Matthias Wietz[1], Jennifer Dannheim[1], Christiane Hasemann[1], Christina Bienhold[1]

[1]DE.AWI
[2]NL.NIOZ
[3]DE.BMBF/PtJ
[4]GEOMAR

Grant-No. AWI_PS143_01

Objectives and scientific programme

The marine Arctic has played an essential role in the history of our planet over the past 130 million years and contributes considerably to the present functioning of the Earth and its life. The past decades have seen remarkable changes in key Arctic variables, including a decrease of sea-ice extent and sea-ice thickness, changes in temperature and salinity of Arctic waters, and associated shifts in nutrient distributions. Since Arctic organisms are highly adapted to extreme environmental conditions with strong seasonal forcing, the accelerating rate of recent climate change challenges the resilience of Arctic life. The stability of a number of Arctic populations and ecosystems is probably not strong enough to withstand the sum of these factors, which might lead to a collapse of subsystems (Paulus 2021) .

Benthos, particularly in deep waters, is a robust ecological indicator for environmental changes, as it is relatively stationary and long-lived, and reflects changes in ecological conditions in the oceans (e.g. organic flux to the seabed) at integrated scales (Gage and Tyler 1991; Piepenburg 2005). To detect and track the impact of large-scale environmental changes in the transition zone between the northern North Atlantic and the central Arctic Ocean, and to determine experimentally the factors controlling deep-sea biodiversity, the Alfred Wegener Institute Helmholtz Center for Polar and Marine Research (AWI) established the deep-sea observatory HAUSGARTEN, which constitutes the first, and until now only open-ocean long-term observatory in a polar region (Soltwedel et al. 2016)

HAUSGARTEN is located in the eastern Fram Strait and includes 21 permanent sampling sites along a depth transect (250 – 5,500 m) and along a latitudinal transect following the 2,500 m isobath crossing the central HAUSGARTEN station (Fig. 2.1). Multidisciplinary research activities at HAUSGARTEN cover almost all compartments of the marine ecosystem from the pelagic zone to the benthic realm. Regular sampling as well as the deployment of moorings and different stationary and mobile free-falling systems (Bottom-Lander, Benthic Crawler), which act as local observation platforms, have taken place since the observatory was established in 1999. Frequent visual observations with towed photo/video systems allow the assessment of large-scale epifauna distribution patterns as well as their temporal development. Geographical features in the HAUSGARTEN area provide a variety of contrasting marine landscapes and landscape elements (e.g. banks, troughs [marine valleys], ridges and moraines, canyons and pockmarks) that generally shape benthic communities over

a variety of different scales (Durden et al. 2020). The habitat-diversity (heterogeneity) hypothesis states that an increase in habitat heterogeneity leads to an increase in species diversity, abundance and biomass of all fauna groups (O'Hara et al. 2020; Dijkstra et al. 2021). Improved technologies, particularly the recent deployment of acoustic and side-scan sonar systems at depth by an Autonomous Underwater Vehicle (AUV) and towed camera sleds within AWI's Deep-Sea Research Group (Purser et al. 2019) have indicated the high-resolution topographical variability of many deep-sea areas, including HAUSGARTEN (Taylor et al. 2017; Purser et al. 2022). So far, the time-series stations maintained across the region do not fully capture the high degree of local heterogeneity (in terms of physical seafloor terrain variables such as slope, rugosity, aspect, depth). Therefore, building on spatial studies conducted during PS136, during *Polarstern* expedition PS143/2 dedicated attempts to collect spatial data to capture the role of this heterogeneity in biodiversity and biomass estimation were carried out with AUV and OFOBS to complement investigations on the temporal variability of benthos in the HAUSGARTEN area. Additionally, a start was made on linking all HAUSGARTEN stations at depths of less than 3,000 m with an AUV photosurvey was made. The aim will be over the next few HAUSGARTEN expeditions to allow a linear assessment of fauna distributions from the shallower stations to the 3,000 m depth contour line.

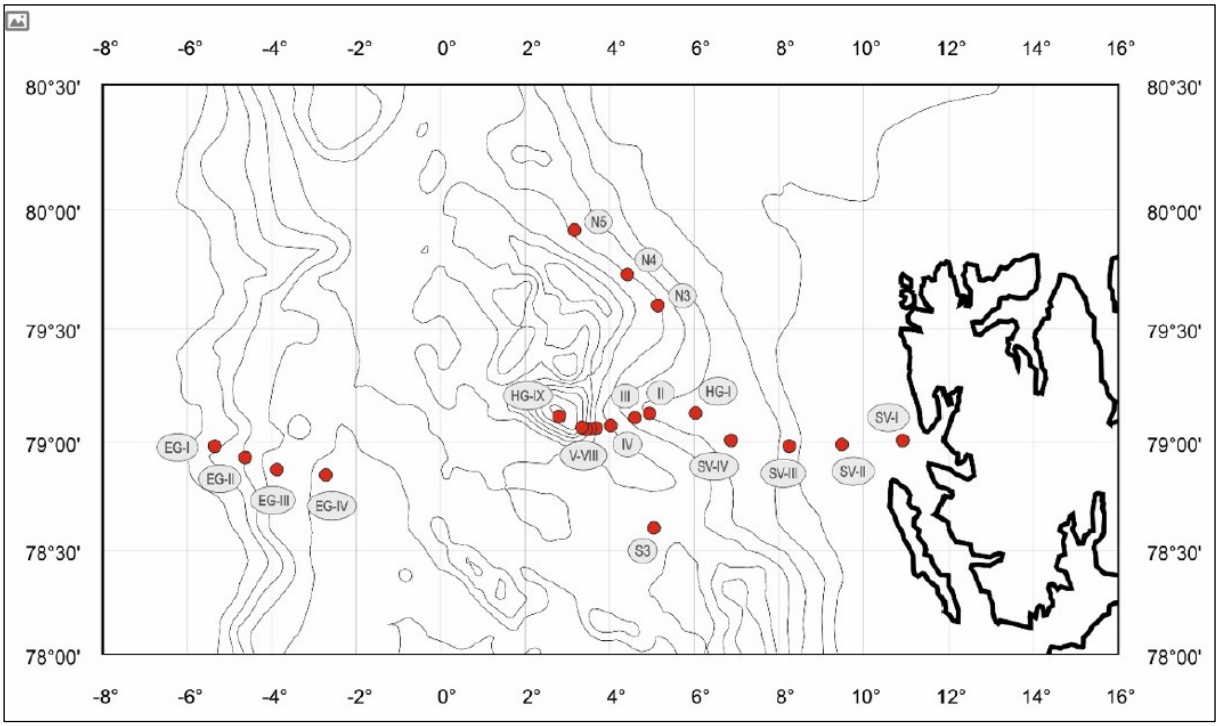

Fig. 2.1: Figure showing the main HAUSGARTEN stations on both sides of the Fram Strait

Unusually, during 2024 the HAUSGARTEN LTER work was split over two cruise legs, PS143/1 and PS143/2. During PS143/1 the benthic boxcore and multicore sampling was conducted, as well as Ocean Floor Observation and Bathymetry System (OFOBS) transects. During PS143/2 the groups work comprised repeating some of the OFOBS stations to glean information on short term term temporal variation, Long Term Lander recovery and deployment, mooring exchange and Autonomous Underwater Vehicle (AUV) exploration and mapping of the seafloor.

Work at sea

Megafauna

Ten Ocean Floor Observation and Bathymetry System (OFOBS) dives were conducted during PS143/2 (Tab. 2.1). During each deployment 200+ images were collected with automated timer every 30 seconds, with additional opportunistic 'hotkey' images of features of interest also captured. Throughout deployments, sidescan bathymetry and HD video of the seafloor were collected, as described in (Purser et al. 2019).

Tab. 2.1: Locations and dates of OFOBS dives conducted during PS143/2. A '*' designates a repeat transect of an OFOBS deployment also made in 2024 during the PS143/1 expedition leg.

OFOBS Dive no.	Station Number	Date	Latitude	Longitude	HAUSGARTEN Station information
1	PS143/2_4-1	16/07/24	79.02960	7.054294	SV-IV
2	PS143/2_7-7	17/07/24	78.61719	5.049517	S3*
3	PS143/2_11-7	18/07/24	79.01641	8.415035	SV-III
4	PS143/2_14-7	18/07/24	78.98093	9.580441	SV-II*
5	PS143/2_19-1	20/07/24	79.13498	6.012749	HG-I*
6	PS143/2_24-1	22/07/24	79.57673	5.246860	N3*
7	PS143/2_56-8	28/07/24	78.98512	-5.487020	EGC-I
8	PS143/2_59-4	29/07/24	79.04787	4.241897	HG-IV*
9	PS143/2_64-1	31/07/24	78.98336	6.958453	Methane Ridge
10	PS143/2_76-11	02/08/24	78.83070	-2.723880	EG-IV

Autonomous Underwater Vehicle (AUV) seafloor mapping

The AUV 'PAUL 3000' conducted a short calibration dive in the first week of the expedition, then carried out 4 successful benthic surveys (Tab. 2.2, Fig. 2.2). AUV Dives 80 and 81 carried out exclusively sonar survey work from a height of approximately 10 – 15 m above seafloor. Dives 82 and 83 conducted both acoustic surveys from comparable heights as well as seafloor photo surveys from approximately 6 m height above seafloor.

Tab. 2.2: Locations and dates of AUV dives conducted during PS143/2. The AUV ID numbers refer to the sequential list of all 'PAUL 3000' AUV dives.

AUV Dive no.	Station Number	Date	Latitude	Longitude	HAUSGARTEN Station information
ID80	PS143/2_3-1	15/07/24	79.00012	7.55413	SV-III to SV-IV
ID81	PS143/2_12-1	18/07/24	79.01653	8.33654	SV-III to SV-II area
ID82	PS143/2_19-1	20/07/24	79.13419	6.09398	HG-1 to SV-III
ID83	PS143/2_60-1	30/07/24	79.13592	4.88218	HG-2 to ridge

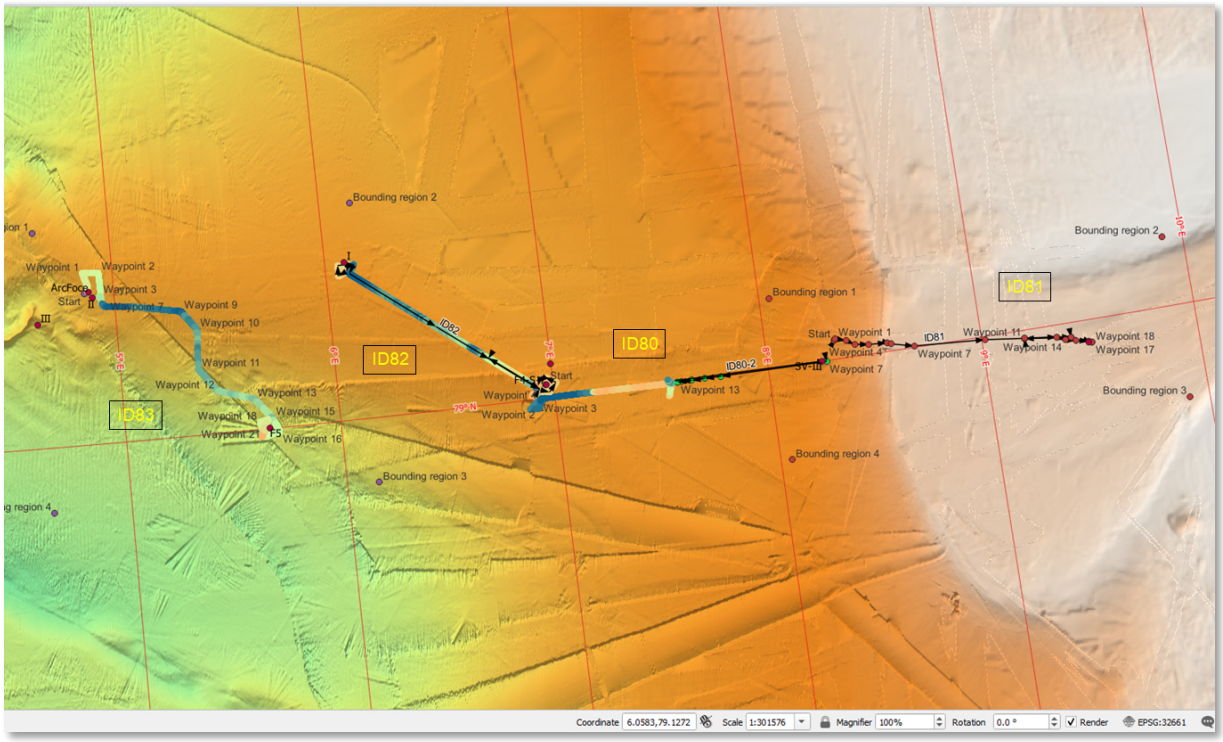

Fig. 2.2: Figure showing the AUV dive courses carried out during PS143/2

Long Term Lander recovery / redeployment

On 21 July (station PS143/2_22-9) a long-term lander was successfully recovered and data from ADCP and time series camera successfully downloaded. The camera showed the rapid seafloor turnover of phytodetritus during an algal fall in 2024 (Fig. 2.3). The fitted sediment trap samples were retrieved and set aside for on shore analysis. The time series camera data successfully recorded 4 images per 24 hrs since deployment in the summer of 2023 during the PS136 expedition. On the 29 July the lander was redeployed, with the same sensor and camera payload (PS143/2_59-3).

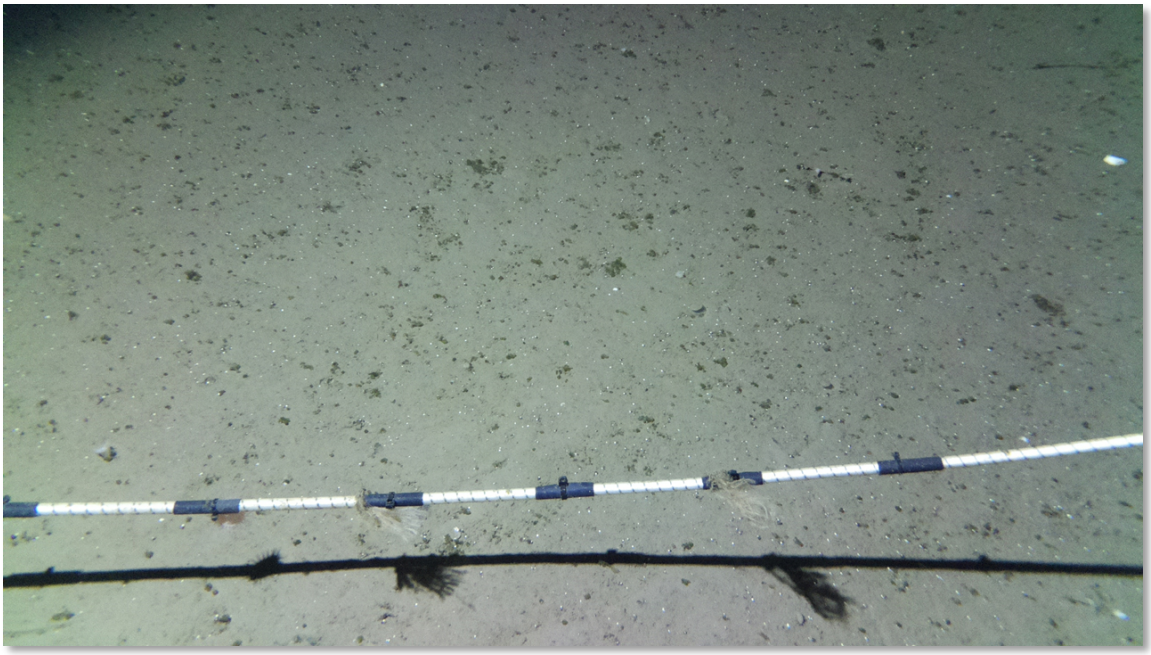

Fig. 2.3: Image of algal fall detritus on the HAUSGARTEN seafloor taken on 17 June 2024 by the Long-Term Lander

Multicorer work

During PS143/2 TV Multicorer (TVMUC sampling was opportunistic and not a key focus of the onboard work, with the majority of sampling for 2024 being taken during PS143/1. Despite this samples were collected. In an addition to the sampling described in Table 2.3, sediments were collected as part of Project HaploSEA, which is funded via Marie Skłodowska-Curie Actions (MSCA) as an MSCA Postdoctoral Fellowship at GEOMAR (Grant agreement ID: 101108076, https://doi.org/10.3030/101108076). The Project is evaluating the use of meta-genetic diversity for biological assessments of deep-sea benthic communities. Sediment samples were collected via the Multicores, with at least three cores per station set aside for this work where possible.

Tab. 2.3: Locations and dates of TVMUC deployments conducted during PS143/2

MUC no.	Station Number	Date	Latitude	Longitude
1	PS143/2_19-2	20/07/24	79.13552	6.07649
2	PS143/2_22-8	21/07/24	79.07827	4.16602
3	PS143/2_25-8	23/07/24	79.93787	3.19281
4	PS143/2_48-6	25/07/24	79.96500	-0.82058
5	PS143/2_54-6	26/07/24	79.90816	-5.23978
6	PS143/2_56-7	27/07/24	78.97553	-5.29832
7	PS143/2_62-3	30/07/24	78.99044	5.67015
8	PS143/2_76-9	02/07/24	78.83453	-2.79650

Preliminary (expected) results

Megafauna

PS143/2 offered the rare opportunity to repeat the traditionally annual time series HAUSGARTEN survey transects between 2 and 6 weeks after surveys conducted during PS143/1. The most immediate observation made following inspection of these two data sets is that there was an algal fall which was visible as widespread phytodetritus during PS143/1 HAUSGARTEN transects was almost all removed from the seafloor by the time of the PS143/2 transect surveys. Example images and a brief description of the typical seafloor from the PS143/2 OFOBS surveys are given below, with image names as used on the PANGAEA data upload:

OFOBS 1 – PS143_2_4-1 - SV-IV

Fig. 2.4: PS143_2_4-1_OFOBS_CAM-1_MANUAL_20240716_012457.jpeg.
Typical soft bottomed SV-IV seafloor with occasional dropstones and grit / pebbles, with encrusting fauna

OFOBS 2 – PS143_2_7-7 - S3

Fig. 2.5: PS143_2_7-7_OFOBS_CAM-1_TIMER_20240717_020641.JPG.
Flat, soft sediment S3 seafloor with very occasional dropstones and sparce fauna.

OFOBS 3 – PS143_2_11-7 - SV-III

Fig. 2.6: PS143_2_11-7_OFOBS_CAM-1_MANUAL_20240718_025359.JPG.
Pebble, grit and dropstone covered seafloor cut with occasional trawl tracks.

OFOBS 4 – PS143_2_14-7 - SV-II

Fig. 2.7: PS143_2_14-7_OFOBS_CAM-1_MANUAL_20240718_181923.JPG.
Very soft SV-II seafloor with a variety of both mobile and sessile fauna.

Fig. 2.8: PS143_2_14-7_OFOBS_CAM-1_MANUAL_20240718_181945.JPG.
A particularly high concentration of Sebastes sp. rockfish shelter amongst a accumulation of rocks on he SV-II seafloor.

OFOBS 5 – PS143_2_19-1 - HG-1

Fig. 2.9: PS143_2_19-1_OFOBS_CAM-1_MANUAL_20240720_021928.JPG.
The soft HG-I seafloor is particularly abundant in polychaete filter feeding worms, particularly to the eastern end of the transect. Occasional 20 – 30 cm diameter outgassing channels are apparent.

Fig. 2.10: PS143_2_19-1_OFOBS_CAM-1_MANUAL_20240720_011007.JPG.
A ray fish has pushed under discoloured, soft seafloor sediments.

OFOBS 6 – PS143_2_24-1 - N3

Fig. 2.11: PS143_2_24-1_OFOBS_CAM-1_MANUAL_20240722_102555.JPG.
A the northerly N3 station dropstones are primarily colonised by large sponges, commonly associated with a number of shrimps.

OFOBS 7 – PS143_2_58-8 - EGC-1

Fig. 2.12: PS143_2_56-8_OFOBS_CAM-1_MANUAL_20240728_001728.JPG.
A basket star brittlestar occupies one of the occasional small stones observed on the EGC-1 transect.

OFOBS 8 – PS143_2_ 59-4 - HG-IV

Fig. 2.13: PS143_2_59-4_OFOBS_CAM-1_TIMER_20240729_224728.JPG.
On this HG-4 transect a piece of wood was observed on the seafloor, in the hydrodynamic lee of a small fauna encrusted rock.

OFOBS 9 – PS143_2_64-1 - Methane Ridge

Fig. 2.14: PS143_2_64-1_OFOBS_CAM-1_MANUAL_20240731_033508.JPG.
On the flanks of the ridge feature investigated during OFOBS 9, Umbellula sp. were particularly abundant as isolated individuals on the ridge flanks.

Fig. 2.15: PS143_2_64-1_OFOBS_CAM-1_MANUAL_20240731_034907.JPG.
Closer to the centre of the ridge occasional well colonised hard rocky stones were visible, supporting a diversity of hydroids, soft corals and anenomes rare in the FRAM strait.

OFOBS 10 – PS143_2_76-11 - EG-IV

Fig. 2.16: PS143_2_76-11_OFOBS_CAM-1_MANUAL_20240802_124831.JPG.
As has been observed during previous expeditions, dropstones and rocks on the western side of the FRAM strait are populated by a lower abundance and biodiversity of filter feeding fauna than those on the east. Here a large barnacle and sponge support a selection of mobile megafauna.

Multicorer samples

Samples were collected for time series analysis by the AWI 'Deep Sea Ecology and Technology' group back on shore, to continue the long-term time series analysis of infauna. Allitionally, later processing and later analyses of a selection of cores will be based on the standardised protocols aiming to analyse whole biodiversity across the tree of life via metabarcoding and novel capture by hybridisation approach. The data will be included in the eDNAabyss-dataset, allowing the comparison of over 15,000 samples worldwide.

Autonomous Underwater Vehicle survey data

The high-resolution images and sidescan data collected during PS143/2 with the AUV will be used to further build the high-resolution topographical map of the HAUSGARTEN and Fram strait seafloor. The images will be used to inform on spatial distribution of megafauna and response to environemental change.

Data management

OFOBS, AUV and Long Term Lander time series camera data will be archived, published and disseminated according to international standards by the World Data Center PANGAEA Data Publisher for Earth & Environmental Science (https://www.pangaea.de) within two years after the end of the expedition at the latest. By default, the CC-BY license will be applied.

This expedition was supported by the Helmholtz Research Programme "Changing Earth – Sustaining our Future" Topic 6, Subtopics 6.1, 6.3 and 6.4.

All benthic data will further be deposited in the data repository CRITTERBASE at AWI, while seafloor still images will also be uploaded to the online image database BIIGLE to enable easy access by other parties.

Molecular data (DNA and RNA data) will be archived, published and disseminated within one of the repositories of the International Nucleotide Sequence Data Collaboration (INSDC, www.insdc.org) comprising of EMBL-EBI/ENA, GenBank and DDBJ.

Many of the physical samples (i.e. Chl *a*, 16S/18S eDNA, phytoplankton and zooplankton biodiversity etc.) will be analyzed at AWI or GEOMAR within approximately one year after the cruise. We plan that the full data set will be available at the latest about two years after the cruise. Samples taken for microscopical and molecular analyses, which cannot be analyzed within two years after the cruise, will be stored at the AWI for at least ten years and available upon request to other researchers.

In all publications based on this expedition, the **Grant No. AWI_PS143_01** will be quoted and the following publication will be cited:

Alfred-Wegener-Institut Helmholtz-Zentrum für Polar- und Meeresforschung (2017) Polar Research and Supply Vessel POLARSTERN Operated by the Alfred-Wegener-Institute. Journal of large-scale research facilities, 3, A119. http://dx.doi.org/10.17815/jlsrf-3-163.

References

Dijkstra JA, Mello K, Sowers D, et al (2021) Fine-scale mapping of deep-sea habitat-forming species densities reveals taxonomic specific environmental drivers. Global Ecology and Biogeography 30:1286–1298. https://doi.org/10.1111/geb.13285

Durden JM, Bett BJ, Ruhl HA (2020) Subtle variation in abyssal terrain induces significant change in benthic megafaunal abundance, diversity, and community structure. Progress in Oceanography 186:102395. https://doi.org/10.1016/j.pocean.2020.102395

Gage JD, Tyler PA (1991) Deep-Sea Biology: A Natural History of Organisms at the Deep-Sea Floor. Cambridge University Press

O'Hara TD, Williams A, Althaus F, et al (2020) Regional-scale patterns of deep seafloor biodiversity for conservation assessment. Diversity and Distributions 26:479–494. https://doi.org/10.1111/ddi.13034

Paulus E (2021) Shedding Light on Deep-Sea Biodiversity – A Highly Vulnerable Habitat in the Face of Anthropogenic Change. Front Mar Sci 8. https://doi.org/10.3389/fmars.2021.667048

Piepenburg D (2005) Recent research on Arctic benthos: common notions need to be revised. Polar Biol 28:733–755. https://doi.org/10.1007/s00300-005-0013-5

Purser A, Hehemann L, Boehringer L, et al (2022) The COSMUS expedition: seafloor images and acoustic bathymetric data from the PS124 expedition to the southern Weddell Sea, Antarctica. Earth System Science Data 14:3635–3648. https://doi.org/10.5194/essd-14-3635-2022

Purser A, Marcon Y, Dreutter S, et al (2019) Ocean Floor Observation and Bathymetry System (OFOBS): A New Towed Camera/Sonar System for Deep-Sea Habitat Surveys. IEEE Journal of Oceanic Engineering 44:87–99. https://doi.org/10.1109/JOE.2018.2794095

Soltwedel T, Bauerfeind E, Bergmann M, et al (2016) Natural variability or anthropogenically-induced variation? Insights from 15 years of multidisciplinary observations at the arctic marine LTER site HAUSGARTEN. Ecological Indicators 65:89–102. https://doi.org/10.1016/j.ecolind.2015.10.001

Taylor J, Krumpen T, Soltwedel T, et al (2017) Dynamic benthic megafaunal communities: Assessing temporal variations in structure, composition and diversity at the Arctic deep-sea observatory HAUSGARTEN between 2004 and 2015. Deep Sea Research Part I: Oceanographic Research Papers 122:81–94. https://doi.org/10.1016/j.dsr.2017.02.008

3. PELAGIC BIOGEOCHEMISTRY

Daniel Scholz[1], Matthias Westphal[2];
not on board: Sinhué Torres-Valdés[1], Adrian Martin[3], Pete Brown[3]

[1]DE.AWI
[2]DE.HSBHV
[3]UK.NOC

Grant-No. AWI_PS143_02

Rationale and Objectives

Current gaps in knowledge concerning nutrient and carbon biogeochemical cycles at the pan-Arctic scale stem from the lack of information necessary to constrain their budgets. Available computations (MacGilchrist et al. 2014; Torres-Valdés et al. 2013, 2016) indicate the Arctic Ocean (AO) is a net exporter of phosphate, dissolved organic phosphorus, silicate, dissolved organic nitrogen and dissolved inorganic carbon (DIC). Net nitrate transports are balanced despite large losses due to denitrification. Silicate export derives largely from riverine inputs, suggesting alterations in river loads might have an impact on exports too, potentially modifying the stoichiometric abundance of nutrients. These computations are based mostly on summer time observations across the main gateways (i.e., Fram Strait, the Barents Sea Opening, Bering Strait and Davis Strait), which hinders our complete understanding given data to resolve temporal variability over seasonal and longer time scales are rather scarce. Because of this, there are still unknowns regarding sources and sinks of these biogeochemically relevant variables. Under ongoing and predicted climate change, identifying and quantifying sinks and sources becomes relevant to: (i) generate baseline measurements against which future change can be evaluated, (ii) assess the impact of climate change on biogeochemical processes (e.g., primary production, organic carbon export, remineralisation), (iii) understand the complex interaction between biogeochemical and physical processes, and how such interactions affect the transport of nutrients downstream and the capacity of the AO to function as a sink of atmospheric CO_2, and to (iv) determine whether long-term trends occur and what is their origin.

To address the points listed above, we began the deployment of FRAM sensors and remote access samplers as follows; whenever enough RAS are available, deployments target core (~250 m) and surface waters of the West Spitsbergen Current and the East Greenland Current since 2018. With these data we aim to assess the role of transports across the Fram Strait, one of the main Arctic gateways, relative to the wider Arctic Ocean nutrient budgets.

The deployments of RAS are done in collaboration with Katja Metfies (AWI), Christina Bienhold (AWI/MPI) and Matthias Wietz (AWI/MPI), who study phytoplankton and bacterial genetics, respectively.

Work at sea

Biochemical in-situ Sensors and remote access samplers (RAS)

We prepared and deployed sensors and remote access samplers (RAS) at the EGC-10 and F4S-8 mooring sites at 54 m depth in the East Greenland Current and at 24 m in the West Spitsbergen Current, respectively. The following tables contain information about the sensors used, their starting date and time as well as the programmed measuring intervals.

Tab. 3.1: Overview of sensors and RAS deployed at EGC-10

Sensor	Parameter	S/N	Start date	Start time [UTC]	Interval
SBE SUNA	NO_3	1166	27.07.24	16:00	2 h
Sunburst SAMI pH	pH	P0186	29.07.24	00:00	4 h
Sunburst SAMI CO2	pCO2	C0155	29.07.24	00:00	2 h
SBE37-SMP-ODO	C,T,D,O_2	20523	28.07.24	12:00	1 h
Wetlabs EcoPar	PAR	522	27.07.24	14:00	1 h
Wetlabs EcoTriplet	CDOM, Chla, backscatter	1552	27.07.24	14:00	4 h
RAS	Water sample	14128_08	31.07.24	12:00	8 days

Tab. 3.2: Overview of sensors and RAS deployed at F4S-8

Sensor	Parameter	S/N	Start date	Start time [UTC]	Interval
SBE SUNA	NO_3	1021	16.07.24	20:00	2h
Sunburst SAMI pH	pH	P0239	18.07.24	00:00	4h
Sunburst SAMI CO2	pCO2	C0185	18.07.24	00:00	2h
SBE37-SMP-ODO	C,T,D,O_2	15438	16.07.24	20:00	1h
Wetlabs EcoPar	PAR	521	16.07.24	22:00	1h
Wetlabs EcoTriplet	CDOM, Chla, backscatter	1425	16.07.24	22:00	4h
RAS	Water sample	14128_09	31.07.24	12:00	8days

We conducted recoveries of the EGC-8 and EGC-9 packages, which measured in the East Greenland Current between 2022 – 2023 and 2023 – 2024, respectively as well as the F4S-7 setup in the West Spitzbergen Current. The table below summarizes the availability of data downloaded after the recoveries.

Tab. 3.3: Overview of successfully recovered data. Ok – sensor recorded data during the entire deployment cycle, no data – sensor recorded no data at all or was not deployed, stopped early – sensor stopped before end of deployment cycle due to malfunction or low power

	EGC-8 [52m]	EGC-9 [53m]	EGC-9 [242m]	F4S-7 [48m])
SBE SUNA	ok	ok	no data	ok
Sunburst SAMI pH	no data	stopped early	no data	stopped early
Sunburst SAMI CO2	ok	ok	no data	stopped early
SBE37-SMP-ODO	ok	stopped early	stopped early	stopped early
Wetlabs EcoPar	ok	ok	no data	ok
Wetlabs EcoTriplet	no data	ok	no data	ok

While the SAMI sensors stopped measuring prematurely due to low battery voltage or clogged sampling tubes, the SBE37 devices of the EGC-9 and F4S-7 all exhibit the same error after about half the operating time. As the serial numbers of the devices are sequential and the devices have worked without any problems before, we assume that this is a hardware malfunction.

The RAS at F4S-7 and EGC-9 at 49 m took all expected samples, the one at EGC-9 at 49 m missed sample numbers 5, 19, 20, 26, 28, 40 and 47 and the sampler at EGC-9 at 242 m did not work at all. We have drawn off 50 ml subsamples of each sampling container for nutrient analysis, to be measured during the next leg.

Additionally, we recorded 51 high-resolution NO_3 profiles at stations shallower than 2,000 m by co-deploying a SUNA nitrate sensor along with the ship's CTD, which provides temperature and salinity data needed to process the sensor records following Sakamoto et al. (2009) The CTD's Niskin bottle nitrate data will be used to further improve the SUNA data quality in terms of offset correction.

Sample collection

In total, 22 CTD casts at 13 different stations were sampled for the later analysis of dissolved inorganic and total dissolved nutrients. Depending on the station depth, samples at 10 m, DCM, below DCM, 50 m, 100 m, 500 m, 1,200 m, 2,000 m, 2,250 m, and above bottom were collected in 50 mL Falcon tubes and stored at -20°C.

In order to improve the data quality of the moored CO_2 and O_2 sensors, DIC and Winkler samples were taken for laboratory analysis and subsequent data comparison only in vicinity of the EGC-10 and F4S-8 mooring locations.

The table below summarizes the stations at which we took seawater samples and their corresponding DCM, below DCM values as well as the station depth. The latter indicates if deep samples were taken at this site.

Tab. 3.4: Overview for the seawater samples for later nutrient analysis with information about the Station ID, station name, the maximum depths and DCM + below DCM values at which the samples were taken.

Cast ID	Station name	Cast type	Max depth [m]	Below DCM [m]	DCM [m]
PS143/2_002-1	SV-IV	deep	1262	NA	NA
PS143/2_002-6	SV-IV	shallow	1263	21	15
PS143/2_007-1	S3	deep	2276	NA	NA
PS143/2_007-6	S3	shallow	2280	40	30
PS143/2_011-1	SV-III	shallow-deep	789	55	30
PS143/2_014-1	SV-II	shallow-deep	215	25	20
PS143/2_015-1	SV-I	shallow-deep	316	25	26
PS143/2_018-1	HG1	deep	1250	NA	NA
PS143/2_018-7	HG1	shallow	1241	42	31
PS143/2_022-1	HG4	deep	2451	NA	NA
PS143/2_022-7	HG4	shallow	2448	30	18
PS143/2_023-1	HG9	deep	5530	NA	NA
PS143/2_023-4	HG9	shallow	5545	35	25
PS143/2_025-1	N5	deep	2477	NA	NA
PS143/2_025-7	N5	shallow	2476	38	31
PS143/2_056-1	EG1	deep	1060	NA	NA
PS143/2_075-1	EG1	shallow	1070	31	10

Cast ID	Station name	Cast type	Max depth [m]	Below DCM [m]	DCM [m]
PS143/2_062-1	F5	shallow-deep	2122	30	20
PS143/2_063-1	F4	shallow-deep	1246	NA	NA
PS143/2_076-1	EG4	Shallow	2526	31	20
PS143/2_076-8	EG4	deep	2529	NA	NA

Preliminary (expected) results

Water samples have to be analysed during the following leg to serve among other purposes for further sensor data processing and quality control. Both datasets will be compiled after quality control measures have been applied.

Data management

Our aim is to compile data from the different devices in a single file once individual data sets have been retrieved, quality controlled and analyzed.

All Data will be archived, published and disseminated according to international standards by the World Data Center PANGAEA Data Publisher for Earth & Environmental Science (https://www.pangaea.de) within two years after the end of the expedition at the latest. By default, the CC-BY license will be applied.

This expedition was supported by the Helmholtz Research Programme “Changing Earth – Sustaining our Future” Topic 2, Subtopic 1 and Topic 6, Subtopic 3.

In all publications based on this expedition, the Grant No. AWI_PS143_02 will be quoted and the following publication will be cited:

Alfred-Wegener-Institut Helmholtz-Zentrum für Polar- und Meeresforschung (2017) Polar Research and Supply Vessel POLARSTERN Operated by the Alfred-Wegener-Institute. Journal of large-scale research facilities, 3, A119. http://dx.doi.org/10.17815/jlsrf-3-163.

References

MacGilchrist GA, Naveira-Garabato AC, Tsubouchi T, Bacon S, Torres-Valdés S, Azetsu-Scott K (2014) The Arctic Ocean carbon sink. Deep Sea Research I 86:39–55. https://doi.org/10.1016/j.dsr.2014.01.002

Torres-Valdés S, Tsubouchi T, Bacon S, Naveira-Garabato AC, Sanders R, McLaughlin FA, Petrie B, Kattner G, Azetsu-Scott K, Whitledge TE (2013) Export of nutrients from the Arctic Ocean. Journal of Geophysical Research: Oceans 118(4):1625–1644. https://doi.org/10.1002/jgrc.20063

Torres-Valdés S, Tsubouchi T, Davey E, Yashayaev I, Bacon S (2016) Relevance of dissolved organic nutrients for the Arctic Ocean nutrient budget. Geophysical Research Letters 43(12):6418–6426.

Sakamoto CM, Johnson KS, Coletti LJ (2009) Improved Algorithm for the Computation of Nitrate Concentrations in Seawater using an in situ Ultraviolet Spectrophotometer. Limnology and Oceanography: Methods 7:132–143.

4. PHYSICAL OCEANOGRAPHY

Wilken-Jon von Appen[1], Rebecca McPherson[1], Simon Reifenberg[1], Hauke Becker[1], Carina Engicht[1], Marlene Meister[1,2], Buu-Lik Duong[1,2], Clemens Rohling[1,3]

[1]DE.AWI
[2]DE.UniOL
[3]DE.UHH

not on board: Christian Haas[1]

Grant-No. AWI_PS143/2_03

Objectives

The physical conditions that lead to enhanced primary and export production in the Arctic Ocean remain unclear. With both, rapid increases in ocean temperatures amplified in the Arctic region and sea ice retreat of the past two decades, the connection between these physical changes and the effect on polar marine ecosystem only increases in importance.

The intermittent presence of sea ice and meltwater affects both the physical and biochemical vertical structure of the water column but also limits in situ observations to summer months when the ice has retreated. The effects of changes in the environmental conditions on the polar marine biodiversity can only be detected through long-term observation of the species and processes. The FRAM multidisciplinary observatory attempts to observe the coupling across the system atmosphere, upper ocean, pelagic, and benthic environments.

The monitoring program of the Atlantic Water (AW) inflow into the Arctic via the West Spitsbergen Current (WSC) started in 1997. PS143/2 will contribute to maintaining this long-standing time series observatory, as the AW inflow conditions drive the changing physical (and also biogeochemical and biological) properties of the Arctic Ocean.

The Frontiers in Arctic Marine Monitoring (FRAM) Helmholtz infrastructure initiative has increased the ability to observe the temporal evolution of the coupled physical-chemical-biological system in the upper water column and troughout the water column to the sea floor. Continuing these interdisciplinary time series will allow for the evaluation of interannual variations in addition to shorter term interactions on submesoscale to seasonal timescales. Two main multidisciplinary time series locations are pursued in the framework of FRAM and its continuation: F4 site at 1,000 m water depth in the inflowing Atlantic Water boundary current (West Spitsbergen Current) and EG4 site at 1,000 m water depth in the outflowing Polar Water boundary current (East Greenland Current). By clearly being embedded in very different water masses representing end points of Arctic conditions, they will allow for a better prediction of what is to be expected in the Arctic Ocean. Submesoscale dynamics take place on horizontal scales of <1km to a few km in Fram Strait. They are a key process that achieves the subduction of Atlantic Water below Polar Water as the Atlantic Water recirulates in Fram Strait. However, the temporal statistics of the submesocale are still unknown.

Ocean-sea ice coupling in the marginal ice zone (MIZ) is related to key mechanisms of rapid Arctic sea ice decline and Arctic Amplification. These include processes affecting heat fluxes in the air-ice-ocean system, ocean mixed layer-halocline coupling, ice melt and ice edge dynamics in the MIZ. We posit that oceanic eddies, fronts and tidal mixing shape the sea ice distribution in the MIZ which leads to locally enhanced ice melting as well as to the generation

of stratified areas with suppressed melting. These processes result in sea ice characteristics that can be distinguished by different gradients of sea ice floe size, concentration, roughness and thickness. Our study also aims to understand the complex physical-chemical-biological interactions that control biogeochemical cycling and ecosystem functioning.

Work at sea

CTD/Rosette Water Sampler

Hydrographic measurements during PS143/2 utilized a CTD system (conductivity, temperature, and depth sensor). The sensors and rosette were supplied by the research vessel. In this section, we first detail the technical setup of the CTD rosette, followed by a description of the general procedure for conducting CTD casts during the cruise. We then provide additional information on the deployments. Please refer to Tab. 4.1 for a summary of all 60 casts, of which positions are shown in Fig. 4.1.

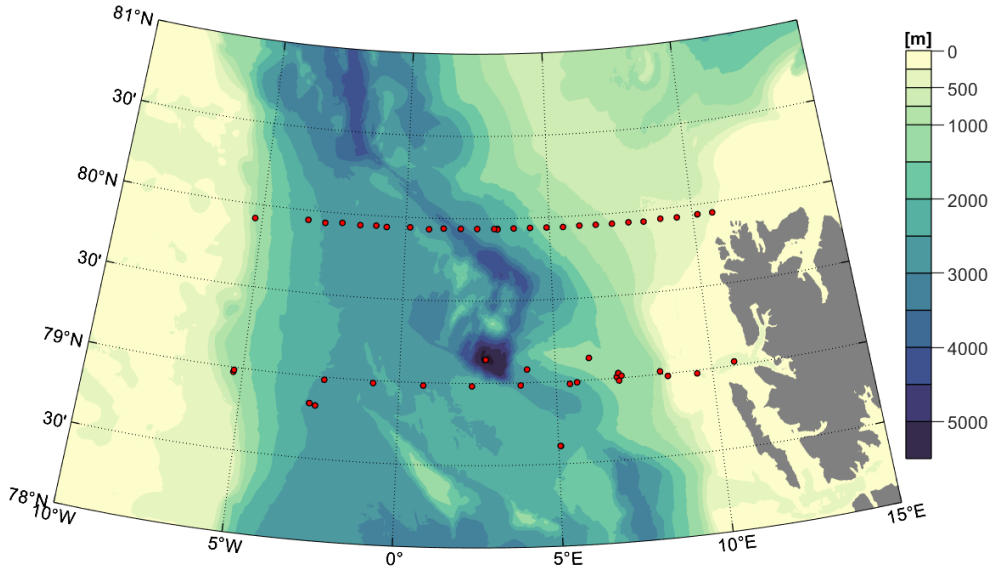

Fig. 4.1: Map showing the CTD stations (indicated by red dots) in the study region

The standard sensor configuration (conf1) of the CTD system was used throughout the cruise included two temperature sensors, two conductivity cells, a pressure sensor, two oxygen sensors, an altimeter, a fluorescence sensor, and a transmissometer, see Tab. 4.2 for more details). Additionally, a Sea-Bird SUNA nitrate sensor (SN 1318) was included on the rosette. Since this sensor has a depth rating of 2,000 m, it was only used during shallower casts. The sensor was programmed to start sampling and internally record data as soon as power was supplied by the SBE911, initiating data acquisition when the CTD was turned on. An Underwater Vision Profiler (UVP) was also attached to the rosette. The UVP automatically begins recording when lowered beyond 20 m and stops when raised above 30 m. The typical CTD deployment procedure was as follows: lowering the rosette to 22 m, waiting up to one and a half minutes for the UVP and CTD pump to activate, then bringing it back to the surface. The downcast then began by lowering the rosette at 0.5 m/s for the first 200 m, increasing up to 1 m/s thereafter. For casts approaching the sea floor, the lowering speed was reduced to 0.5 m/s approximately 100 m above the seabed, with further reductions when nearing the bottom, especially if the altimeter signal was weak. When the altimeter functioned correctly, full-depth casts were stopped 10 m above the seabed.

Tab. 4.1: Sensor configurations for the CTD system used during PS131

	SN	Channel	Description	Calibration Date
CTD			SBE 911plus	
Temperature	2685	F0	SBE3	11-08-2023
Temperature sec.	2423	F3	SBE3	01-08-2023
Conductivity	2446	F1	SBE4	13-07-2023
Conductivity sec.	2078	F4	SBE4	25-07-2023
Pressure	0485	F2	SBE9	14-11-2017
Oxygen	0880	V4	SBE43	06-12-2023
Oxygen sec.	4274	V5	SBE43	24-06-2023
Altimeter	1228	V2	Benthos PSA-916	--
Fluorescence	1670	V1	WET Labs ECO-AFL/FL	30-11-2023
Beam Transmission	946R	V0	WET Labs C-Star	16-07-2023

Furthermore, a bbe FluoroProbe (FLP, TS-24-15) was mounted on the rosette measuring the fluorescence of and identifying different groups of algae. Reliable measurements are possible down to 200 m depth, which is why it was only used during ‘shallow’ CTD casts.

Water samples were collected at all biological stations (see chapter 4). The niskin bottles were triggered on the upcast, with a 60-second wait at each target depth to sample the 'true' ambient water mass and allow lagging sensors to stabilize. These water samples are partly used for calibrating salinity and oxygen measurements. The results from on-board salinometry are presented below. Water sampling for the biological working groups usually aimed for the deep chlorophyll maximum (DCM) in the water column. During downcasts, one of the biologists stood aside to set the target depths aiming for the DCM and ‘below DCM’. It was not uncommon that the shape, intensity and location of the DCM changed between down- and upcast, for which reason the heaving speed was sometimes reduced to 0.2 m/s for the upper 50m of the water column facilitating spontaneously adjusted stops of the rosette.

Measurement differences between primary and secondary sensors (temperature, conductivity, and oxygen) were observed throughout the cruise. No clear malfunctions could be observed (Fig. 4.2).

For PS143_02_021_06.hex, the station and cast number differed from the action log of the vessel. There it was registered as 022_06.

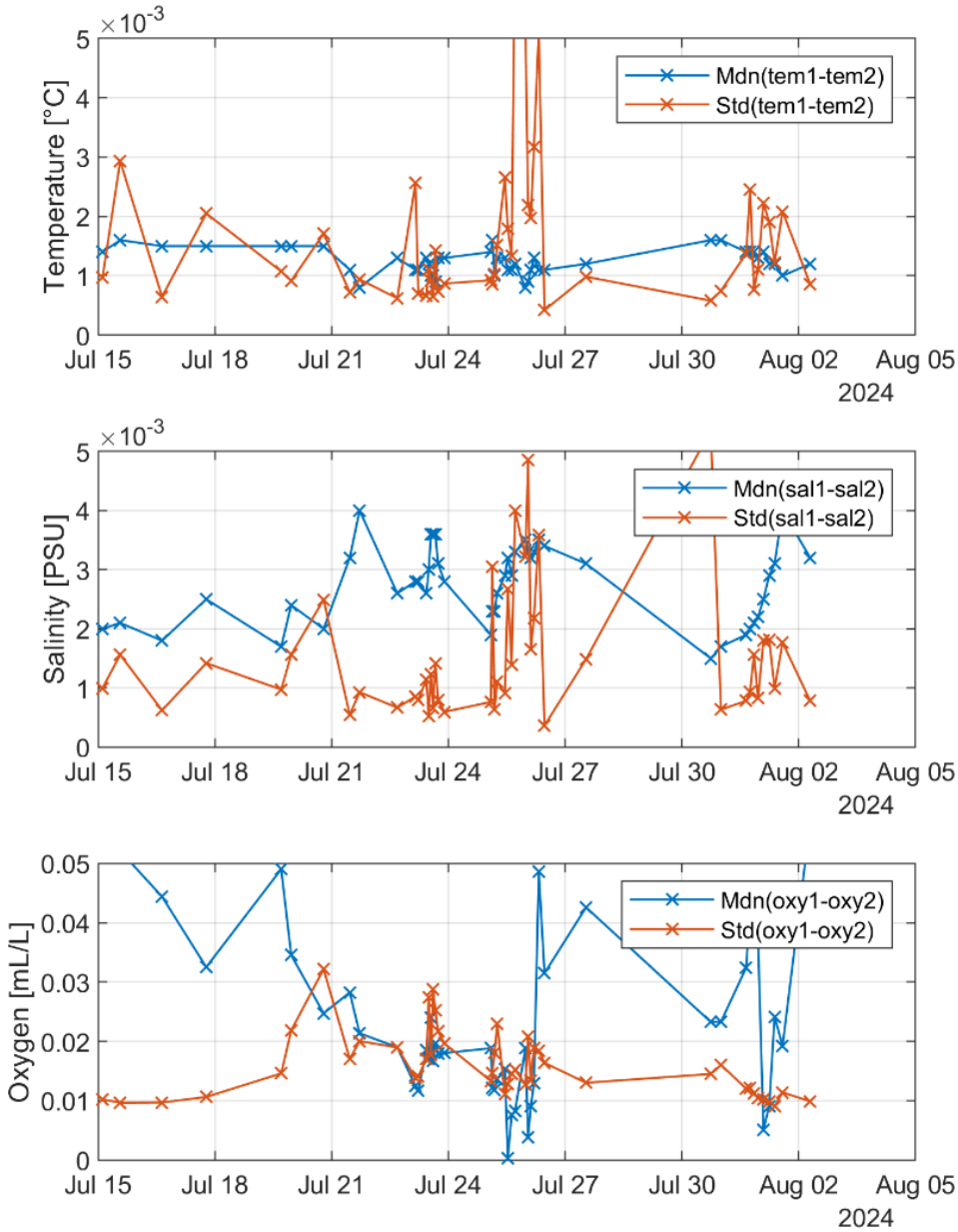

Fig. 4.2: Time series of the mean (in blue) and standard deviation (in orange) of the measurement difference between primary and secondary sensors

Tab. 4.2: Meta-data of all CTD stations from PS143/2. The station names refer to the file numbers of the CTD data, an exception is station 021_06.

Station as in Log	Start time [UTC]	Lat [°N]	Lon [°E]	Cast Depth [dbar]	Description	Comments
001_01	15-07-2024 02:44	79.0067	6.9407	1218	Test station with bottles	
002_01	15-07-2024 13:38	79.0308	6.9977	1280	SV-IV deep with bottles	CTD computer froze before cast at around 10:00 UTC. Unit was restarted.

Station as in Log	Start time [UTC]	Lat [°N]	Lon [°E]	Cast Depth [dbar]	Description	Comments
002_06	15-07-2024 20:18	79.0290	7.0053	203	SV-IV shallow with bottles	First attempt aborted due to underwater unit-error. Second attempt successful.
007_01	16-07-2024 15:27	78.6093	5.0693	2315	S3 deep with bottles	Several spooling errors.
007_06	16-07-2024 22:37	78.6092	5.0582	202	S3 shallow with bottles	
011_01	17-07-2024 18:41	79.0168	8.3345	801	SV-III deep with bottles	Niskin #12 leaked
011_06	17-07-2024 23:54	79.0177	8.3332	202	SV-III shallow with bottles	
014_01	18-07-2024 11:34	78.9808	9.5070	216	SV-II with bottles	
015_01	18-07-2024 22:13	79.0235	10.7237	319	SV-I with bottles	
018_01	19-07-2024 16:55	79.1338	6.0908	1253	HG-I deep with bottles	
018_06	19-07-2024 23:05	79.1342	6.0938	1254	HG-I shallow with bottles	
022_01	20-07-2024 19:02	79.0802	4.0863	2486	HG-IV deep with bottles	Spooling error. Valve of niskin #11 and #13 replaced.
022_06	21-07-2024 02:11	79.0803	4.0917	203	HG-IV shallow with bottles	Saved as PS143_02_021_06.hex
023_01	21-07-2024 11:10	79.1422	2.7348	5664	HG-IX deep with bottles	Valve of niskin #22 replaced. Several spooling errors. Niskin #12 leaked. Beam transmission jumping from 95% to 98% at 1200m depth during downcast. 20min winch repair at 2120m depth during upcast.
023_04	21-07-2024 17:15	79.1428	2.7600	2956	HG-IX shallow with bottles	Cast was used for fixing errors on the winch at depth. Niskin #6 did not close. Niskin #12 leaked.
025_01	22-07-2024 16:28	79.9383	3.1923	2525	N5TE section deep with bottles	Valve of niskin #12 changed.
025_07	22-07-2024 23:30	79.9378	3.1927	203	N5TE section shallow with bottles	
026_01	23-07-2024 03:41	79.9392	3.7553	509	N5TE section without bottles	First cast without closing bottles.

Station as in Log	Start time [UTC]	Lat [°N]	Lon [°E]	Cast Depth [dbar]	Description	Comments
027_01	23-07-2024 05:25	79.9400	4.3268	507	N5TE section with bottles, Bio-Station	Niskin #6 did not close.
028_01	23-07-2024 10:26	79.9387	4.8982	507	N5TE section with bottles but no samples	Niskin #6 checked by Labor-Elo. All bottles closed to check functionality of it. Niskin bottle did close.
029_01	23-07-2024 11:52	79.9372	5.4718	507	N5TE section without bottles	
030_01	23-07-2024 13:15	79.9400	6.0428	507	N5TE section without bottles	
031_01	23-07-2024 14:33	79.9383	6.6145	506	N5TE section without bottles	
032_01	23-07-2024 15:56	79.9380	7.1815	507	N5TE section without bottles	
033_01	23-07-2024 17:37	79.9378	7.7578	507	N5TE section, Bio-Station	
034_01	23-07-2024 21:35	79.9333	8.2830	493	N5TE section without bottles	Echolot was completely off. Altimeter checked in time. Presence of ice.
035_01	23-07-2024 23:12	79.9402	8.8710	467	N5TE section without bottles	
036_01	24-07-2024 00:35	79.9363	9.4497	467	N5TE section without bottles	
037_01	24-07-2024 02:04	79.9390	10.1683	446	N5TE section without bottles	
038_01	24-07-2024 03:16	79.9387	10.6965	291	N5TE section without bottles	Echolot jumping between 300-400 and “000”m.
040_01	24-07-2024 12:06	79.9398	10.1773	443	N5TE section with bottles, Bio-Station	
041_01	25-07-2024 02:11	79.9347	3.1928	506	N5TW section without bottles	Presence of ice.
042_01	25-07-2024 03:03	79.9375	3.0785	506	N5TW section without bottles	
043_01	25-07-2024 04:27	79.9383	2.4842	506	N5TW section without bottles	
044_01	25-07-2024 06:07	79.9383	1.9162	506	N5TW section with bottles, Bio-Station	
045_01	25-07-2024 10:47	79.9392	1.3158	506	N5TW section without bottles	
046_01	25-07-2024 12:38	79.9325	0.8067	506	N5TW section without bottles	Presence of ice.

Station as in Log	Start time [UTC]	Lat [°N]	Lon [°E]	Cast Depth [dbar]	Description	Comments
047_01	25-07-2024 14:59	79.9403	0.1478	506	N5TW section without bottles	
048_01	25-07-2024 17:07	79.9355	-0.6663	506	N5TW section with bottles, Bio-Station	
049_01	25-07-2024 23:30	79.9403	-1.0317	506	N5TW section without bottles	
050_01	26-07-2024 01:07	79.9365	-1.5853	507	N5TW section without bottles	
051_01	26-07-2024 02:50	79.9420	-2.2142	506	N5TW section without bottles	
052_01	26-07-2024 04:45	79.9343	-2.8057	506	N5TW section without bottles	
053_01	26-07-2024 07:43	79.9418	-3.4047	506	N5TW section without bottles	
054_01	26-07-2024 11:16	79.9150	-5.2492	968	N5TW section with bottles, Bio-Station	
056_02	27-07-2024 12:53	78.9715	-5.2958	1057	EG-I deep with bottles, Bio-Station	
062_01	30-07-2024 17:45	78.9905	5.6698	2157	F5 with bottles, Bio-Station	
063_01	31-07-2024 00:06	79.0127	7.0955	1262	F4 with bottles	Calibration of glider and mooring sensors.
067_01	31-07-2024 13:21	78.9855	8.5713	264	T78.59 section without bottles	
068_01	31-07-2024 15:37	78.9843	7.0100	506	T78.59 section without bottles	
069_01	31-07-2024 18:02	78.9827	5.4412	507	T78.59 section without bottles	
070_01	31-07-2024 20:24	78.9843	3.8703	506	T78.59 section without bottles	
071_01	31-07-2024 22:57	78.9822	2.3150	507	T78.59 section without bottles	
072_01	01-08-2024 02:15	78.9828	0.7633	507	T78.59 section without bottles	
073_01	01-08-2024 05:48	78.9841	-0.8297	507	T78.59 section without bottles	
074_01	01-08-2024 09:07	78.9833	-2.3888	508	T78.59 section without bottles	
075_01	01-08-2024 14:03	78.9837	-5.2791	1073	T78.59 section, EG-I shallow with bottles, Bio-Station	

Station as in Log	Start time [UTC]	Lat [°N]	Lon [°E]	Cast Depth [dbar]	Description	Comments
076_01	01-08-2024 22:53	78.8349	-2.8048	203	EG-IV shallow	Accidental stop of winch at 30m depth during upcast for three minutes.
076_08	02-08-2024 07:03	78.8340	-2.7933	2570	EG-IV deep with bottles	
077_01	02-08-2024 16:52	78.8228	-2.6090	10	EG-IV shallow 2 with bottles	Pumps did not turn on.

Salinometry

We collected 34 water samples for high-precision salinometry from the CTD Rosette during the second leg PS143/2. In addition to these samples, 37 water samples from the first leg PS143/1 were also measured. Here we describe the sampling, and preliminary results from the salinometer.

The samples were taken from the Niskin bottles of the CTD rosette before any other water sampling. Before taking the actual sample, the sample bottles were filled twice until the water spilled over in order to rinse them, and the rubber cap was rinsed while the bottles were emptied in between. Then the bottles were closed, rinsed with fresh water from outside, sealed with an aluminum cap, and stored. We then obtained high-precision salinity measurements with an Optimare Precision Salinometer (OPS, SN 006) for potential recalibration of the conductivity sensors. An overview of all taken samples as well as the results from the salinometry can be found in Tab. 4.3.

We measured these samples in five salinometry sessions of 10, 10, 13, 24, and 14 bottles, i.e. 71 samples in total. The day before each session, the salinity bottles were heated in a water bath to approximately 30°C. Then, the pressure within the bottles was released with an injection needle after the warm bath. Afterwards, the bottles were allowed to cool down to room temperature for about 20 hours. Before using the OPS, the samples were shaken thoroughly for overcoming any stratification in the bottle. While being sampled by the OPS, the opening of the bottles was sealed with parafilm to inhibit evaporation. The metal inlet tube of the OPS was cleaned with a Kim-wipe between the samples.

A salinometry session starts with the standardization of the OPS using standard seawater. The respective bottle was sealed with the original cap and regularly sampled at the end of each session again, if enough water remained in the bottle after the standardization. The salinity of the standard did not decrease in any session. A decrease would be indicative of faults in the salinometry session.

Overall, our preliminary analysis suggests that the absolute differences of both salinity measurements from the CTD compared to the OPS salinity were generally < 0.004 PSU, with one exception. For cast PS143_2_001_01, Niskin bottle #4 (at 1,000 m depth), there was a considerably large difference between the salinity from primary and secondary sensor. While the value from Sal11 (secondary) compares well to the OPS measurement, the Sal00 is off by >0.3 psu. Also, for bottle 25 (sampled during PS132_2_002_01), the rubber lid popped off after the bottle was rinsed with fresh water and was then put back on, the data point is removed from the analysis.

Excluding this outlier, the conductivity measurements seem to be of appropriate quality for the planned studies and analyses. The mean difference of primary (secondary) CTD sensor and the OPS was -0.0020 psu (0.0019 psu) during the first leg and 0.0007 psu (0.0038 psu) for the

second leg (dashed lines in Fig. 4.3). That is, there is a slight drift in both sensors between the two cruise legs.

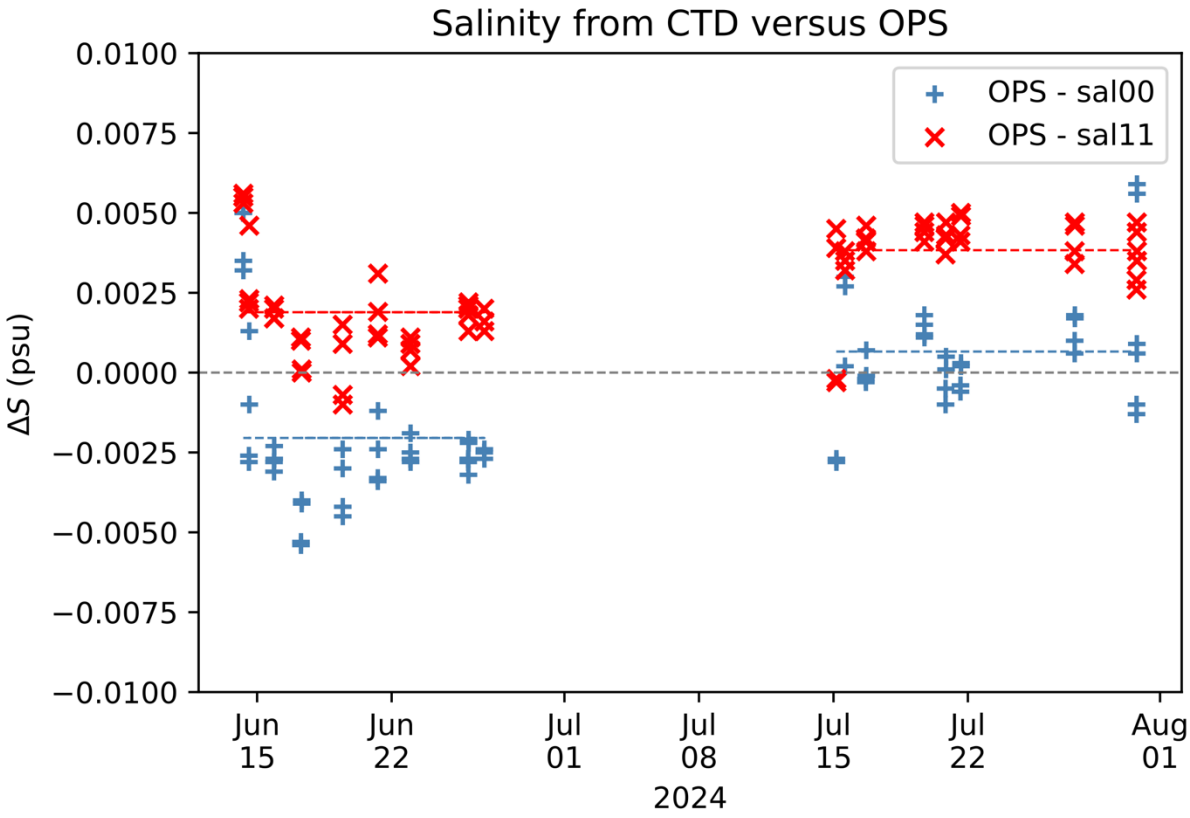

Fig. 4.3: Differences of salinity measured with the high-precision salinometer (OPS) and the two sensors sal00 (primary, blue) and sal11 (secondary, red) from the CTD Rosette. Two outliers (>0.3) from the primary sensor are outside the plotting range, see main text. The dashed lines show the mean deviation for each cruise leg.

Tab. 4.3: Overview of salinometry

Station	Date [2024]	Depth [m]	Niskin	OPS [psu]	Sal00 [psu]	Sal11 [psu]	Session
PS143/1_002_01	14.06.24	200	2	34.9930	34.9880	34.9875	5
PS143/1_002_01	14.06.24	200	2	34.9930	34.9880	34.9875	5
PS143/1_002_01	14.06.24	100	5	34.9580	34.9545	34.9524	5
PS143/1_002_01	14.06.24	100	5	34.9577	34.9545	34.9524	5
PS143/1_002_05	14.06.24	1000	13	34.9114	34.9124	34.9091	2
PS143/1_002_05	14.06.24	1000	13	34.9137	34.9124	34.9091	2
PS143/1_002_05	14.06.24	2000	5	34.9139	34.9167	34.9119	3
PS143/1_002_05	14.06.24	2000	5	34.9141	34.9167	34.9119	3
PS143/1_004_03	15.06.24	1800	5	34.9127	34.9158	34.9110	2
PS143/1_004_03	15.06.24	1800	5	34.9130	34.9158	34.9110	2
PS143/1_004_03	15.06.24	1400	7	34.9122	34.9145	34.9101	2

Station	Date [2024]	Depth [m]	Niskin	OPS [psu]	Sal00 [psu]	Sal11 [psu]	Session
PS143/1_004_03	15.06.24	1400	7	34.9118	34.9145	34.9101	2
PS143/1_006_06	19.06.24	400	17	34.8552	34.8594	34.8559	3
PS143/1_006_06	19.06.24	400	17	34.8549	34.8594	34.8559	3
PS143/1_006_06	19.06.24	750	10	34.8759	34.8789	34.8750	1
PS143/1_006_06	19.06.24	750	10	34.8765	34.8789	34.8750	1
PS143/1_009_08	21.06.24	1800	5	34.9142	34.9176	34.9131	1
PS143/1_009_08	21.06.24	1800	5	34.9143	34.9176	34.9131	1
PS143/1_009_08	21.06.24	1200	9	34.9090	34.9114	34.9071	1
PS143/1_009_08	21.06.24	1200	9	34.9102	34.9114	34.9071	1
PS143/1_015_06	22.06.24	1100	5	34.9107	34.9132	34.9098	2
PS143/1_015_06	22.06.24	1100	5	34.9105	34.9132	34.9098	2
PS143/1_015_06	22.06.24	750	11	34.9584	34.9603	34.9573	3
PS143/1_015_06	22.06.24	750	11	34.9575	34.9603	34.9573	3
PS143/1_020_01	25.06.24	2500	2	34.9221	34.9249	34.9201	2
PS143/1_020_01	25.06.24	2500	2	34.9222	34.9249	34.9201	2
PS143/1_020_01	25.06.24	1800	4	34.9126	34.9158	34.9113	1
PS143/1_020_01	25.06.24	1800	4	34.9131	34.9158	34.9113	1
PS143/1_020_01	25.06.24	1400	6	34.9126	34.9148	34.9105	1
PS143/1_020_01	25.06.24	1400	6	34.9127	34.9148	34.9105	1
PS143/1_021_06	26.06.24	1800	5	34.9127	34.9154	34.9114	3
PS143/1_021_06	26.06.24	1800	5	34.9130	34.9154	34.9114	3
PS143/1_021_06	26.06.24	2000	3	34.9136	34.9161	34.9116	3
PS143/1_005_01	17.06.24	4500	3	34.9255	34.9308	34.9244	3
PS143/1_005_01	17.06.24	4500	3	34.9254	34.9308	34.9244	3
PS143/1_005_01	17.06.24	2000	6	34.9159	34.92	34.9159	3
PS143/1_005_01	17.06.24	2000	6	34.9160	34.92	34.9159	3
PS143/2_001_01	15.07.24	1000	4	34.9138	34.6078	34.9099	4
PS143/2_001_01	15.07.24	1000	4	34.9144	34.6078	34.9099	4
PS143/2_001_01	15.07.24	500	7	34.9633	34.9661	34.9636	4
PS143/2_001_01	15.07.24	500	7	34.9634	34.9661	34.9636	4
PS143/2_002_01	15.07.24	1000	12	34.9128	34.9134	34.9098	4
PS143/2_002_01	15.07.24	1000	12	34.9136	34.9134	34.9098	4
PS143/2_002_01	15.07.24	500	15	35.0024	34.9994	34.9989	4
PS143/2_002_01	15.07.24	500	15	35.0021	34.9994	34.9989	4
PS143/2_007_01	16.07.24	2000	5	34.9171	34.9173	34.9129	4
PS143/2_007_01	16.07.24	2000	5	34.9170	34.9173	34.9129	4
PS143/2_007_01	16.07.24	1000	13	34.9140	34.9133	34.9094	4
PS143/2_007_01	16.07.24	1000	13	34.9132	34.9133	34.9094	4
PS143/2_018_01	19.07.24	1000	8	34.9140	34.9122	34.9096	4

Station	Date [2024]	Depth [m]	Niskin	OPS [psu]	Sal00 [psu]	Sal11 [psu]	Session
PS143/2_018_01	19.07.24	1000	8	34.9137	34.9122	34.9096	4
PS143/2_018_01	19.07.24	750	15	34.9135	34.9124	34.9089	4
PS143/2_018_01	19.07.24	750	15	34.9136	34.9124	34.9089	4
PS143/2_022_01	20.07.24	1000	5	34.9178	34.9188	34.9141	4
PS143/2_022_01	20.07.24	1000	5	34.9183	34.9188	34.9141	4
PS143/2_022_01	20.07.24	2000	12	34.9128	34.9123	34.9081	4
PS143/2_022_01	20.07.24	2000	12	34.9124	34.9123	34.9081	4
PS143/2_023_01	21.07.24	1000	5	34.9191	34.9195	34.9148	4
PS143/2_023_01	21.07.24	1000	5	34.9189	34.9195	34.9148	4
PS143/2_023_01	21.07.24	2000	12	34.9050	34.9047	34.9	4
PS143/2_023_01	21.07.24	2000	12	34.9049	34.9047	34.9	4
PS143/2_056_02	27.07.24	1000	1	34.8900	34.889	34.8862	5
PS143/2_056_02	27.07.24	1000	1	34.8896	34.889	34.8862	5
PS143/2_056_02	27.07.24	500	12	34.8612	34.8594	34.8565	5
PS143/2_056_02	27.07.24	500	12	34.8611	34.8594	34.8565	5
PS132/2_062_01	30.07.24	2000	3	34.9172	34.9185	34.9146	5
PS132/2_062_01	30.07.24	2000	3	34.9175	34.9185	34.9146	5
PS132/2_062_01	30.07.24	500	7	34.9504	34.9448	34.9469	5
PS132/2_062_01	30.07.24	500	7	34.9507	34.9448	34.9469	5
PS132/2_062_01	30.07.24	1000	5	34.9124	34.9118	34.908	5
PS132/2_062_01	30.07.24	1000	5	34.9127	34.9118	34.908	5

Mooring recoveries and deployments

Recoveries

During expedition PS143/2, a total of 11 moorings were recovered in the central HAUSGARTEN area and close to East Greenland (Fig. 4.4, Tab. 4.5). A total of 7 of these moorings were deployed in the summer of 2022 (during PS131) thus in the water and measuring for 2 years; 3 were deployed in the summer of 2023 (during PS136) thus measuring for 1 year; while a short-term mooring (F4-W-5-ST) was deployed at beginning of PS143/2 and recovered towards the end of the cruise, measuring for a total of 3 weeks. A further 2 long-term landers were recovered, both which had been deployed in 2023.

A total of 101 instruments (hydrographic and biological) were recovered without major complications with minimal instrument loss (5 lost and 8 which did not record as programmed; a total of 12% of the deployed instrumentation). The lost instrumentation was due to a combination of assumed trawling activity near Svalbard (F4-OZE-3) in which the line containing an AZFP and Sonovault (and floats) was cut, and two near-bottom instruments (a SBE37 and RCM11, and two acoustic releasers) on HG-IV-FEVI-46 which were lost during recovery. Primarily, the instruments which did not record as programmed were due to instrument, not programming, error. These instruments in particular will be examined and testing further, either at AWI or sent to the respective manufacturers.

Upon recovery, there were some line entanglements towards the bottom of several moorings, particularly HG-IV-FEVI46. This was due to little wind which kept the ship and floats relatively

stationary and allowed the loose line between the sediment traps to rise into itself. This did not damage the instruments, merely slowed down the recovery process.

The winch and profiler on F4-W-5-ST were recovered by Zodiac at the end of the cruise, having been released separately to the bottom part of the mooring. The second part of the mooring, of which was composed of line and floats, was recovered in the usual way over the side of the ship. The recovered winch system on F4-W-5-ST did not appear to have worked over the 3-week deployment as programmed, as the top profiler was first observed on the surface when arriving at the station, and had not spooled back down to the winch itself as programmed. Upon first inspection, it appears that the winch itself was in working order; the issue was with the programme. Further examination found that the winch has successfully completed one profile but failed to re-spool. More tests are necessary to determine the exact reason and how to improve this, though this result was, to an extent, anticipated. One of the reasons for deploying this 'short-term' (ST) winch system was to get much faster feedback if the winch system was indeed working as planned instead of waiting until the following summer and its recovery. By then, it would be also too late to correct any mistake found before the next deployment. In this sense, the mooring itself was a success despite the lack of data.

Almost all hydrographic instrumentation and the ADCPs that were downloaded onboard after recovery appeared to have sampled continuously over the respective deployment periods. Not every instrument on the moorings deployed in 2022 lasted throughout the two-year duration, presumably due to battery failure. Interestingly, the hydrographic instruments deployed on HG-EGC-8, which were programmed to run for one year but were deployed for 2 years, all measured successfully for the whole two years they were in the water.

There was little to no sea ice at any of the mooring stations, including on the East Greenland continental shelf (HG-EGC-8 and HG-EGC-9), contrary to the very thick ice cover during their deployments in 2022 and 2023 respectively which prohibited the recovery of HG-EGC-8 in 2023. For all mooring activities, the sea state was generally very calm though visibility poor (between 100 – 500 m). The ocean conditions were ideal for mooring recovery, and contribute to the high success rate of instrument recovery.

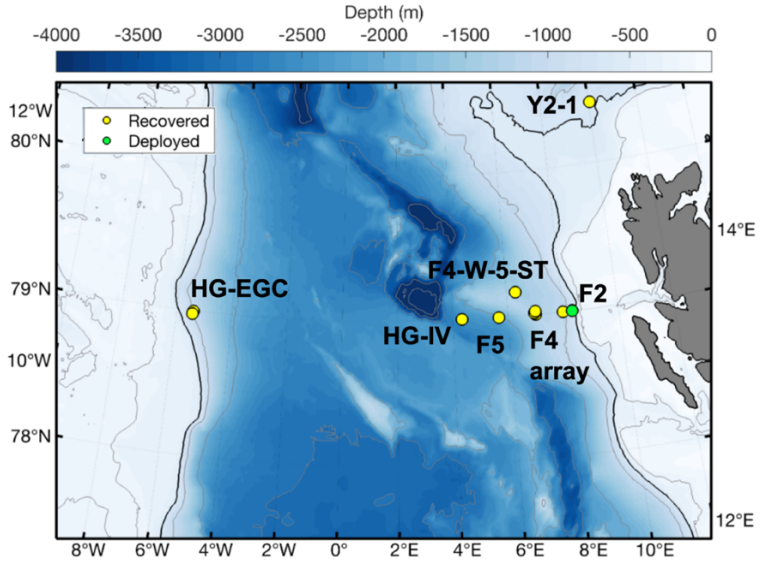

Fig. 4.4: Summary of the location of all the mooring recoveries (yellow) and deployments (green) over the course of PS143/2. Details of each mooring can be found in Tab. 4.5.

Deployments

Over the course of the cruise, a total of 10 moorings were deployed (Tab. 4.4). Most of these moorings were deployed at the typical central HAUSGARTEN stations and near East Greenland, continuing the long-term observations there (Fig. 2.1). Generally minor modifications in the placement of sensors were made during deployment, particularly in the upper 250 m, to better resolve the physical and biological structure of the upper water column. One long-term lander was also deployed, equipped with a current meter and camera to measure for one year.

An additional set of moorings were also deployed at the F4 location during PS143/2. The standard cluster at F4 is 3 moorings placed 1,400 m apart in a triangle formation (namely F4-22, F4-S-8, and F4-W-5); this was increased to a total of 5 moorings, including the short-term winch (F4-W-5-ST) and F4-H-1, during the cruise. On the three non-winch moorings, hydrographic sensors were placed with a high vertical resolution of 20 m apart, from 50 m down to 250 m where an ADCP was located, in order to capture buoyancy and velocity gradients in the Atlantic Water layer. A measuring device (‘Messrad’) was used to ensure a consistent 20 m depth difference between each instrument. From these instruments, horizontal gradients can be well-resolved in order to track mesoscale/sub-mesoscale eddy activity in the West Spitsbergen Current. After the recovery of F4-W-5-ST at the end of the cruise, the F4 cluster remains as 4 moorings in the water; F4-22 will be recovered in summer 2026 while the rest will be recovered next summer in 2025.

The sea state was generally very calm throughout the deployments and little to no sea ice at each station. There were no issues with instruments or line during any of the deployments.

Tab. 4.4: Summary of all the mooring stations for both deployments and recoveries during PS143/2

Name	Longitude		Latitude		Depth	Top	Deployment time UTC					Deployment station	Recovery time UTC					Recovery station
	Degrees	Minutes	Degrees	Minutes	Meters	Meters	Year	Month	Day	Hour	Minute		Year	Month	Day	Hour	Minute	
Recoveries																		
F2-21	8	19.91 E	79	0.01 N	786	20	2022	7	8	15	52	PS131_25-1	2024	7	18	8	32	PS143_2_013_01
F3-20	7	59.93 E	78	59.98 N	1074	38	2022	7	8	13	42	PS131_24-1	2024	7	19	8	47	PS143_2_017_01
F4-21	7	0.03 E	79	0.02 N	1224	50	2022	7	7	8	54	PS131_15-1	2024	7	16	5	47	PS143_2_005_01
F4-OZA-3	6	19.91 E	79	10.00 N	1416	89	2022	7	8	9	33	PS131_23-1	2024	7	20	8	45	PS143_2_020_01
F4-S-7	6	57.75 E	79	00.67 N	1253	20	2023	6	6	21	23	PS136_020_01	2024	7	15	5	33	PS143_2_001_03
F5-20	5	39.97 E	79	0.02 N	2091	34	2022	7	7	16	25	PS131_17-1	2024	7	30	10	30	PS143_2_061_01
HG-IV-FEVI-46	4	19.77 E	78	59.95 N	2599	39	2023	6	1	9	20	PS136_008_02	2024	7	29	14	40	PS143_2_059_01
HG-EGC-8	5	23.74 W	78	59.78 N	1011	47	2022	8	3	17	37	PS131_106-1	2024	7	27	10	39	PS143_2_056_01
HG-EGC-9	5	25.65 W	78	58.72 N	979	48	2023	6	13	16	4	PS136_033_07	2024	7	27	7	39	PS143_2_055_01
Y2-1	10	3.65 E	80	25.00 N	693	128	2022	7	18	9	53	PS131_59-1	2024	7	24	7	22	PS143_2_039_01
F4-W-5-ST	7	0.06 E	79	1.41 N	1243	110	2024	7	16	11	39	PS143_2_006_01	2024	7	31	6	4	PS143_2_065_01
LT-Lander-2023	4	13.33 E	79	1.86 N	2516	2514	2023	6	15	23	52	PS136_038_01	2024	7	21	7	35	PS143_2_022_09
ArcFoce-Lander	4	52.91 E	79	8.11 N	1493	1491	2023	6	15	21	33	PS136_037_01	2024	7	30	7	26	PS143_2_060_02
Deployments																		
F2-22	8	19.88 E	79	0.03 N	773	23	2024	7	19	8	7	PS143_2_016_01						
F3-21	7	59.74 E	79	0.13 N	1061	43	2024	7	19	14	15	PS143_2_017_02						
F4-22	7	0.04 E	79	0.01 N	1197	47	2024	7	17	13	38	PS143_2_009_01						
F4-S-8	7	2.05 E	79	0.70 N	1222	19	2024	7	17	16	50	PS143_2_010_01						
F4-W-5	6	58.02 E	79	0.71 N	1213	134	2024	7	20	14	20	PS143_2_021_01						
F4-H-1	7	4.05 E	79	0.02 N	1221	38	2024	7	17	9	39	PS143_2_008_01						
F4-W-5-ST	7	0.06 E	79	1.41 N	1243	111	2024	7	16	11	39	PS143_2_006_01						
F5-21	5	40.03 E	79	0.01 N	2068	44	2024	7	30	15	46	PS143_2_061_02						
HG-IV-FEVI-48	4	19.91 E	79	0.00 N	2531	34	2024	7	29	19	40	PS143_2_059_02						
HG-EGC-10	5	23.83 W	78	59.78 N	979	49	2024	7	28	8	16	PS143_2_057_01						
LT-Lander-2024	4	13.40 E	79	1.86 N	2526	2524	2024	7	29	20	33	PS143_2_059_03						

Recovery of moored acoustic recorders

Three passive acoustic recorders (SV1097, SV1391, SV1088) moored at different locations (F4-21, F5-20, Y2-01) were successfully recovered (Tab. 4.5). An attempt was also made to recover a fourth recorder (SV1387) moored at F04-OZA3. However, during the recovery

process, it became apparent that the top part of the mooring, including the recorder, was missing, suggesting it had been torn off prior to recovery. The recorders were all SonoVaults (manufactured by Develogic GmbH, Hamburg). While SV1097 and SV1088 were standard SonoVault underwater acoustic recorders with RESON TC4037 hydrophones, SV1391 was a new version with an active HTI-96-min (exportable) hydrophone. This version uses two external battery packs attached to a pressure case containing the recorder electronics and the hydrophone. All of them had been deployed during *Polarstern* expedition PS131. Deployment positions of the recorders are marked in Fig. 4.5.

Tab. 4.5: Recovery information for the different recorders. Note the SV1387 could not be recovered as part of the mooring including the device was torn off prior to recovery.

Recorder SN/Type	Mooring	Deployment date	Recovery date	Recording period	Sampling frequency /kHz	Comment
SV1097 standard	F4-21	07.07.2022	16.07.2024	01.07.2022 – 04.08.2023	48	
SV1387 standard	F4-OZA3	08.07.2022	(20.07.2024)	-	48	Upper part of mooring including the recorder ripped off prior to recovery
SV1088 standard	Y2-01	18.07.2022	24.07.2024	16.07.2022 – 23.07.2023	96	Data contain electronic Noise
SV1391 HTI	F5-20	07.07.2022	31.07.2024	01.07.2022 – 07.07.2023	96	

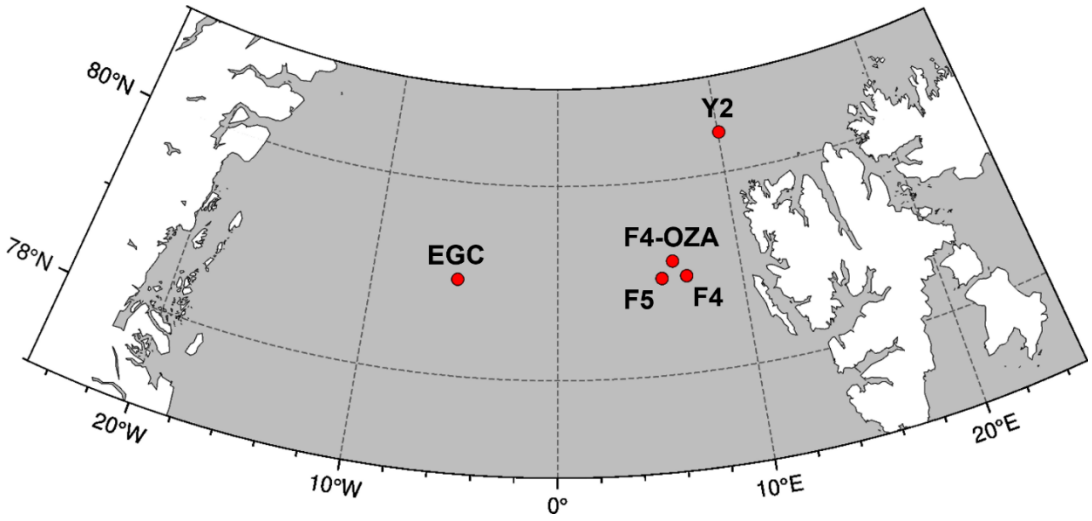

Fig. 4.5: Mooring positions for recorders recovered/deployed during PS143/2

After recovery, the acoustic recorders were rinsed with freshwater to remove biological fouling. If possible, the status of the recovered recorders was checked by connecting them to a laptop via a serial connection and using the 'Develogic Device Control' software (Version 1.0.4.26525, provided by the manufacturer). The recorders were then left to dry for at least one day to prevent damage to the electronics from any water trapped in the threading of the recorder's housing. The areas around the sealed openings were carefully dried with compressed air and tissues before opening.

Once opened, all SD cards, which had been labeled prior to deployment with the recorder's serial number, the recording module number, and the SD card slot, were removed and backed up. The acoustic data were copied using a custom-written Python script. Up to eight SD cards were copied simultaneously, with the data saved into monthly and daily folders on two 10 TB WD Red HDD drive and one 4 TB Sans Disk Extreme Portable SSD. The backup process included renaming the files based on each file's internal timestamp (WAV header) to the format 'YYYYMMDD-HHMMSS_ARKXXX-ZZ_SVXXXX.wav' (with X representing the IDs of the mooring and SonoVault recorder, respectively, and Z indicating the consecutive numbering of this mooring, i.e., the number of the current servicing cycle at a respective mooring).

Deployment of moored acoustic recorders

Three SonoVault recorders (SV1095, SV1096, SV1389) were deployed in three moorings (F4-22, EGC-10, F5-21) during PS143_2 (Fig. 4.4, Fig. 4.5, Tab. 4.6). Prior to the deployment, newly formatted SD cards were placed into the SD card slots on each recording module. Each recorder contains 35 SD cards. SD-card sizes were chosen based on the required total storage capacity resulting from planned deployment duration and sampling frequency. Total storage capacities are listed alongside the sampling settings in the table below. Data is stored with 24-bit resolution and a file length of 600 seconds duration (Tab. 4.6). In addition to the recorders, two AZFPs were deployed: the first (AZFP 55112) at F4-22, and the second (AZFP 55183) at F5-21.

Tab. 4.6: Deployment information for different recorders

Recorder SN/Type	Mooring	Deployment date	Sampling frequency /kHz	Sampling scheme	Total storage /TB	approx. storage capacity /year(s)	Comment
SV1095 standard	F4-22	17.07.2024	96	30min ON / 30min OFF; Start on 2024-07-11 00:00	5.50	1.21	Secured with an additional rope to the mooring line to prevent slipping
SV1096 standard	EGC-10	28.07.2024	48	continuously	8.75	1.93	
SV1389 HTI	F5-21	30.07.2024	48	continuously	9.50	2.09	In the first file the signal needs approx. 15s until it is stable

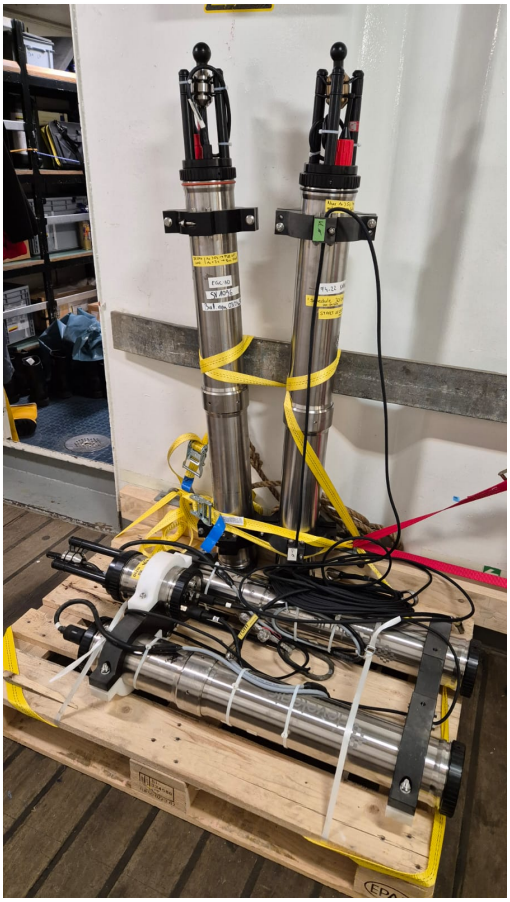

Fig. 4.6: Passive acoustic recorders deployed during PS143/2

Fig. 4.7: SV1095 prior to deployment. The recorder was secured with an additional rope to the mooring line to prevent slipping.

Vessel mounted ADCP

From 12 July 2024 17:59 to 05 August 2024 15:53 we measured profiles of ocean current velocity in the upper 350 m while underway with a vessel-mounted Acoustic Doppler Current Profiler (VMADCP). The RDI Ocean Surveyor instrument (150 kHz) was mounted in the 'Kastenkiel' of *Polarstern*. The instrument was configured in narrowband mode and set up to use 4 m bin size (configuration file cmd_OS150NB_trigger_off.txt as shown in Tab. 4.8), covering a range from 20 m to about 300 m.

Overall, the system worked without major problems, but there were software issues that resulted in data gaps between 19/07/2024 13:20:00 - 15:30:00 and 23/07/2024 13:20:00 - 13:50:00. The data were collected in data files (.ENX, *.ENR, *.ENS, *.N1R, *.N2R, *.NMS, *.STA, *.LTA, *.VMO, *.LOG). The format is 'Filename' followed by a three digit file number. The file names for the corresponding data are listed in Tab. 4.7.

The setup of navigational input was used from the vessel's GPS system. The software VmDas (Teledyne RD Instruments) was used to set the ADCP's operating parameters and to record the data. Finally, the data conversion was done using Matlab routines of the Ocean Surveyor Sputum Interpreter (OSSI) (osheader.m, osdatasip.m, osrefine.m, osbottom.m). Hereby the VMADCP data was corrected by using a misalignment angle of 0.3810 degrees and an amplitude factor of 1.007638 (Fig. 4.8 and 4.9).

The data was reviewed during the cruise and no data quality issues were identified. The first three pings as well as the last pings may have to be excluded from further data analysis as they show signs of unreliable quality. Several transects were made through the Fram Strait, resulting in ADCP data recorded at approximately the same latitude. One of the transects at 79°N is shown in Fig. 4.9. As far as can be judged, the directions of the currents are as expected. The first three pings and pings deeper than 250 m were excluded as they showed signs of unreliable quality.

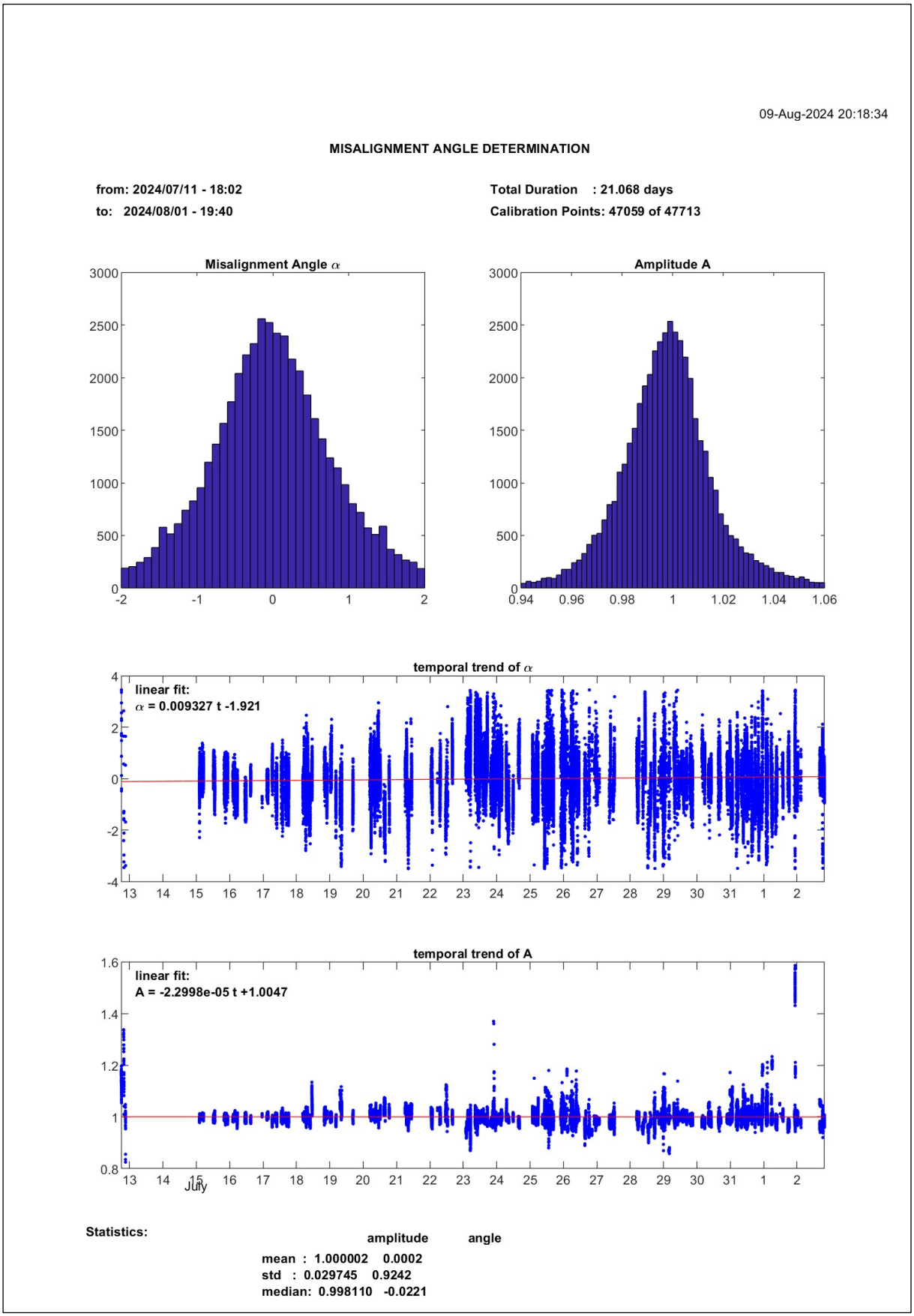

Fig. 4.8: Misalignment determination

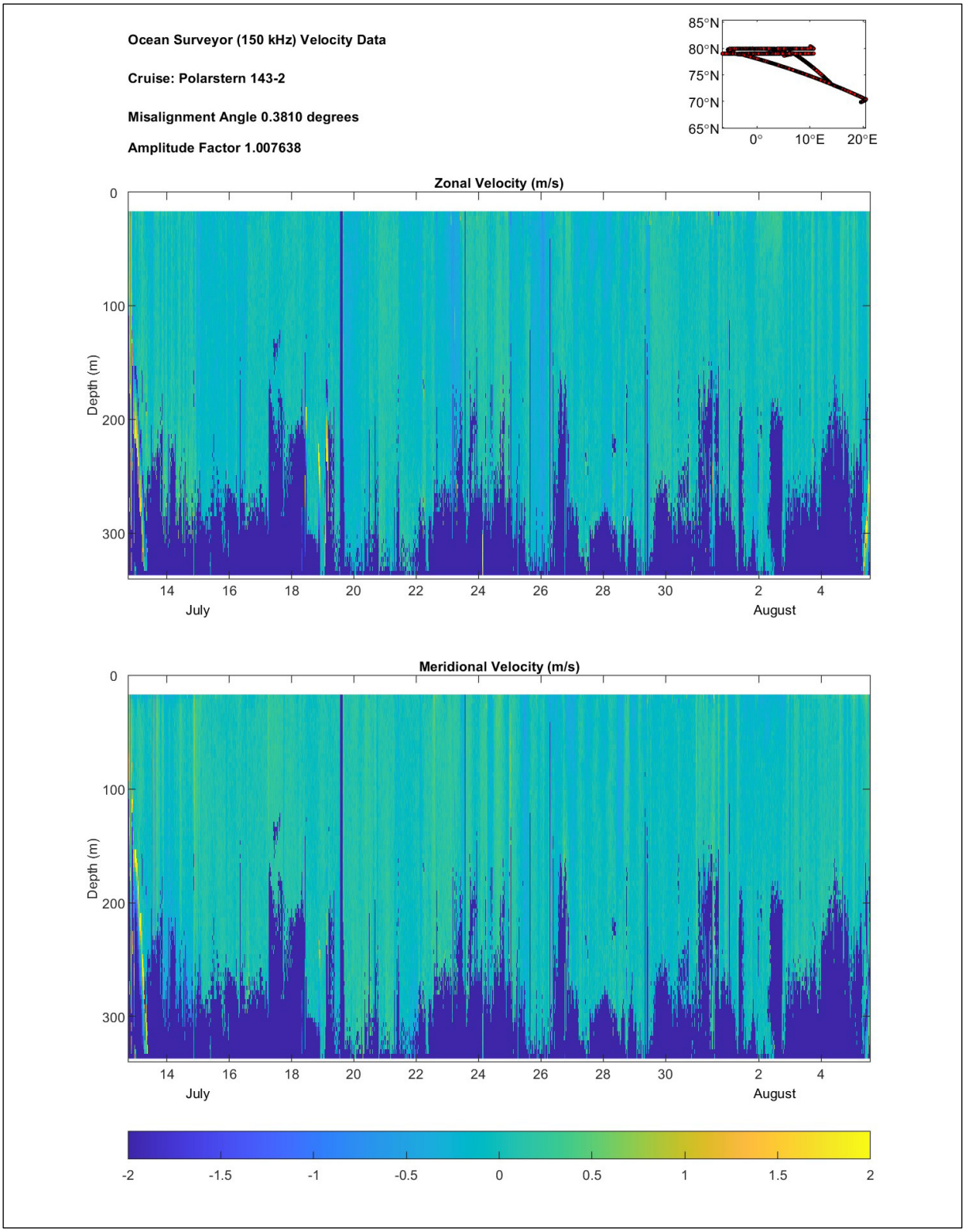

Fig. 4.9: Resulting ocean velocities [m s^{-1}] during PS143/2

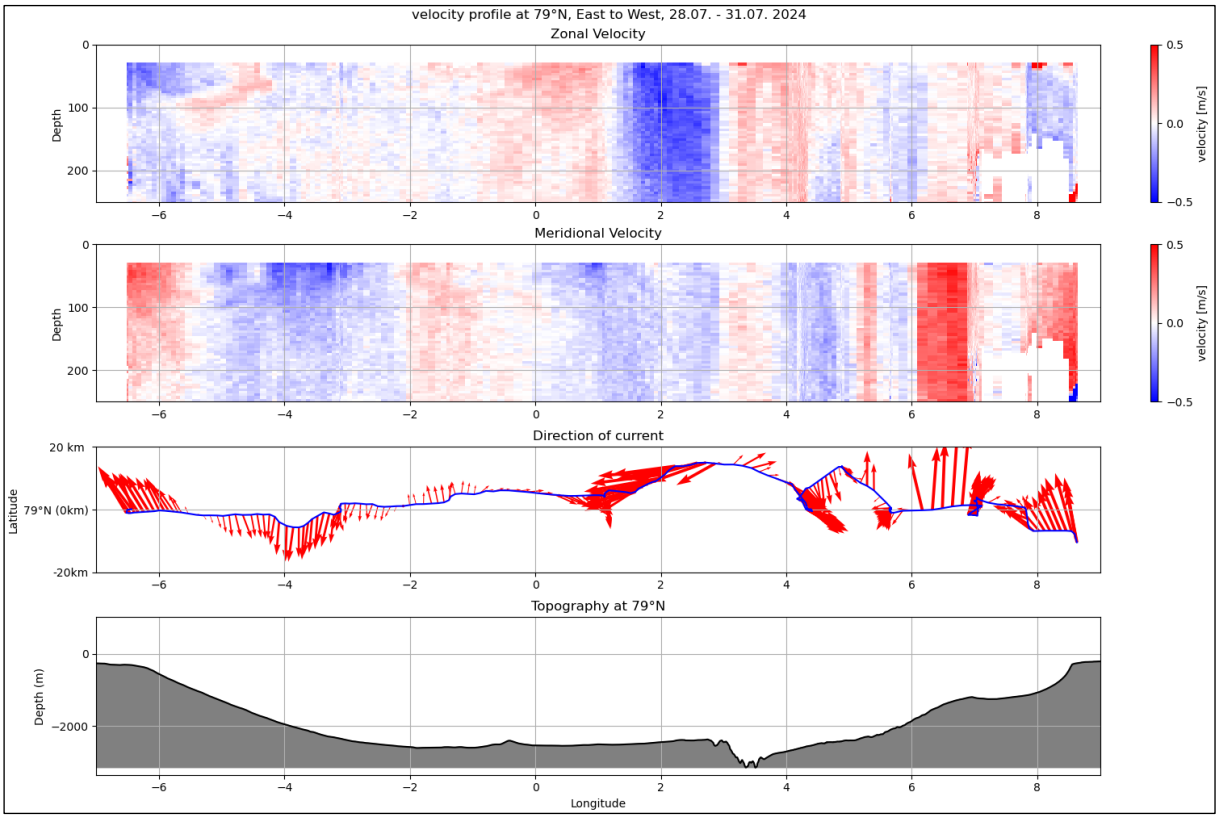

Fig. 4.10: Velocity profile at 79°N, recorded between 28.07.2024 – 31.07.2024 from east to west

Tab. 4.7: VMADCP command file cmd_OS150NB_trigger_off.txt

```
;-------------------------------------------------------------------------\
; ADCP Command File for use with VmDas software.
;
; ADCP type:      150 Khz Ocean Surveyor
; Setup name:     for Polarstern in 6/2014
; Setup type:     Low resolution, long range profile (Narrowband)
;
; NOTE:  Any line beginning with a semicolon in the first
;        column is treated as a comment and is ignored by
;        the VmDas software.
;
; NOTE:  This file is best viewed with a fixed-point font (e.g. courier).
; Modified Last: 12Jun2014
;-------------------------------------------------------------------------/

; Restore factory default settings in the ADCP
cr1
```

```
; set the data collection baud rate to 9600 bps,
; no parity, one stop bit, 8 data bits
; NOTE:  VmDas sends baud rate change command after all other commands in
; this file, so that it is not made permanent by a CK command.
cb411

; Set for narrowband single-ping profile mode (NP), 100 (NN) 4 meter bins (NS),
; 2 meter blanking distance (NF), 390 cm/s ambiguity vel (WV)
WP000
NP001
NN080
NS0400
NF0400
;WV390

; Disable single-ping bottom track (BP),
; Set maximum bottom search depth to 1200 meters (BX)
BP000
;BX12000

; output velocity, correlation, echo intensity, percent good
ND111100000

; Ping as fast as possible
TP000000

; Since VmDas uses manual pinging, TE is ignored by the ADCP
; and should not be set.
;TE00000000

; Set to calculate speed-of-sound, no depth sensor, external synchro heading
; sensor,  pitch or roll being used, no salinity sensor, use internal transducer
; temperature sensor
EZ1011101

; Output beam data (rotations are done in software)
EX00000

; Set transducer misalignment (hundredths of degrees).
```

```
; Ignored here but set in VmDAS options·
;EA000000

; Set transducer depth (decimeters)
ED00110

; Set Salinity (ppt)
ES35

;set external triggering and output trigger; no trigger
CX0,0

;set external triggering and output trigger
;CX1,3

; save this setup to non-volatile memory in the ADCP
CK
```

Tab. 4.8: Filenames and collected times

Filename	Time [UTC]	Comments
Werft_Test_2024002_000	12-07-2024 17:59 – 14-07-2024 13:19	
PS_143_2_002_000	14-07-2024 13:20 – 16-07-2024 18:04	
PS_143_2_003_000	16-07-2024 18:05 – 24-07-2024 05:24	Data gaps: 19.07.2024 13:20:00 – 15:30:00 23.07.2024 13:20:00 – 13:50:00
PS_143_2_004_000	24-07-2024 05:25 – 28-07-2024 01:29	
PS_143_2_005_000	28-07-2024 01:30 – 28-07-2024 22:29	
PS_143_2_006_000	28-07-2024 22:30 03-08-2024 18:36	
PS_143_2_007_000	03-08-2024 18:37 – 05-08-2024 13:53	

Triaxus towed ocean profiler of the AWI (topAWI)

The remotely operated towed vehicle Triaxus from MacArtney serves as a platform for multiple instruments and allows gathering a high-resolution dataset. The system is towed behind the ship either in a saw-tooth pattern or at a constant depth. The planned use of the system for expedition PS143/2 was to measure several high-resolution transects between Svalbard and East Greenland. This goal could not be achieved due to several successive system errors that occurred during the expedition.

Due to a damage of the towed body in 2022, a repair at the manufacturer was necessary before the cruise, which was also used for necessary maintenance work. After a one-year contract assignment process in 2023, it was promised that the system would be returned from repair and service in February 2024. The actual delivery of the system was at the end of May 2024, one week before the freight deadline for *Polarstern*. As a result, the system could not be tested in advance of the expedition.

Chronological timeline of repair

14.07.2024: First pre-dive check

Detection of a fault in the high-voltage supply due to a negative self-test of the Isometer. The pre-dive check was cancelled prematurely due to the personal danger of error. After two days of troubleshooting, a fault high-voltage relay was diagnosed as the cause and the corresponding fault was repaired.

16.07.2024: Preparation for deployment

In preparation for the first deployment, the ballasting of the system was checked. A further pre-dive check was executed to prepare the system for deployment, which had to be cancelled quickly after a fault location due to excessive power consumption when the system was switched on. After one day of troubleshooting, a polarity reversal of the high-voltage supply was identified and adjusted, which might be happen during winch maintenance at the manufacturer.

18.07.2024: Checking the system after polarity reversal

After correcting the polarity reversal error, the system was checked for errors in the 4th pre-dive check. After switching on the towing system, the power consumption was within the expected range. However, when the motor control system was checked, a malfunction was detected in the entire motor electronics. After six days of troubleshooting with the support of several colleagues and consultation with the manufacturer, a defect in the motor distribution, the motor controller and the motor feedback of one of the five motors was identified as the cause and the corresponding components were replaced. Due to the lack of measurability and the limited options for action on our part by the manufacturer, several iteration steps with associated pre-dive checks were necessary.

26/27.07.2024: Establishment of operational readiness

In collaboration with five colleagues, the system was made ready for use and the first successful pre-dive check was carried out. Also, all sensors were checked for deployment.

28.07.2024: First deployment

After the 11th pre-dive check, the system was deployed for the first time together with the new depressor. After a brief check of all functions, all sensors were switched on and the first scientific measurement was carried out. After approx. 6 hours, the deployment had to be cancelled due to communication problems called "Downlink Error" and the system had to be recovered for safety reasons.

30.07.2024: "Downlink error" check

After the communication error did not occur again during the 12th pre-dive check and a test run lasting several hours (error frequency on 28 July 2024 from a few hours to a few seconds), all components that could be replaced in one day and could have a connection to the error, were replaced and the system was then checked with a successful pre-dive check.

31.07.2024: Second deployment

After an error-free 14th pre-dive check, the system was launched at station 66_1. When switching on the sensors, an error occurred in the primary conductivity sensor of the CTD, which also controls the pumps, so that the CTD could not measure. However, this error was not repaired, as after two hours of operation the communication error "Downlink Error", again led to the operation being cancelled. Due to the limited time available, the error could not be found or repaired before the end of the expedition and therefore the system cannot be used again.

Tab. 4.10: Details of the Triaxus deployments during PS143/2

dive	name	Syear	Smonth	Sday	Shour	Sminute	Eyear	Emonth	Eday	Ehour	Eminute	SLonDeg	SLonMin	SLonEW	SLatDeg	SLatMin	SLatNS	ELonDeg	ELonMin	ELonEW	ELatDeg	ELatMin	ELatNS	cable	minz	maxz	station	comment
1	EGC_test	2024	7	28	13	26	2024	7	28	19	43	5	25.60	W	79	8.08	N	5	40.73	W	78	59.47	N	1050	10	250	058_01	downlink error
2	WSC_test	2024	7	31	10	8	2024	7	31	12	28	7	49.81	E	78	59.26	N	8	38.08	E	78	53.65	N	1000	10	250	066_01	downlink error

Sea Ice Monitoring System (SIMS)

Fig. 4.11: Setup of the SIMS in front of Polarstern

To resolve the ice thickness variability and gradients and their temporal change across the MIZ, we used the Sea Ice Monitoring System (Haas 1998) deployed off an aluminium beam on the bow of *Polarstern* (Fig. 4.11). The SIMS measures ice thickness continuously along the ship's track by calulating the difference of distance measurements to the Ice surface and to the salt water underneath the ice. The distance to the ice surface is measured with an ultrasonic ranger (Senix Corp., ToughSonic 30) and the distance to the salt water is inferred from measurements with an electromagnetic induction sounder (Geonics Ltd., EM-31 MK2). Additionally surface Albedo information and GPS data has been recorded and storded with the sea ice thickness data. The SIMS was operated from the 22 July 12:30 UTC until the 1 August 14:00 UTC with a recording frquenuency of 1Hz. The instrument recorded continuously without any major breaks or problems. The System could not be started before entering the MIZ because of technical difficulties with the EM sounder and had to be stopped before leaving the MIZ, where minimal swell garantied easier crane operation.

Ice Observation Camera

A surveillance camera (Reolink, W430) was installed directly at the ship's bow overlooking the SIMS and the ice underneath and ahead (see Fig. 4.12). Between 20 July 01:48 and 1 August 14:03 a photograph was taken every two seconds. The timelapse has two data gaps. From the 20 July 5:54 until 21 July 03:09 the camera was not supplied with power and from 23 July 11:26 until 24 July 10:41 the power adapter was broken because of a humidity induced shortage. Due to foggy conditions images can be blurred by sleet or rain drops on the lens.

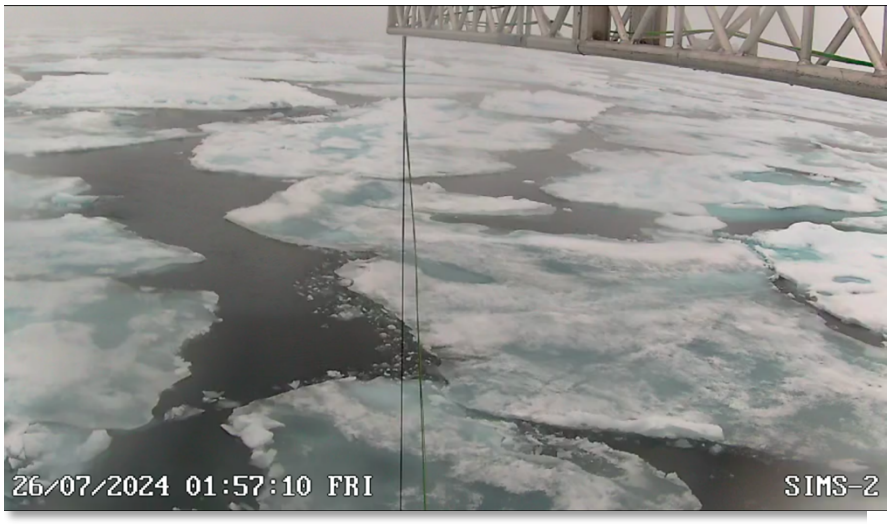

Fig. 4.12: Image taken from the bow of Polarstern on 26 July at 01:57:10 UTC

Preliminary results

CTD/Rosette Water Sampler

A high-resolution transect (N5TE) had been conducted along 79.95°N from 3.12°E toward the continental shelf of west Svalbard (Fig. 4.1) covering the WSC and presumably its multiple branches. An intense signature in temperature accompanied by an intermediate maximum in salinity might indicate the inner branch. A series of "yo-yo" casts (Niskin bottles are kept open during the upcast) was performed until reaching an anticyclonic structure of sea ice, which had been observed via satellite images the days before and aimed for to do a biological station.

The crossing of this ice structure is indicated by a surface layer of cold and fresh water with a reaching down to around 100m depth. After mooring work further in the north and an additional biological station positioned around the second last station of N5TE, the transect was extended to the west by N5TW. This half of the transect captured a distinct layer of cold and fresh PW, the boundary layer of the AW and its eastern restriction. A strong subsurface thermohaline frontal structure could be observed (Fig. 4.13). Note the temporal gap between station 25 and 41. Approaching the end of N5TW multiple casts were cancelled due to time reasons leading to a distinct spatial gap between station 53 and 54. A second westward CTD transect (not shown) with a spatial spacing of 18 nm between casts was intiated on 31 July along 78.98°N after a failed operation of the topAWI. For further information on the CTD casts outside of these transects, refer to Tab. 4.2.

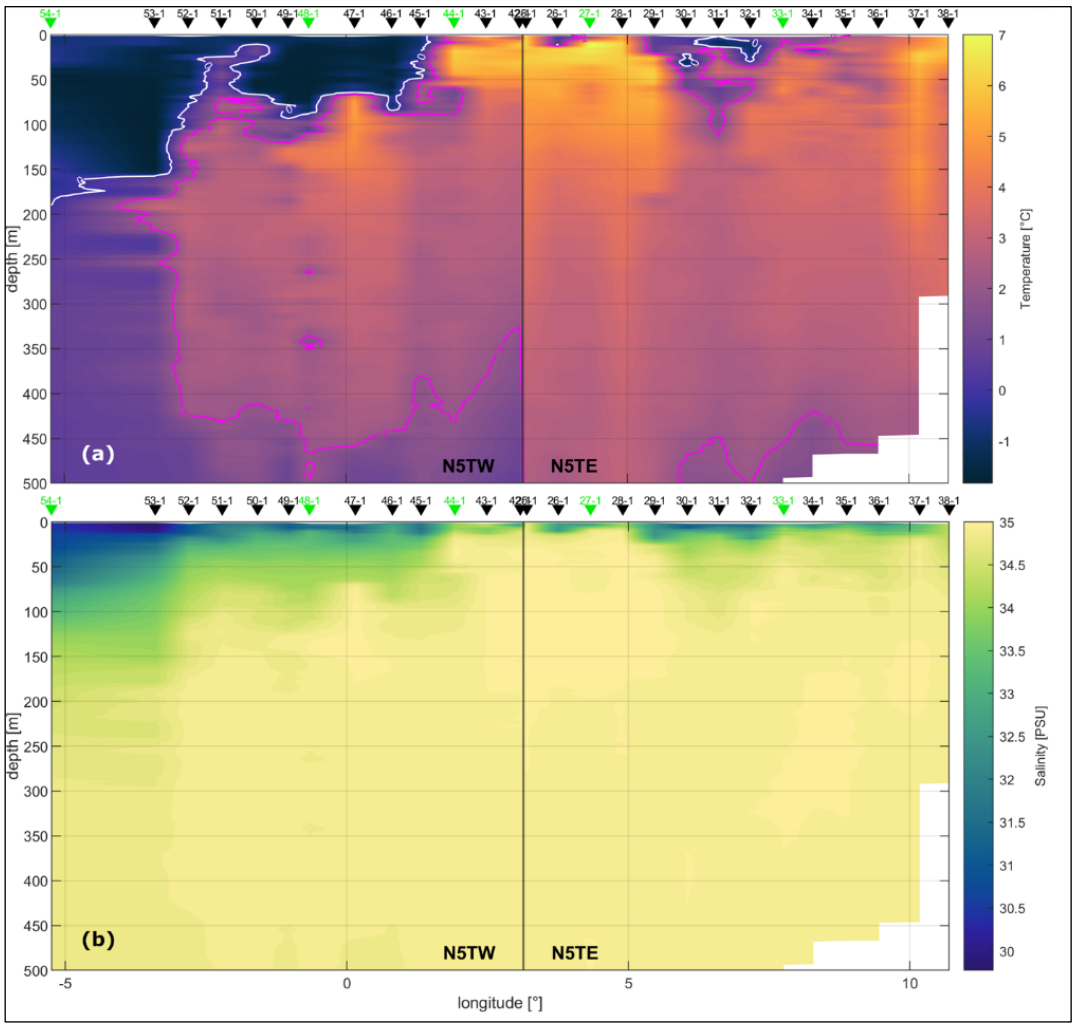

Fig. 4.13: Hydrographic section along 79.95°N for (a) temperature in [°C] with the white and pink contour indicating the 0°C- and 2°C-isotherm, respectively, and for (b) salinity in [PSU]. The scatters on top mark the actual positions of the CTD casts. Furthermore, green scatters represent the Bio-stations. The vertical grey line indicates the temporal gap between the start of N5TE and N5TW.

Moorings

The mooring work conducted during PS143/2 are part of a long-term observation campaign, mainly focused with measuring the changes and variability of the hydrography, biology and biogeochemistry in West Spitsbergen Current (WSC) from seasonal to decadal timescales. The WSC carries warm, saline water from the North Atlantic into Fram Strait. Approximately half of the warm Atlantic Water (AW) that flows northwards in the WSC is recirculated westwards across Fram Strait towards East Greenland; the rest continues northwards and enters the central Arctic Ocea. The AW in the WSC is the major source of oceanic heat and salt for the Arctic Ocean and changes in the properties of the AW inflow strongly influence both ocean and sea ice conditions there.

The mooring F2 is stationed in the core of the WSC which follows the continental shelf of Svalbard and primarily carries the inflow of AW into the central Arctic Ocean. Records in the near-surface, at 22 m, show a pronounced seasonal cycle of the AW (Fig. 4.14). Towards the end of the summer months, temperatures peak between July and October up to almost 8°C with a corresponding highly variable freshening signal. At the end of the winter months, between March and April, temperatures decrease towards 2°C and have a stable, high salinity value. The strength of the inflow can be inferred from the changing depth of the instrument, with vertical mooring motion (‘knockdowns’) due to strong horizontal currents. The largest knockdowns occurred during the winter months, often reaching 100 m, indicating a stronger flow than during summer where knockdowns were generally much weaker (about 20 m).

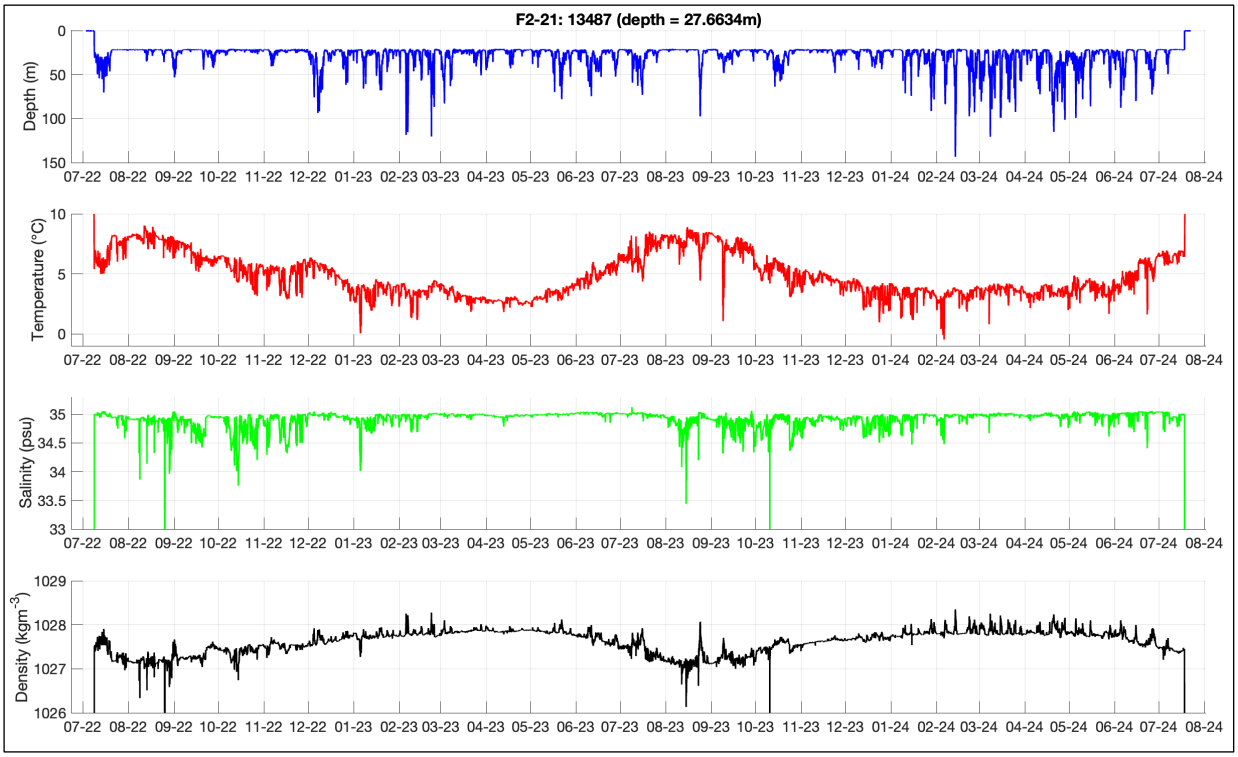

Fig. 4.14: Measurements from a two-year record of (from top to bottom) pressure, temperature, salinity and density from a SBE37 at 27 m depth on mooring F2-21

The current velocities at F2 show a dominant northwards direction of the core of the WSC (Fig. 4.15), where it flows close to the eastern continental shelf edge. This is contrary to the flow at F4, which sits in the offshore branch of the WSC (Fig. 4.15) and reveals a more variable flow

direction, illustrated by the wide spread of the current ellipses which represent a diverse range of current directions.

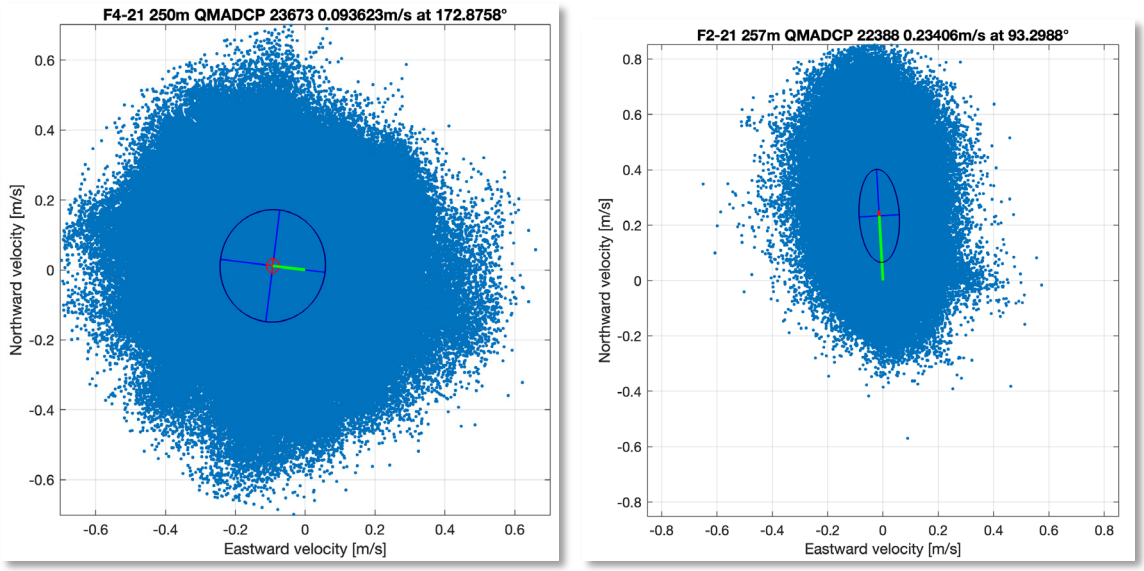

Fig. 4.15. Scatterplots of velocities from ADCPs at 250 m deep in the WSC at (left) F4 (offshore branch) and (right) F2 (WSC core). The green lines represent the mean current speed and direction, with the black ellipse indicating the standard deviation.

Over the last 25 years of observations, a long-term warming trend of the Atlantic Water in the WSC has emerged. From 1997 to 2022, the AW has warmed by a total of almost 1°C, corresponding to an increase of 0.31°C/decade. Thus, it is anticipated that the temperature records from the mooring recoveries in the boundary current, when combined with the previous records, will also show a continued warming trend.

Thermosalinograph

The thermosalinograph was operated continuously during the cruise. Standard settings were used. The data were screened during the cruise and no significant problems were identified.

The salinity and temperature distribution in the Fram Strait is shown in Fig. 4.16. As expected, the western part of the Fram Strait shows colder and less saline water from the arctic ocean, while in the eastern part the water is more saline and warmer, as expected from Atlantic water

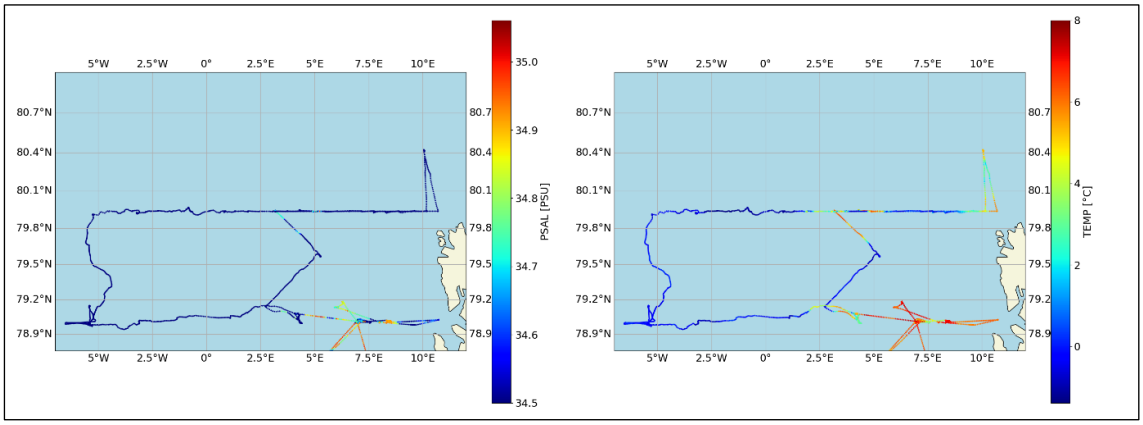

Fig. 4.16: Temperature and salinity distribution in the Fram Strait measured by the thermosalinograph during PS 143/2

Sea ice coverage

During PS143/2 two dedicated east west Transects in the Fram Strait were conducted with the SIMS to collect data on the sea-ice coverage. In Fig. 4.17 sea ice data from the 80° North transect is shown. Ice concentration correlates well with the ice visible on the SAR Image from the Copernicus Sentinal 1 mission captured on the 25 July 2024 at 07:04:41.084Z (Fig. 4.18), when *Polarstern* was approximately at 79.934 N and 1.915 E.

Sea Ice thickness distributions show the occurence of melting, first and multi year ice during the transect. (Fig. 4.17)
It must be mentioned that sea ice thickness measurements depend on the course the officer on duty navigates through the ice. Following leads and avoiding ice contact yields biased measurements. Therefore, short statements from the officer on duty have been documented, where general ice conditions and a subjective assessment of whether large ice floes, small ice floes, or all ice floes were circumnavigated, have been recorded.

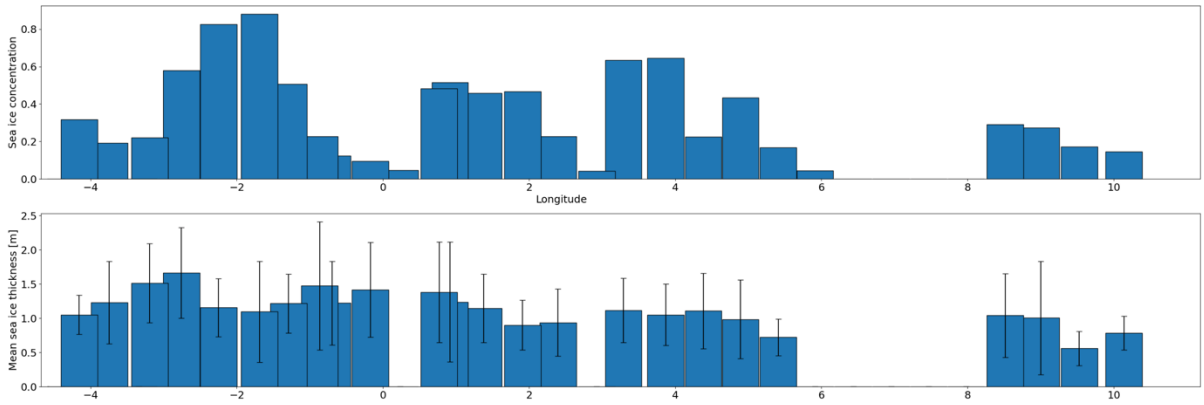

Fig. 4.17: Measured ice concentration and mean ice thickness of 10km sections along the 80°North Fram Strait transect

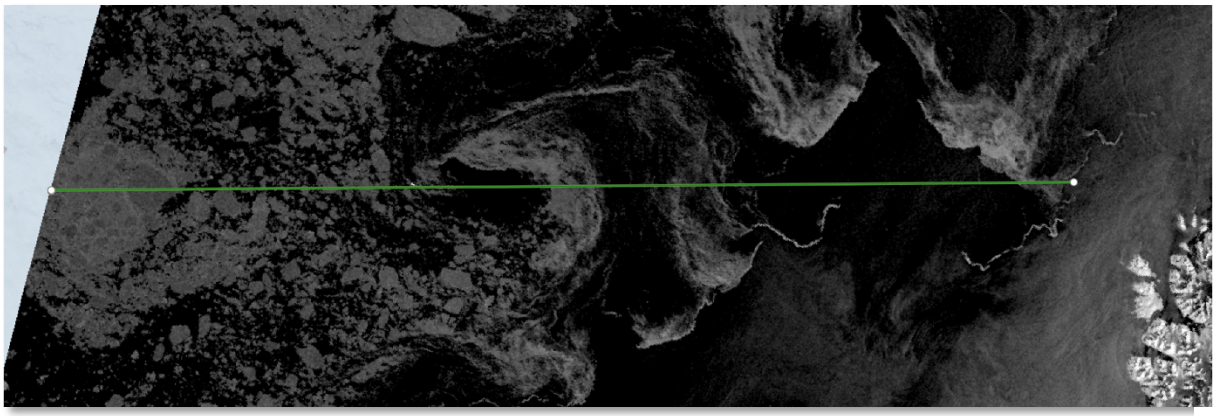

Fig. 4.18: SAR Image from the Copernicus Sentinal 1 mission captured on 25 July 2024 at 07:04:41.084Z

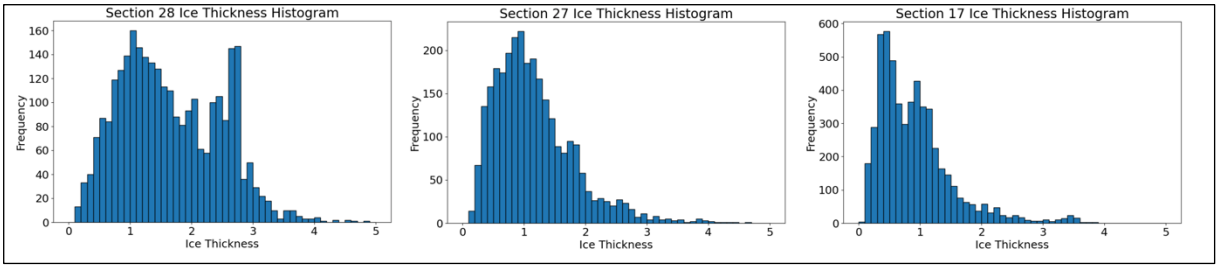

Fig. 4.19: Sea ice thickness distributions from 3 selected 10 km sections from the 80°North transect. The Sections 17, 27 and 28 are located around 1.9°E, 2.2°W and 2.8°W respectively.

Data management

All sensor data will be archived, published and disseminated according to international standards by the World Data Center PANGAEA Data Publisher for Earth & Environmental Science (https://www.pangaea.de) within two years after the end of the expedition at the latest. By default, the CC-BY license will be applied.

This expedition was supported by the Helmholtz Research Programme “Changing Earth – Sustaining our Future” Topic 2, Subtopic 1 and Topic 6, Subtopic 3.

In all publications based on this expedition, the **Grant No. AWI_ PS143/2_03** will be quoted and the following publication will be cited:

Alfred-Wegener-Institut Helmholtz-Zentrum für Polar- und Meeresforschung (2017) Polar Research and Supply Vessel POLARSTERN Operated by the Alfred-Wegener-Institute. Journal of large-scale research facilities, 3, A119. http://dx.doi.org/10.17815/jlsrf-3-163.

References

Haas C (1998) Evaluation of Ship-based electromagnetic–inductive thickness measurements of Summer Sea ice in the Bellingshausen and Amundsen Seas, Antarctica. Cold Reg. Sci. Technol., 27(1):1–16. https://doi.org/10.1016/S0165-232X(97)00019-0

5. PEBCAO – PLANKTON ECOLOGY AND BIOGEOCHEMISTRY IN THE CHANGING ARCTIC OCEAN

Barbara Niehoff[1], Celina Behrendt[1], Astrid Bracher[1], Magdalena Dolinkiewicz[1], Tabea Galonska[1], Christian Konrad[1], Kerstin Korte[1], Sophia Hirschmann[2], Christian Hohe[1], Tania Klüver[2], Ellen Oldenburg[1,3], Benjamin Pontiller[2], Ovidiu Popa[3], Marlis Reich[4], Ina Schmidt[5], Carolin Uhlir[1],

not on board: Felipe Artigas[6], Anja Engel[2], Morten Iversen[1], Alexandra Kraberg[1], Eva-Maria Nöthig[1]

[1]DE.AWI
[2]DE.GEOMAR
[3]DE.UniD
[4]DE.UniHB
[5]DE.UniHRO
[6]FR.CNRS-LOG ULCO

Grant-No. AWI_PS143/2_04

Outline

The Arctic Ocean has gained increasing attention in recent decades due to the drastic decrease in sea ice and increase in temperature at a rate, which is approximately twice as fast as the global average. It is also expected that ocean acidification will influence the chemical equilibrium and the elemental cycling in the surface ocean. The effects of such changes on the **P**lankton **E**cology and **B**iology in the **A**rctic **O**cean (PEBCAO) can be detected by long-term observations and process studies. The PEBCAO group began its studies on plankton ecology in the Fram Strait (~79°N) in 1991, intensified its efforts in 2009, and since 2014, PEBCAO is part of the FRAM (Frontiers in Arctic Monitoring) Ocean Observatory team and provide information on intra- and inter-annual variations in plankton ecology, biogeochemical parameters, and microbial (prokaryotic and eukaryotic) biodiversity. In a holistic approach, we combine classical bulk measurements of biogeochemical parameters, microscopy, optical methods, satellite observations, and molecular approaches. These measurements have been complemented by dedicated process studies in the Nansen and Amundsen Basin of the Central Arctic Ocean (CAO), and by participation in the MOSAiC drift experiment. We are also involved in the development and deployment of automatic platforms and sampling technology for long-term monitoring in the Arctic Ocean with a focus on the LTER HAUSGARTEN.

Our long-term observations in Fram Strait revealed changes in productivity and biodiversity. For instance, the chlorophyll-a (Chl *a*) values in summer increased in the eastern but not in the western Fram Strait (Nöthig et al. 2015 & 2020). This is in accordance with the increasing contributions of *Phaeocystis pouchetii* and nanoflagellates to the summer phytoplankton community. This change in community composition may have had an effect on the particulate organic carbon (POC) during summer (Engel et al. 2019) as the amount of POC decreased over the last years. We also observed that *Themisto compressa*, an invading amphipod species from temperate waters, increased in abundance (Kraft et al. 2013; Schröter et al. 2019). All this suggests that the Fram Strait ecosystem is undergoing profound changes, likely induced by climate conditions warranting sustained observation.

Sea ice is one of the major players in ecosystem processes since it affects the solar radiation fluxes due to its reflective properties, its melting is impacting stratification, and it is a habitat and feeding ground for various organisms of the polar ecosystem. Sea ice origin even governs the community distribution of e.g. sea ice protists (Hardge et al. 2017), and thus changing

transport routes and thinning sea ice (Krumpen et al. 2019) might have major implications on the biodiversity of the sea ice biota. In addition, the changing sea ice scape increases light availability on larger and smaller scales, allowing phytoplankton to grow in previously ice-covered regions (Massicotte et al. 2019). A long-term trend towards thinner sea ice has profound implications for the timing and position of the seasonal ice zone (including MIZ) and the anticipated ice-free summers in the future will have major impact on the entire ecosystem and alter biogeochemical cycles in the Arctic.

Meltwater stratification is particularly pronounced in the marginal ice zone (MIZ) of the Arctic Ocean which is defined as an area of the ocean covered with 15-80% sea ice and characterized by extensive sea ice melt (Aksenov et al. 2017; Strong and Rigor 2013). In consequence, the MIZ is a key area of Arctic marine primary production (Gradinger and Baumann 1981). Overall, there has been an increase in the areal extent of the MIZ reflected by low surface salinity and stratification in the seasonal ice zone of the Arctic Ocean. Observations from recent expeditions suggest, that the area impacted by sea ice melt in the Fram Strait might extend south-eastwards. This was particular obvious in summer 2021, when the sea ice edge in June extended to south of 79°N at ~ 4°E. It is currently unclear whether increased melt-water amounts and stratification will lead to increased export of particulate organic carbon or whether the products of primary production will remain at the surface and drive a regenerating system. Arctic regions impacted by melting sea ice support specific plankton community composition (Weiss et al. 2024; Oldenburg et al. 2024), and may either increase particle export (Lalande et al. 2019; Fadeev et al. 2021) or retain particles at the surface for a while, depending on the physical structure of the respective water parcels at the surface (v. Appen et al. 2021). Retention rates of biomass in the upper water column might change in the future, due to expected changes in plankton communities and trophic networks in consequence to Arctic environmental change. These changes might include that small algae gain importance in mediating element and matter turnover as well as energy fluxes in Arctic pelagic systems. However, currently cryo-pelagic coupling of microalgal communities and the role of sea-ice algae in primary production under the ice, and particularly in the MIZ has to be better understood to estimate consequences of sea ice decline on Arctic primary production and carbon cycles. A combination of measurements of classical parameter (particulate organic carbon, nitrogen, biogenic silica) and molecular biodiversity studies provided first insights into microbial distribution and Chl *a* biomass in the Arctic Ocean and suggest a high contribution of small microalgae to Chl *a* biomass in the Central Arctic Ocean (Metfies et al. 2016; Hardge et al. 2017). Many zooplankton species are affected by these changes at the base of the food web as they rely on phytoplankton as food source. Furthermore, zooplankton community composition may shift due to the increasing inflow of warmer Atlantic water into the Fram Strait. Altered zooplankton trophic interactions and community compositions will have consequences for the carbon sequestration and flux. Also, Mycoplankton (defined here as saprotrophic and parasitic fungi and pseudofungi (oomycetes)) may have a considerable ecological impact, e. g. by controlling the population size of bloom-forming species (Buaya et al. 2019). In polar regions, however, the diversity and dynamics of the mycoplankton remain to be discovered (Hassett et al. 2019 a,b). Another, yet understudied group are Bacteriophages, or phages, which are viruses that infect and replicate within bacterial hosts and play an essential role in regulating microbial populations and ecosystem dynamics (Suttle 2007). The virome of extreme environments such as polar regions has only rarely been investigated due to challenges such as limited access to the ecosystem and low biomasses (Heinrichs et al. 2024). Understanding the diversity, structure, and functions of polar phages is, however, critical to advancing our knowledge of the microbial ecology and biogeochemical processes in these environments.

Comprehensive understanding of the impact of changing environmental conditions on ecosystem functions and functionality, thus, requires studying the system on different spatial and temporal scales. This can be accomplished by combining different observation approaches, providing different kinds of information: (i) satellite-based observations can

provide geographically large-scale information on changes in ecosystem functions, such as Chl *a* concentrations over bigger time-scales; (ii) the deployment of sediment traps and automated water samplers for molecular biodiversity studies over extended periods of time (mainly one or two years from summer to summer) in different parts of the Arctic Ocean can provide insight into algal biodiversity and matter export during different sea ice scenarios over the annual cycle; (iii) underway sampling and towed optical plankton observations can provide high-resolution information on plankton distribution in the upper water column; (iv) classical CTD sampling and net-tows provide samples for vertical characterization of plankton distribution in the water column.

Objectives

Overall, the overarching objectives of PEBCAO are to improve the mechanistic understanding of biogeochemical and microbiological feedback processes in the changing Arctic Ocean, to document ongoing and long-term changes in the biotic and abiotic environment and to assess the potential future consequences of these changes. In particular we aim to identify climate-induced changes in the biodiversity of pelagic ecosystems and, concomitantly, in carbon cycling and sequestering and improve our mechanistic understanding of linkages between key environmental parameters and ecosystem functionality in the Arctic Ocean. The objectives are addressed using a range of methodologies:

Heterotrophic bacteria play a vital role in global biogeochemical cycles. To better understand bacterial activity, one objective was to determine bacterial abundance, biodiversity and production. By linking compound dynamics with rate measurements and community structure, we will gain further insights into the flow of carbon through the Arctic food web. To address the effects of global change on microbial biogeochemistry in the Arctic Ocean, we aim to continue monitoring concentrations of organic carbon, nitrogen, and phosphorus, as well as specific compounds like amino acids, carbohydrates, and gel particles. To assess cell abundances, we sample for microscopic counts and flow cytometry that allows us to determine phytoplankton (< 50 µm), bacteria, and viral abundances. Phytoplankton primary production has been determined by radioisotopes and distinguished into particulate primary production (carbon remaining in the cells) and dissolved primary production (organic carbon subsequently released by cells). In addition, primary production has been assessed *in situ* using fast repetition rate fluorometry (FRF) with the FastOcean ADP profiling system.

We expect that the small algae at the base of the food web gain importance in mediating element and matter turnover as well as energy fluxes in Arctic pelagic systems. In order to detect changes, also in this smallest fraction of the plankton, traditional microscopy have been complemented by optical (see below) and molecular methods that are independent of cell-size and morphological features, and we will determine their contribution to Chl *a* biomass. Changes in Eukaryotic microbial communities are tightly linked to prokaryotic community composition. The assessment of the biodiversity and biogeography of Arctic Eukaryotic microbes, including phytoplankton and their linkages to prokaryotic microbial communities, will be based on analyses of eDNA via 18S meta-barcoding. A suite of automated sampling devices in addition to classical sampling via Niskin bottles attached to a CTD/Rosette Water Sampler has been used to collect samples for eDNA analyses. This includes the automated filtration device AUTOFIM deployed on *Polarstern* for underway filtration, automated Remote Access water Samplers (RAS) and long-term sediment traps deployed on the FRAM moorings for year-round sampling. The automated and long-term studies on phytoplankton will be complemented by following sinking aggregate dynamics at high temporal resolution throughout a whole year using the BOP system to determine daily size-distribution, abundance and size-specific sinking velocities of settling particles.

Underway measurements of the surface phytoplankton with two devices, the FluoroProbe and the CytoSub, will help to detect spatial changes in the community. The CytoSub (a Flow Cytometer) quantified the phytoplankton community, especially the picoplankton size class,

ranging from 0.2 to 2 µm. The Flow Cytometer measured the light scatter of each cell which provides information on the internal or external complexity of the cell. The fluorescence (red, orange, yellow) indicates the type of cell. All those light signals are transformed to electrical signals and are made visible in a cytogram (Thyssen et al. 2015). We will also use the FluoroProbe (bbe Moldaenke GmbH, Germany), which is a multispectral fluorometer to (1) measure total chlorophyll fluorescence and to (2) discriminate among four spectral algal groups (brown algae, cyanobacteria, green algae, and cryptophytes) and coloured dissolved organic matter (CDOM) (Artigas et al. 2019). In Arctic oceanic waters, *Phaeocystis pouchetii* is blooming in July (Schoemann et al. 2005), while the biomass of diatoms is decreasing during summer after a strong spring bloom (Soltwedel 2023). With the CytoSub, we will aim to detect *P. pouchetii* cells in different life stages and with the Fluoroprobe we will discriminate haptophytes from brown algae. The dominating phytoplankton class is eukaryotic picophytoplankton, especially chlorophytes such as *Micromonas polaris* and *Micromonas commoda* (Bachy et al. 2022), and these can be detected with the CytoSub (RedPico) and, if their biomass is large, with the FluoroProbe.

Optical measurements of the phytoplankton will be acquired continuously during PS143/2. We will determine total phytoplankton and group specific Chl *a* concentrations, as well as the absorption by other particles and colored dissolved organic matter. We will broaden the sampling frequency of information on phytoplankton, particulate and chromophoric dissolved organic matter (CDOM) abundance and composition by taking continuous optical measurements which directly give information on inherent and apparent optical properties (IOPs, and AOPs, respectively). We collect a high spatial and temporal resolved data set on phytoplankton (total and composition) and its degradation products at the surface and for the full euphotic zone using continuous optical observations during the entire cruise and at specific transects operated by towing the Triaxus platform, respectively. This large data set will be calibrated using high precision measurements on discrete water samples and combined with ocean colour satellite data to upscale the station-based information on linkages between the various trophic layers and biogeochemical cycling. Further, these data will be used for validating several ocean color satellite products (e.g., Oelker et al. 2022; Xi et al. 2021; Bracher et al. 2009).

Similarly to the phytoplankton community, the zooplankton community composition may shift due to the increasing inflow of warmer Atlantic water into the Fram Strait. Altered zooplankton trophic interactions and community compositions will have consequences for the carbon sequestration and flux. Most of our knowledge on zooplankton species composition and distribution has been derived from traditional multiple net samplers, which integrate depth intervals of up to several hundred meters. Nowadays, optical systems, such as the zooplankton recorder LOKI (Light frame On-sight Key species Investigations), continuously take pictures of the organisms during vertical casts. Linked to each picture, hydrographical parameters are being recorded, i.e. salinity, temperature, oxygen concentration, and fluorescence. This will allow us to exactly identify distribution patterns of key taxa in relation to environmental conditions. We will also use the UVP5 (Underwater Vision Profiler), which is mounted on the ship´s CTD to also tackle zooplankton distribution patterns, albeit with much less taxonomic resolution than with LOKI.

Moreover, Bacteriophages, or phages, which are viruses that infect and replicate within bacterial hosts, play an essential role in regulating microbial populations and ecosystem dynamics (Suttle 2007). The virome of extreme environments such as polar regions has only rarely been investigated due to challenges such as limited access to the ecosystem and low biomasses (Heinrichs et al. 2024). One objective during PS143/2 therefore was to enhance our understanding the diversity, structure, and functions of polar phages which is critical to advancing our knowledge of the microbial ecology and biogeochemical processes in these environments.

We also included research dedicated to protistan parasites. These are severely understudied in the marine realm although they are likely to affect the population dynamics of phytoplankton

(including bloom timing and magnitude) and zooplankton. We therefore conducted a baseline study of the diversity of different parasite groups and their association with potential hosts. This investigation will also form the basis for future biogeographic studies. The analyses will combine different microscopy techniques (LM, SEM, CFLM) as well as molecular data, the latter facilitating observation of parasitism even at times where easily discernible parasite life-cycle stages are absent. We initiated cultures for fungal plankton (in addition to oomycete cultures established on PS143/1). Co-cultures of parasites and their hosts will be used for experiments planned in the upcoming INDIFUN-AI BMBF project in which we wish to investigate the utility of using parasites and saprotrophic fungi as indicators of environmental change.

In summary, during PS143/2 the following objectives are addressed:

- Monitoring biogeochemical parameters
- Determine autotrophic and heterotrophic microbial activities
- Monitoring plankton species composition and biomass distribution
- Assessing the flux of particulate organic matter to the seafloor
- Investigating selected phyto- and zooplankton (including their parasites)
- Determining the composition of organic matter and gel particles
- Sampling mycoplankton to study diversity and dynamics (PS143/1 & PS143/2)
- Studying host-parasite systems in phyto- and mycoplankton

Work at sea

Biogeochemistry (Benjamin Pontiller, Sophia Hirschmann, Tania Klüver)

Throughout the cruise, discrete seawater samples were collected at selected stations from the CTD-Rosette and processed for a range of biological and biogeochemical parameters to quantify organic matter in the Fram Strait and to estimate its turn-over. During PS143/2, 11 of the regular HAUSGARTEN stations and 6 additional stations were visited, spanning an East-West transect at roughly 80°N (N5). At each station, the euphotic zone was sampled using a "shallow" cast, collecting samples from the surface, chlorophyll a maximum (Chl *a* max), below Chl *a* max., at 50 m, and at 100 m depths. At selected stations, a deep cast was performed to collect samples for amino acids, carbohydrates, and gel particles at five depths ranging from 200 m to a depth of 1,200 m (Tab. 5.1). In addition to the CTD sampling, 9 stations along a West-East transect at 79°N were sampled from the underway system (Tab. 5.2).

Dissolved Biogeochemical Parameters:

- Dissolved Organic Carbon and Total Dissolved Nitrogen (DOC/TDN): Seawater was filtered through 0.45 µm GMF syringe filters into combusted glass vials, acidified with hydrochloric acid (Suprapur), and stored at 4 °C until analysis via High-Performance Liquid Chromatography (HPLC).
- Dissolved Amino Acids (DAA) and Combined Carbohydrates (DCHO): These samples were filtered using 0.45 µm Acrodisc filters, stored in combusted glass vials, and kept at -20 °C.
- Dissolved Inorganic Carbon (DIC): Samples were treated with mercury (II) chloride and stored at 4 °C.
- Nutrients (NUT): These samples were filtered through 0.4 µm cellulose acetate filters and stored at -20 °C.

- Total Alkalinity (TA): Samples were filtered through 0.45 µm Acrodisc filters and stored at 4 °C.

Particulate Biogeochemical Parameters:

- Transparent Exopolymer Particles (TEP) and Coomassie Stainable Particles (CSP): Seawater samples were filtered using 0.4 µm polycarbonate filters, stained with Alcian Blue and Coomassie Brilliant Blue dyes respectively, and stored at -20 °C until microscopic and colorimetric analyses.
- Confocal Laser Scanning Microscopy (CLSM) and CLASI-FISH: Samples to analyze gel particle-associated bacterial community structure were filtered through black 0.4 µm polycarbonate filters and stored at -20 °C.
- Lipid Analysis: Samples were filtered using 0.2 µm hydrophilic Durapore filters, flash-frozen in liquid nitrogen, and stored at -80 °C.

Phytoplankton and bacterial parameters:

- Bacterial (BA), Picophytoplankton (PA) and Viral (VA) Abundance: Samples were fixed with GDA 25% and frozen at -80 °C. Analysis by flow cytometry will be conducted at GEOMAR.
- Phytoplankton Primary Production (PP) and Bacterial Biomass Production (BBP): These rates were determined onboard using radioactive tracers ^{14}C sodium bicarbonate and 3H-leucine, respectively. Due to technical issues with the incubation cabinet, PP measurements were only taken at 0 °C.
- Arctic Bacterioplankton Function (RNAmetaT): Samples were collected at all stations from the surface, DCM, 50 m, and 100 m depths, preserved with RNALater, flash-frozen, and stored at -80 °C until further processing in the home laboratory.

Tab. 5.1: Biogeochemical parameters sampled from the CTD-Rosette Water Sampler. Abbreviations as follows: DOC: dissolved organic carbon; DCHO: dissolved carbohydrates; DAA: dissolved amino acids; NUT: inorganic nutrients; TEP: transparent exopolymer particles; CSP: Coomassie stainable particle; RNAmetaT: bacterial RNA for metatranscriptomic analysis; LIP: lipids; BA/PA/VA: bacterial, picophytoplankton, and virus abundances; BBP: bacterial biomass production; PP: phytoplankton primary production; DIC: dissolved inorganic carbon; TA: total alkalinity.

Station	**ID**	**DOC/ DCHO /DAA**	**NUT**	**TEP/ CSP**	**CLSM**	**RNA metaT**	**LIP**	**BA/PA/ VA**
PS143/2_2-1	SV-IV deep	x	x	x	x	-	x	x
PS143/2_2-6	SV-IV shallow	x	x	x	x	x	x	x
PS143/2_7-1	S3 deep	x	x	x	x	-	x	x
PS143/2_7-6	S3 shallow	x	x	x	x	x	x	x
PS143/2_11-1	SV-III	x	x	x	-	x	x	x
PS143/2_14-1	SV-II shallow	x	x	x	x	x	x	x
PS143/2_15-1	SV-I shallow	x	x	x	-	x	x	x
PS143/2_18-1	HG-I deep	**x**	x	x	-	-	x	x
PS143/2_18-7	HG-I shallow	x	x	x	-	x	x	x
PS143/2_22-1	HG-IV deep	x	x	x	x	x	x	x
PS143/2_22-7	HG-IV shallow	x	x	x	x	x	x	x
PS143/2_23-4	HG-IX shallow	x	x	x	x	x	x	x
PS143/2_23-1	HG-IX deep	x	x	x	x	-	x	x

Station	ID	DOC/ DCHO /DAA	NUT	TEP/ CSP	CLSM	RNA metaT	LIP	BA/PA/ VA
PS143/2_25-1	N5 deep	x	x	x	x	-	x	x
PS143/2_25-7	N5 shallow	x	x	x	x	x	x	x
PS143/2_27-1	N5TE3 shallow	x	x	x	-	x	x	x
PS143/2_33-1	N5TE8 shallow	x	x	x	-	x	x	x
PS143/2_40-1	N5TE11 shallow	x	x	x	-	x	x	x
PS143/2_44-1	N5TEW3 shallow	x	x	x	-	x	x	x
PS143/2_48-1	N5TW7 shallow	x	x	x	-	x	x	x
PS143/2_54-1	N5TW14 shallow	x	x	x	-	x	x	x
PS143/2_56-2	EG-I deep	x	x	x	x	-	x	x
PS143/2_75-1	EG-I shallow	x	x	x	x	x	x	x
PS143/2_76-1	EG-IV shallow	x	x	x	x	x	x	x
PS143/2_76-8	EG-IV deep	x	x	x	x	-	x	x

Tab. 5.2: Biogeochemical parameters sampled from the underway system. Abbreviations as follows: DOC: dissolved organic carbon; DCHO: dissolved carbohydrates; DAA: dissolved amino acids; NUT: inorganic nutrients; TEP: transparent exopolymer particles; CSP: Coomassie stainable particle; BA/PA/VA: bacterial, picophytoplankton, and virus abundances; BBP: bacterial biomass production.

Station	ID	DOC/ DCHO/ DAA	NUT	TEP/CSP	BA/PA/VA	BBP
PS143/2_79TU1	79TU1	x	x	x	x	x
PS143/2_79TU2	79TU2	x	x	x	x	x
PS143/2_79TU3	79TU3	x	x	x	x	x
PS143/2_79TU4	79TU4	x	x	x	x	x
PS143/2_79TU5	79TU5	x	x	x	x	x
PS143/2_79TU6	79TU6	x	x	x	x	x
PS143/2_79TU7	79TU7	x	x	x	x	x
PS143/2_79TU8	79TU8	**x**	x	x	x	x
PS143/2_79TU9	79TU9	x	x	x	x	x

To investigate the influence of anthropogenic pollution on the microbial community and biogeochemistry we aimed at collecting microplastic particles (> 300 µm) throughout the cruise from the underway system of *Polarstern*. As no particles were found during the cruise, an incubation experiment was continued that had started during cruise PS143/1 with water from station SV-II collected from 10 m depth with the CTD rosette water sampler. A total of 24 glass jars were filled with one litre of seawater each and seven different types of plastic were incubated in triplicates at 4°C. The experiment ended during PS143/2 on 3 August 2024. Samples for metatranscriptomic and 16S rRNA gene amplicon sequencing were taken to investigate the biodiversity and function of plastic-associated bacteria focusing on potential pathogens and their resistome. In addition to the molecular data, DOC and bacterial abundance data were taken.

For continuous underway surface sampling a Single Turnover Active Fluorometry system (LabSTAF, Chelsea Technologies, UK) was used throughout the cruise to obtain data on phytoplankton photosynthesis, fitness, and primary productivity (Fig. 5.1). Measurements were taken every 25–30 minutes, except for a few time points due to interrupted water supply from the underway system; the instrument performed according to plan and generated a vast amount of raw data. Quality control and analysis of this data will be carried out in the following months.

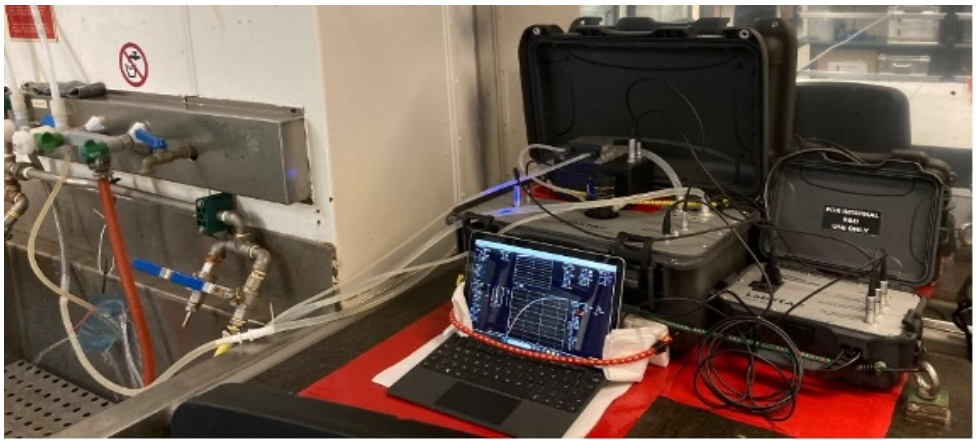

Fig. 5.1: Setup of the LabSTAF system

Protistian and Microbial Plankton (Katja Metfies, Celina Behrendt, Tabea Galonska, Kerstin Korte, Marlis Reich, Alexandra Kraberg, Eva-Maria Nöthig)

Seawater samples (Tab. 5.1) were taken at 5 – 12 depths by a CTD/rosette sampler in the HAUSGARTEN area and on the east-west transect on 79.9 N. Aliquots were filtered for analyzing biogeochemical parameters such as Chl *a* (unfractionated, and fractionated on 10 µm, 3 µm, and 0.2 µm), particulate organic carbon and nitrogen (POC and PN), and biogenic silica (PbSi), respectively. Furthermore, unfiltered CTD water samples were fixed with formalin (final concentration 0.5 – 1.0 %) for later quantitative assessment of the phytoplankton community by inverted microscopy. Additional samples were collected from 5 depths via the CTD-rosette from the top 100m depth for molecular analyses in order to assess microbial community compositions by 18S meta-barcoding. Samples for 18S meta-barcoding analyses were fractionated by three filtrations on 10.0, 3.0, and 0.4 µm filters.

Tab. 5.3: Stations with phytoplankton hand-net hauls (20µm mesh size)

Sampling Event	**Station ID**	**Date**	**Latitude**	**Longitude**	**Tow length [m]**	Weather conditions
PS143_2/2-1	SV4	15.7.24	79°1.8199'N	06°54.740'N	20	cloudy
PS143_2/7-1	S3	16.07.24	79°36.551'N	05°20.074'N	20	sunny
PS143_2/11-1	SV3	17.07.24	79°01,059'N	05°20.074'N	20	sunny
PS143_2/14-1	SV2	18.07.24	79°58.850'N	09°30.415'N	20	light cloud
PS143_2/18-1	HGI	19.07.24	79°8.0360'N	06°05,564'N	20	cloudy
PS143_2/21-1	HGIV	20.07.24	79°04.824'N	04°05,306'N	20	sunny
PS143_2/22-5	HGIX	21.07.24	79°8,5140'N	02°44.020'N	20	cloudy

Sampling Event	Station ID	Date	Latitude	Longitude	Tow length [m]	Weather conditions
PS143_2/25-2	N5	22.07.24	79°56.296'N	03°11.634'N	20	foggy
PS143_2/33-2	NSTE8	23.07.24	79°56.264'N	07°45.630'N	20	foggy
PS143_2/40-2	NSTE11	24.07.24	79°56.388'N	10°10.622'N	15-17	foggy
PS143_2/44-2	NSTW3	25.07.24	79°56.326'N	01°55.083'N	15-17	foggy
PS143_2/48-2	NSTW5	25.07.24	79°56.123'N	00°39.977'N	15	foggy
PS143_2/54-2	NSTW14	26.07.24	79°54.742'N	05°14.964'N	15	foggy
PS143_2/56-2	EGC1	27.07.24	78°58.288'N	05°17.740'N	15	foggy
PS143_2/75-2	EG1	01.08.24	78°59.980'N	79°1.8199'N	17	foggy

To address spatial variability of microbial plankton communities, we complemented sampling for molecular analyses using the CTD-rosette with sampling via the underway sampling system AUTOFIM, permanently installed on board *Polarstern*. We used the device to collect samples with a volume of ~ 2 litres during two transects along ~79.9N and ~78.9 N degrees with a resolution of 30 min (~ 3 nm). All filters for eDNA were frozen at -80°C until further analyses in the laborato ry on shore.

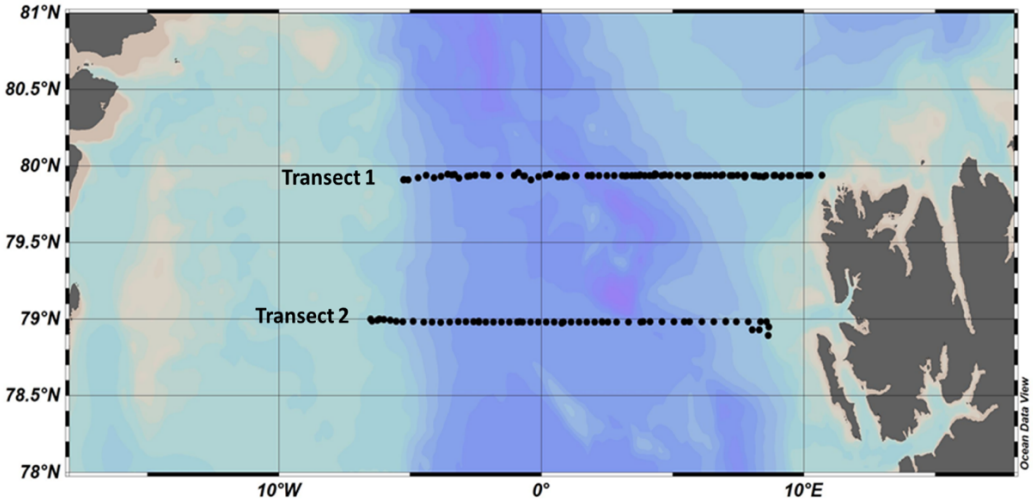

Fig. 5.2: Map illustrating the locations of eDNA samples collected underway along the two transects with the automated filtration device AUTOFIM

A subset of CTD samples collected from the depth of the Chl *a* maximum for eDNA analyses (Fig. 5.2, Tab. 5.4) were subjected on board ship to sequencing of the 18S gene via MINION/Nanopore-technology. Genomic DNA was isolated using the PowerWater Kit (Qiagen, Germany) and sequencing was accomplished according to a manufacturers protocol with a primer-set targeting the V4 region of the 18S gene.

Tab. 5.4: Samples subjected to 18S meta-barcoding

Sample	Station	Water	Month	Cruise
PS143_1_N3_10m	N3	MIZ	June	143_1
PS143_1_N4_10m	N4	MIZ	June	143_1

Sample	Station	Water	Month	Cruise
PS143_1_N5_10m	N5	MIZ	June	143_1
PS143_1_S3_10m	S3	Atlantic	June	143_1
PS143_1_SV2_10m	SV2	Svalbard Shelf	June	143_1
PS143_1_SV3_10m	SV3	Svalbard Shelf	June	143_1
PS143_1_SV4_10m	SV4	Svalbard Shelf	June	143_1
PS143_1_EG1_10m	EG1	Ice covered	June	143_1
PS143_1_EG2_10m	EG2	Ice covered	June	143_1
PS143_1_EG3_10m	EG3	Ice covered	June	143_1
PS143_1_EG4_10m	EG4	Ice covered	June	143_1
PS143_1_HG1_10m	HG1	Atlantic	June	143_1
PS143_1_HG2_10m	HG2	Atlantic	June	143_1
PS143_1_HG3_10m	HG3	Atlantic	June	143_1
PS143_1_HG4_10m	HG4	Atlantic	June	143_1
PS143_1_HG5_10m	HG5	Atlantic	June	143_1
PS143_1_HG6_10m	HG6	Atlantic	June	143_1
PS143_1_HG7_10m	HG7	Atlantic	June	143_1
PS143_1_HG8_10m	HG8	Atlantic	June	143_1
PS143_1_HG9_10m	HG9	Atlantic	June	143_1
PS143_2_N5_10m	N5	MIZ	July	143_2
PS143_2_S3_10m	S3	Atlantic	July	143_2
PS143_2_SV2_10m	SV2	Svalbard Shelf	July	143_2
PS143_2_SV3_10m	SV3	Svalbard Shelf	July	143_2
PS143_2_SV4_10m	SV4	Svalbard Shelf	July	143_2
PS143_2_HG1_10m	HG1	Atlantic	July	143_2
PS143_2_HG4_10m	HG4	Atlantic	July	143_2
PS143_2_HG9_10m	HG9	Atlantic	July	143_2
PS143_2_0Grad_10m	0Grad	MIZ	July	143_2
PS143_2_1,5Grad_10m	1.5Grad	MIZ	July	143_2

To study live phytoplankton by light microscopy, vertical net hauls with a hand net were carried out. The hand net had a mesh size of 20 µm and the tows were standardized to a tow length of 20 m. Where this was not possible due to the strength and/or direction of the currents, this was noted in the metadata (see Tab. 5.3).

Mycoplankton

To assess the Mycoplankton community, water samples were taken from the rosette deployed at the HAUSGARTEN stations (Tab. 5.5). These samples were size-fractionated (500 µm and 50 µm) and filtered on 0.2 µm filters to (A) analyse the community composition with long-read sequencing of the rDNA operon, and (B) microscopically resolve morphological diversity and obtain absolute cell abundances. In addition, fungus-specific growth media were inoculated with seawater and spread on solid medium to isolate individual strains. For isolation work, waters from the surface or Deep Chl *a* Max were used. The isolation as well as the processing and evaluation of the filters will be continued in the laboratory of AG Reich at the University of Bremen with molecular tools, yieliding data on mycoplankton composition, distribution and

morphology. In addition, fungus-specific medium was inoculated with seawater from selected stations. Over the next month, we aim to isolate arctic fungal species from these samples. The isolates will serve as model organisms to carry out specific experiments, e.g. to investigate the role of fungi as a food source for zooplankton.

Tab. 5.5: Sample types at the AWI-HAUSGARTEN stations for assessing mycoplankton communities. All samples were pre-filtered per station and depth, and subsamples were taken from each of the two fractions (i.e. <500µm and <50µm). At some stations, in addition a plankton net sample was taken (0-20m).

Station ID	Water depth [m]	eDNA	Fluorescence microscopy	Isolation
SV4	1000	x	X	
SV4	500	x	X	
SV4	100	x	X	
SV4	50	x	X	
SV4	21	x	X	
SV4	15	x	X	x
SV4	10	x	X	
S3	2778	x	X	
S3	2000	x	X	
S3	1000	x	X	
S3	500	x	X	
S3	100	x	X	
S3	50	x	X	
S3	40	x	X	
S3	30	x	X	
S3	10	x	X	
SV2	10			x
HG1	1235	x	X	
HG1	1000	x	X	
HG1	500	x	X	
HG1	100	x	X	
HG1	50	x	X	
HG1	42	x	X	
HG1	31	x	X	
HG1	10	x	X	x
HG4	2445	x	X	
HG4	2000	x	X	
HG4	1000	x	X	
HG4	500	x	X	
HG4	100	x	X	
HG4	50	x	X	

Station ID	Water depth [m]	eDNA	Fluorescence microscopy	Isolation
HG4	30	x	X	
HG4	18	x	X	
HG4	10	x	X	x
HG9	5330	x	X	
HG9	2000	x	X	
HG9	1000	x	X	
HG9	500	x	X	
HG9	100	x	X	
HG9	50	x	X	
HG9	35	x	X	
HG9	25	x	X	
HG9	10	x	X	x
EG1	1000	x	X	
EG1	500	x	X	
EG1	100	x	X	
EG1	50	x	X	
EG1	32	x	X	
EG1	20	x	X	
EG1	10	x	X	x
F5	20			x
EG4	2000	x	X	
EG4	1000	x	X	
EG4	500	x	X	
EG4	100	x	X	
EG4	50	x	X	
EG4	31	x	X	
EG4	20	x	X	
EG4	10	x	X	x
EG1	0-20			x
EG4	0-20			x

Phages and Viruses (Ovidiu Popa, Ellen Oldenburg)

To study the diversity and distribution of phages and viruses at different sampling sites and depths during PS143/2 we collected 10L of seawater with the CTD/rosette sampler at four depths (surface, DCM, 50m and 100m) at 10 HAUSGARTEN stations (Fig. 5.3). In addition, samples were collected from surface, 10 m, DCM and 100 m at the five east-west transect stations.

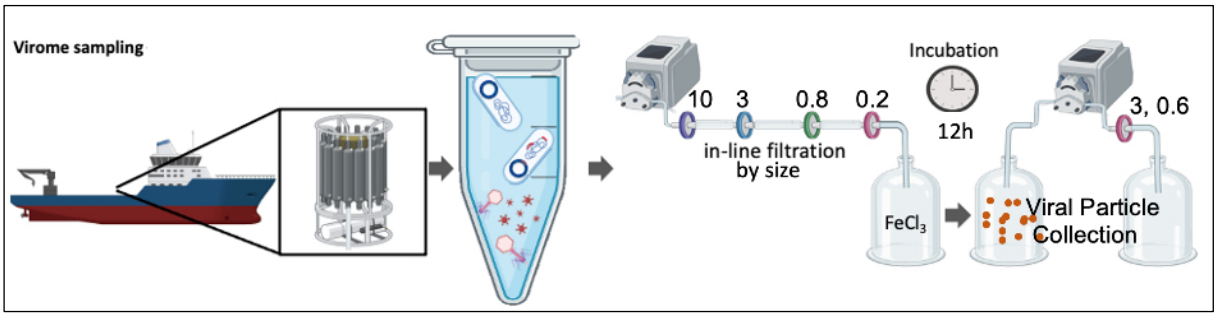

Fig. 5.3: Overview of the sampling procedure for filtration by size and viruses during PS 143/2. Water (10 L) was collected from the upper 100m using the CTD Rosette. Samples containing free-living and enclosed viral particles, along with putative hosts, undergo multiple filtration steps to separate the cells by size. Viral fraction enrichment is achieved through incubation with $FeCl_3$ followed by subsequent filtering.

In total, 227 samples (phytoplankton, microplankton and prokaryotes) and 120 virus samples were collected. All samples will be later analysed using state of the art metagenomic approaches. By analyzing the genetic composition of these components, we aim to understand their impact on the dynamics and adaptation of their host organisms.

Filtration by Size (227 filters):

- Sample Volume: 5L of seawater
- Filter Pore Sizes: 10 µm, 3 µm, 0.8 µm, and 0.2 µm
- Purpose: To separate cells by size and distinguish between plankton, microplankton, and prokaryote fractions.
- Storage: All filters containing different samples were stored at -20°C for later laboratory processing.

Viral Particle Collection (120 filters):

- Sample Volume: 10L of seawater (post 0.2 µm filtration step, containing viral particles that passed through the filter)
- Incubation: Incubated with $FeCl_3$ for 12 hours at room temperature in the dark to form viral iron flocculates (John et al. 2011).
- Concentration: Viral iron flocculates were concentrated on one 3 µm and two 0.6 µm filters.
- Storage: All filters containing the iron flocculates were stored at -80°C for later laboratory processing.

This two-step filtration design allows us to distinguish between viruses that are cell-attached or intracellular (present in the larger fractions but absent in the $FeCl_3$ treated samples) and free-floating viruses (only found in the $FeCl_3$ fraction). The total volume of $FeCl_3$ treated seawater that was filtered on each station at four depth is shown in Tab. 5.6.

Tab. 5.6: Total volume of $FeCl_3$ treated seawater that was filtered on one 3 µm filter and on two 0.6 µm filters at different stations (column names; NT5 charactrizes the station sampled on the east-west transect at 79°N, all other stations are located in the AWI Hausgarten) and depth (row names). Cell color gradient corresponds to the water volume from blue (blue (0L) to red (10L).

	SV4	F4W 5ST	SV3	SV2	HGI	HGIV	HGIX	N5	N5T E2	N5T E8	N5T E11	N5T W3	N5T W7	N5T W14	EGI	E IV
urface	2	7	6	6.5	3.5	7	8.5	7	5.5	6.5	6.5	4.5	7.5	7.5	5	9.
DCM	1.5	8	5.5	5.5	3	3	9	8	7.5	6	8	4.8	7	8	8	8.
at 50m or 10m (NT5)	6	6.5	8	10	5	5	8.2	8	0	9.5	8	3	6	8.3	9	9.
100m	4	8	7.3	10	7	7	10	8	9	9	9	8	8	9	9	8.

Zooplankton (Barbara Niehoff, Magdalena Dolinkiewic)

Mesozooplankton biodiversity and large-scale distribution patterns of zooplankton were investigated in the Eastern Fram Strait and in the East Greenland Current at the monitoring stations of the AWI-HAUSGARTEN observatory (Tab. 5.5), and on the east-west transect at 79°N using a Multinet midi (Hydrobios, Germany, 150 µm mesh size). In the AWI-HAUSGARTEN, the net was towed vertically to sample five standard depths layers (1,500-1,000-500-200-50-0 m). At the EGC Station, the bottom depth was shallower than 1,500 m, and thus the depth intervals were adjusted, yielding a higher resolution of the upper water column. The transect was focused on the upper 500 m of the water column in order to elucidate the influence of ice conditions on the plankton community, and here sampling intervals were 500-200-100-50-20m. All net samples were immediately preserved in 4 % formalin buffered with hexamethylenetetramine. In the laboratories at AWI, these samples will be analyzed with the optical system ZooScan (Hydroptics, France) to determine zooplankton species composition and abundance (Cornils et al. 2022).

At three stations (Tab. 5.7), an addional Mulitnet cast was conducted to determine carbon and nitrogen contents of zooplankton organisms. Such data are available for the large *Calanus* spp. and for female *Metridia longa*, information on other taxa is, however rare. Therefore, we here focused on yet less studies Copepoda taxa, (i.e. the genera *Aetidiopsis*, *Gaetanus*, *Heterorhabdus*, *Metridia*, *Paraeuchaeta*, *Scaphocalanus* and *Spinocalanus*). In addition, we collected specimen of the taxa Ostracoda, Polychaeta, Amphipoda and Euphausiacea. Immediately after capture, the samples were transported into a cooling container (5°C), and single organisms were sorted alive and determined to the lowest possible taxonomical level and developmental stage. Depending on the size of the organism, we transferred either groups or single specimens into tin caps and stored these at -20°C until later measurements of carbon and nitrogen contents at AWI.

To analyze the vertical distribution of zooplankton species with high spatial resolution, the optical system LOKI (Lightframe On-sight Key species Investigation, Tab. 5.7). LOKI was equipped with a 150 µm plankton net and took high resolution images of zooplankton organisms and particles at a rate of 18 frames sec^{-1} while being towed vertically from 1,000 to

0 m. Simultaneously, depth, temperature, oxygen content and fluorescence were recorded to relate the zooplankton abundance to the environmental conditions. As a novel approach, another LOKI was mounted to the TRIAXUS (see chapter 3) aiming at the horizontal distribution of zooplankton key species. This LOKI also produced images which allow for taxa identification, however, the TRIAXUS system was only deployed for a short time due to technical problemns and, thus, this imaging data set is not sufficient for a meaningful analysis. We also installed an Underwater Vision Profiler (UVP, Hydroptic, France) on the water rosette, which collected images and particle data on each deep cast of the CTD, and on each of CTD cast to 500m of the transect, yielding more than 30 profiles. The image data will later be processed at AWI.

Tab. 5.7: List of stations of Multinet and LOKI deployments during PS143/2. At each station one sample were preserved for the analyses of zooplankton abundance; at selected station one additional cast was conducted and single live organismens were sorted alive for carbon and nitrogen content measurements. LOKI casts could not always be performed (-) due to either technical issues or limited time. Station IDs refer either to the AWI-HAUSGARTEN monitoring stations or to the location of sampling on the transect.

Station	Date	Station ID	Multinet	Analyses	LOKI
PS143/2_02	15.07.24	SV4	x	Abundance	x
PS143/2_07	16.07.24	S3	x	Abundance	x
PS143/2_11	17.07.24	SV3	x	Abundance	x
PS143/2_14	18.07.24	SV2	x	Abundance + CN	x
PS143/2_15	19.07.24	SV1	x	Abundance	x
PS143/2_18	19.07.24	HG-I	x	Abundance	x
PS143/2_21	20.07.24	HG-IV	x	Abundance	x
PS143/2_23	21.07.24	HG-IX	x	Abundance + CN	-
PS143/2_25	22.07.24	N5	x	Abundance	x
PS143/2_27	23.07.24	N5TE3	x	Abundance	x
PS143/2_33	23.07.24	N5TE8	x	Abundance	x
PS143/2_40	24.07.24	N5TE11	x	Abundance	x
PS143/2_44	25.07.24	N5TEW3	x	Abundance	x
PS143/2_48	25.07.24	N5TW7	x	Abundance	x
PS143/2_54	26.07.24	N5TW14	x	Abundance	-
PS143/2_56	27.07.24	EGI	x	Abundance	-
PS143/2_75	01.08.24	EGI	x	Abundance	x
PS143/2_76	02.08.24	EG-IV	x	Abundance + CN	x

Phytooptics (Astrid Bracher, Christian Hohe, Carolin Uhlig)

The contribution of the Phytooptics group was the acquisition of high resolved information on the amount and composition of phytoplankton and its pigments, coloured dissolved organic matter (CDOM) and particles along the cruise transect. These data collection enables via the complementation to satellite and previous field data acquisition the analysis of long-term trends in Fram Strait. In addition to that, these *in-situ* data are important for the validation of the group's own satellite products on underwater lght properties and phytoplankton compositionon. The continuous surface and profile biooptical data were regularly calibrated with measurements at discrete water samples determining the phytoplankton pigment composition

using High Pressure Liquid Chromatography (HPLC) method and the optical properties using spectrophotometric instrumentation.

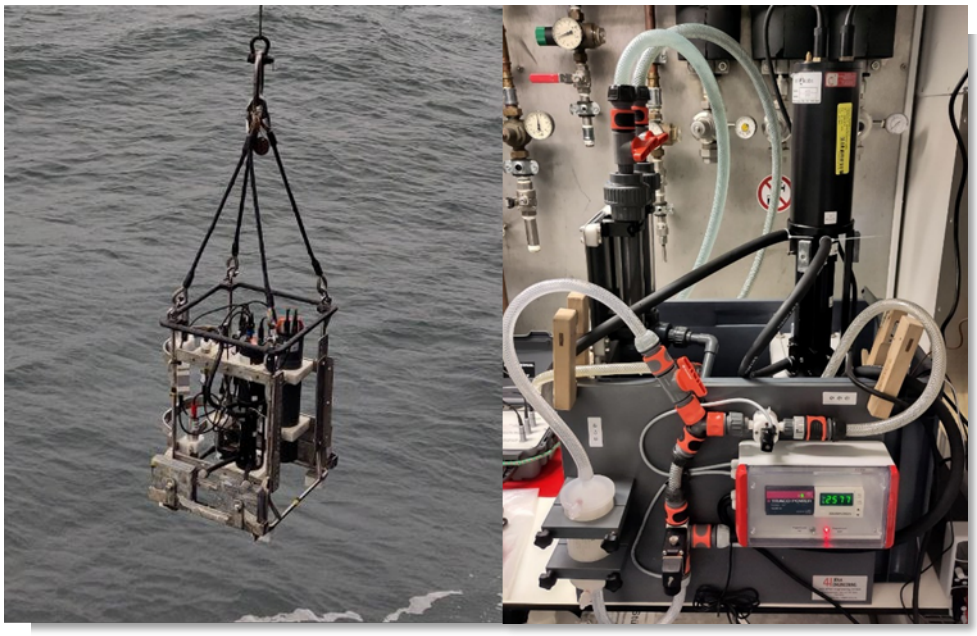

Fig. 5.4: Left: Underwater light field measurements with TRIOS RAMSES radiometers detecting the hyperspectral up- and downwelling radiation and the WETLABS AC-s (including pressure sensor, data logger and battery) measuring extinction and absorption. Right: Continuous measurements of the extinction and absorption of light in Arctic surface waters using a WETLABS AC-s mounted to the Polarstern surface seawater pump system. From those measurements directly, the absorption and scattering of particles and CDOM is determined for the whole spectrum in the visible resolved with about 3 nm resolution. This data then can be decomposed various specific algorithms to determine the particle size distribution and the various phytoplankton pigment composition.

Active and passive bio-optical measurements for the survey of the underwater light field, specific light attenuation, particle and phytoplankton composition and distribution were performed continuously on the surface water but also in the profile during Triaxus operation and at 18 light profiler stations were also CTD casts took place. In particular the following work was carried out:

(a) Continuous measurements of inherent optical properties (IOPs) with a hyperspectral spectrophotometer: For the continuous underway surface sampling an *in-situ*–spectrophotometer (ACS; Wetlabs) was operated in flow-through mode from shortly after leaving the port of Tromsø until and one day before arriving at the end of the expedition (see Fig. 1.1). The instrument was mounted to a seawater supply taking surface ocean water. A flow-control with a time-programmed filter was mounted to the ACS to allow alternating measurements of the total and the CDOM inherent optical properties of the sea water. Flow-control and debubbler-system ensured water flow through the instrument with no air bubbles. The ACS needed to be operated on the seawater supply at the Nasslabor-1, with seawater pumped via the membrane pump through the Teflon tubing in order to deliver living phytoplankton cells continuously throughout the cruise. The instrument was calibrated daily by measurements with MilliQ water. Operation was except for the daily calibrations (with MilliQ) continuously, except

for an eight-hour break during the night of 24 July when the software broke down and unfortunately was only noticed in the early morning.

(b) A second ACS instrument was mounted on a steel frame together with a depth sensor and a set of hyperspectral radiometers (RAMSES; Trios) and operated as light profiler during 18 CTD stations (see Fig. 5.4, Tab. 5.1) during daylight and out of the shipy. The frame was lowered down to maximal 100 or 120 m with a continuous speed of 0.1 m/s or during daylight with additionally stops at 5, 10, 15, 20, 25, 30 and 40, 50, 60, 100 (120) m to allow a better collection of radiometric data. The Apparent Optical Properties of water (AOPs) (hyperspectral surface reflectance and light attenuation from surface to depth within the water column) were calculated based on downwelling and upwelling irradiance measurements in the surface water profile (down to the 0.1% light depth) from the radiometers calibrated for the incident sunlight with measurements of a radiometer on deck. The ACS measured the inherent optical properties (IOPs: total attenuation, scattering and absorption) in the water profile.

(c) Because of many technical problems caused at maintenance by the company, the TRIAXUS was operated only twice for three and one hour on 28 and 31 July 2024, respectively. Both operations were stopped because of a pressure dependent problem that only occurs below 150 m depth. Luckily still we could measure about 50 up- and downcast profiles, each at about 1 m/s profiling speed, of hyperspectrally resolved AOPs (surface reflectance, diffuse attenuation, water leaving radiance) and IOPs (absorption, scattering) optical properties. For the acquisition of the hyperspectral AOPs from one downwelling RAMSES sensor and hyperspectral IOPs from another ACS instrument.

(d) Water samples from both underway and CTD stations were filtered in the laboratory to have the following samples and measurement: (1) HPLC phytoplankton pigment samples (pore size 0.7 µm filtered pads were immediately stored onboard in the -80°C freezer); (2) Particle and phytoplankton absorption spectra (ap, ad, and aph) were obtained by measuring a second set of filtered pads for each sample; and (3) CDOM absorption spectra were obtained by measuring the filtered water samples with 0.2µm pore size filters. Surface water was sampled from the seawater pump on *Polarstern* with an interval of 3 hours to fully cover the whole cruise track. In additon five depths were sampled by the CTD-rosette during CTD casts within the top 100 m. The filtrate water samples were analyzed for CDOM absorption onboard with a 2.5-m path length liquid waveguide capillary cell system (LWCC, WPI) following Levering et al. 2017 (for further detailed for our setup see Alvarez et al. 2022). Particulate and phytoplankton absorption coefficients were determined with the quantitative filter techniques using sample filtered onto glass-fiber filters QFT-ICAM and measuring them in a portable QFT integrating cavity setup Röttgers et al. 2016). The RAMSES station data and discrete water sample absorption measurements were analysed on bord to end products.

Underway and station measurements with CytoSub and FluoroProbe (Ina Schmidt)

To continuously measure the phytoplankton community composition, abundance, and the biomass variably at high frequency, we connected the CytoSub and the FluoroProbe (Fig. 5.5) to the same underway sea water supply as the ferry box. Measurements were only interrupted while the ships pump was not working in the ice. During stations, the FluoroProbe will be also used in a modified profiling configuration, to measure in-vivo fluorescence down to 50-200m. In total, 15 profiles were made. Water from different depths, collected with the CTD rosette, will be used to create discrete depth profiles with the CytoSub, by applying four protocols (one especially for Picophytoplankton, one for Nano-, one Microphytoplankton and one for taking pictures of Microphytoplankton). 20 stations were sampled with 4 to 6 depths.

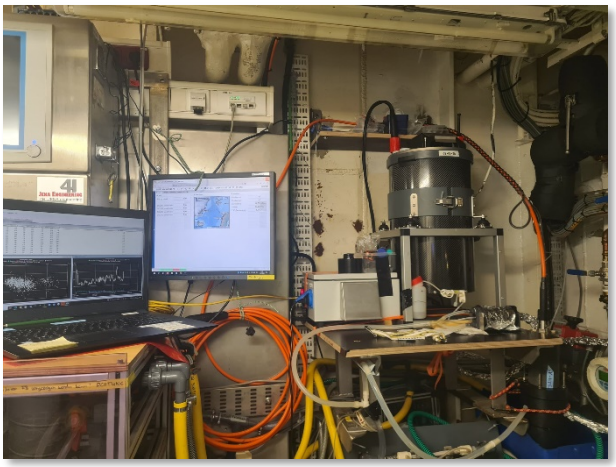

Fig. 5.5: Setup of Flow Cytometer and FluoroProbe during PS143/2 (credits: I. Schmidt)

The CytoSub (CytoBuoy, Netherlands) is specifically designed to characterize each particle and to record the corresponding optical features and a pulse shape, which can be combined with imagery of selected particles, mainly in the bigger size range. Moreover, this automated Flow Cytometer does not only focus on Pico- and Nanophytoplankton (as current benchtop FCM do) but can measure the whole size range up to Microphytoplankton single cells and colonies, for example of *Phaeocystis* spp. which is giving a big advantage compared to traditional flow cytometry. The CytoSub will provide an opportunity to assess microbial functional diversity continuously at and between stations and facilitate investigations of interactions and associations between different populations and their reaction to environmental changes.

Recovery of automated samplers (Christian Konrad, Katja Metfies, Daniel Scholz)

Recovery and deployment of the BOP system

The BOP system, being part of a larger mooring, allows to follow aggregate dynamics at high temporal resolution at different seasons throughout a whole year, using an *in-situ* camera system to determine daily size-distribution, abundance and size-specific sinking velocities of settling particles (Fig. 5.6). During PS136, such system was deployed with the mooring F4S-7 deployment, installed at approx. 496 m. To tackle the particles, a settling cylinder through which particles can sink, a perpendicular camera system recorded image sequences daily. At the bottom of the settling cylinder, collection cups, that were programmed to rotate so each cup, collected material for a certain period. The cups were filled with a viscous gel, which preserves the size and three-dimensional structures of particles sinking into the gel. This makes it possible to identify and quantify different particle types as well as their compositions. After one year of deployment, we recovered the BOP system from the mooring on 7 July 2024 during PS143/2.

We also deployed a new version of the BOP system, which was equipped with two rotating tables and capable of collecting sinking particles in 40 gel-cups and deployed this system with the F4-W5 mooring at station PS143.2_21-1 on 20 July 2024 at 79°00.099'N and 08°58.069'E (for details of the moorings, please, see chapter 3). We aligned the particle sampling with to the sampling of the deep ocean sediment traps, moored on the same mooring, and ensured that we would have several gel cups open for three days each during each collection period of the deep ocean sediment traps. This was to ensure that we would not have particles falling on

top of each other, which would prevent image analyses on the particles collected in the gel traps. We programmed the camera for measurements of particle type, size-distribution, abundance, and sinking velocities to switch on at 12:00 (UTC) and capture one image every four seconds for 28 minutes.

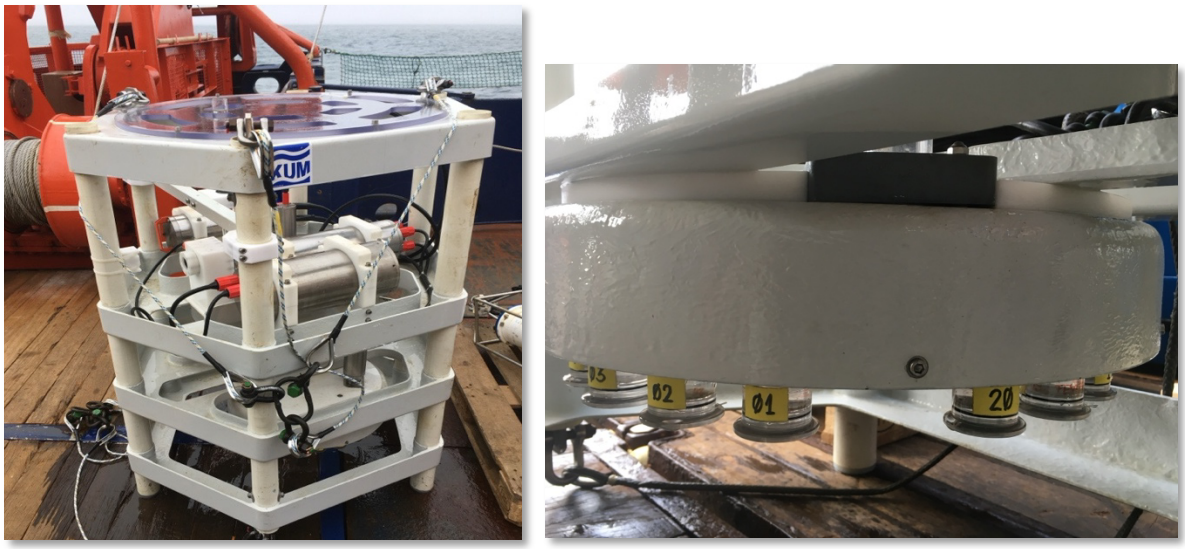

Fig. 5.6: The BOP system with the glass settling column and camera system (left image) and the rotation table with collection cups (right image).

The PEBCAO-team also accomplished the preparation and post-deployment processing of sediment traps and automated water samplers (RAS) deployed on moorings at the stations F4, EGC and Y in the MIZ. Overall, we recovered six sediment-traps, three RAS and deployed seven sediment-traps and two RAS (Tab. 2.1, 2.2, 5.8, 5.9, 5.10).

Tab. 5.8: Recovery of sediment traps during PS143/2

Event	Device-Name	Lat	Long	Depth [m]	Deployment period
1-3	F4S-7	N 79°00.700	E 006°57.720	185	15.06.2023-15-06-2024
1-3	F4S-7	N 79°00.700	E 006°57.720	595	15.06.2023-15-06-2024
59-1	HG IV Fevi 46	N 79°00.015	E 004°19.907	204	15.06.2023-15-06-2024
59-1	HG IV Fevi 46	N 79°00.015	E 004°19.907	2348	15.06.2023-15-06-2024
56-1	EGC8	N 78°59.777	E 005°23.744	501	05.08.2022-15.06.2023
55-1	EGC-9	N 78°58.721	W 005°25.645	442	15.06.2023-15-06-2024
22-9	Lander	N 79°01.849	E 004°13.754	2533	17.06.2023-15.06.2024

Tab. 5.9: Deployment of sediment traps during PS143/2

Event	Device-Name	Lat	Long	Depth [m]	Deployment period
10-1	F4S-8	N 79°00.701	E 007°02.053	190	31.07.2024-31.05.2025
10-1	F4S-8	N 79°00.701	E 007°02.053	603	31.07.2024-31.05.2025
59-2	HGIV Fevi 48	N 70°00.000	E 004°19.911	194	31.07.2024-31.05.2025
59-2	HGIV Fevi 48	N 70°00.000	E 004°19.911	2333	31.07.2024-31.05.2025
57-1	EGC10	N 78°59.783	W 005°23.835	489	31.07.2024-31.05.2025
59-3	Lander	N 79°01.777	E 004°13.317	2530	31.07.2024-31.05.2025

Tab. 5.10: Recovery of Remote Access Sampler (RAS) during PS143/2

Station	Device-Name	Lat	Long	Depth [m]	Deployment period
1-3	RAS – F4-S7	N79° 0.7098	E6° 57.81	23	06/2023 – 05/2024
55-1	RAS - EGC 8	N78° 58.721	W5°25.645	52	08/2022 – 07/2023
56-1	RAS - EGC 9	N 78° 59.78	W5° 23.74	49	06/2023 – 05/2024

Preliminary (expected) results

Biogeochemistry (Benjamin Pontiller, Sophia Hirschmann, Tania Klüver)

Bacterial biomass production (BBP) was determined on board via radioisotope (^{3}H-Leucine) incubations (Fig. 5.7 A and B). Preliminary results showed the highest heterotrophic activity in the surface layer above 30 m depth, with pronounced peaks at the easternmost station (N5TE11) and N5. These BBP peaks coincided with peaks in water temperature (likely Atlantic water inflow) and phytoplankton post-bloom conditions at the time of sampling. In addition, bacterial production measurements along a 79°N transect, sampled in higher resolution, showed high bacterial biomass production between 4°E - 10°E above 40 m depth (Fig. 5.7 C and D).

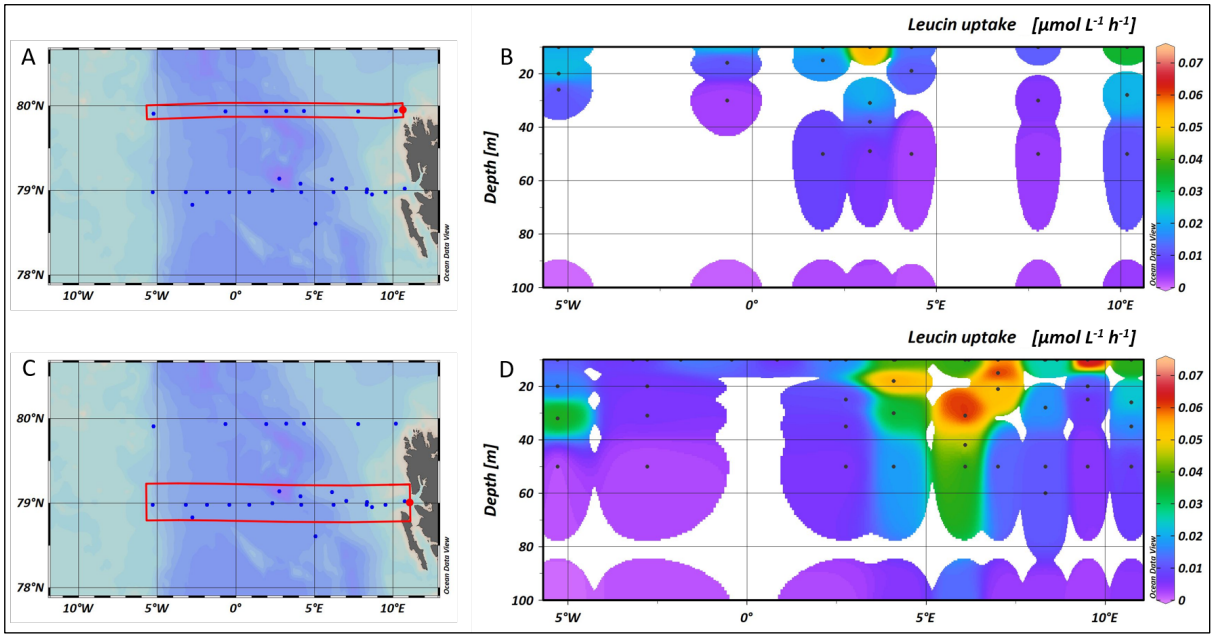

Fig. 5.7: Bacterial biomass production (BBP) along an East-West transect at roughly 80°N (A and B) and an East-West transect at 79°N (C and D): Transects are marked in red and BBP expressed as leucine uptake at in-situ temperature in the upper 100 m. Actual depths from where discrete seawater samples were obtained are marked with black dots.

Preliminary analysis of primary production (PP) measurements considering two different size fractions (POC and DOC) along the 79°N transect showed a similar pattern as BBP (Fig. 5.8 C and D) with the highest bicarbonate incorporation rates above 20 m depth (Fig. 5.8). The fact, that PP_{DOC} was roughly 2-fold higher compared to PP_{POC} at station SV-III, suggests a larger contribution of Cyanobacteria compared to larger phytoplankton (Fig. 5.8 C). Flow Cytometry and 18S metabarcoding results will provide more detailed information on the community composition.

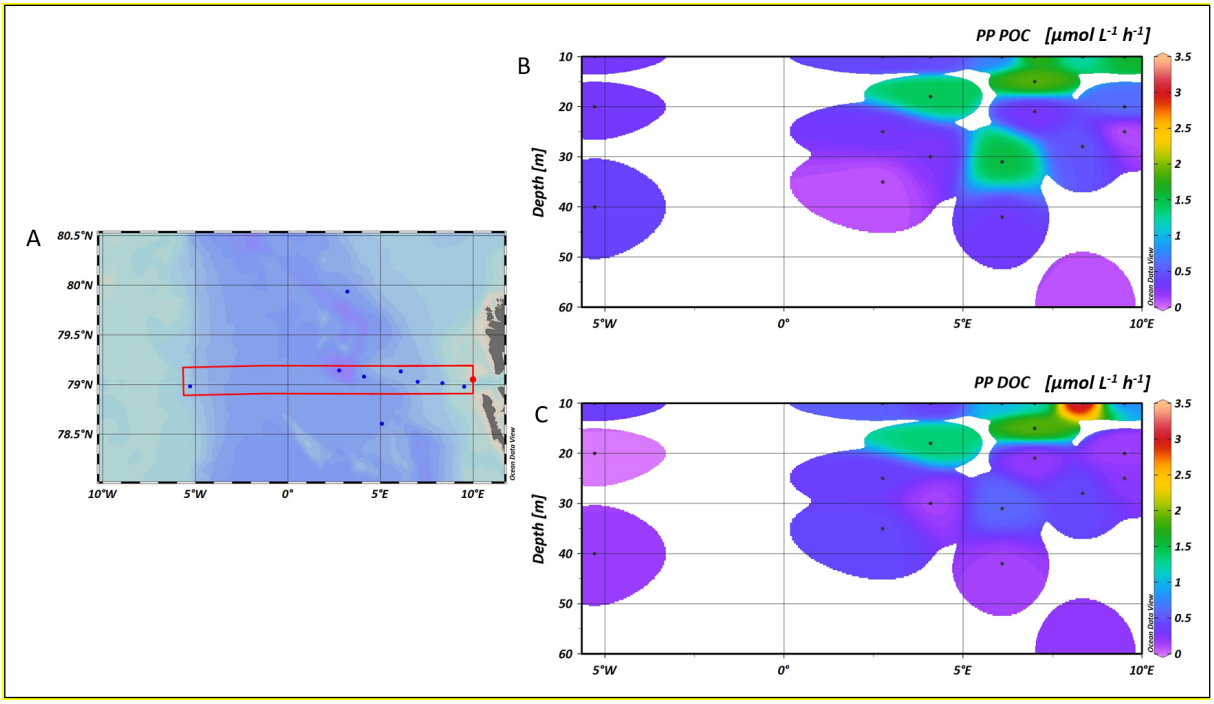

Fig. 5.8: Phytoplankton primary production (PP) along an East-West transect at 79°N: Transect marked in red (A), PP at in-situ temperature in the upper 100 m split into particulate organic carbon (PP POC) (B) and dissolved organic carbon (PP DOC) (C). Actual depths from where discrete seawater samples were obtained are marked with black dots.

Protistian and Microbial Plankton (Katja Metfies, Celina Behrendt, Tabea Galonska, Kerstin Korte, Marlis Reich, Alexandra Kraberg, Eva-Maria Nöthig)

Eukaryotic microbial community composition

The results of the 18S metabarcoding suggests that the eukaryotic community composition was different between different water-masses and areas with different ice-coverage (Fig. 5.9). Similarities between the microbial communities was highest between ice-free water of the West Spitsbergen Current and the Svalbard shelf. The grouping of the stations was done according to previous asignments of stations to watermasses during past studies in the observation area. Significant differences were also observed in eukaryotic microbial community composition between the two cruise legs (Fig. 5.10). Sampling for eDNA took place with an approximate time-lag of ~ 2-4 weeks. The significant differences in community composition between the two cruise legs suggest quick turnover.

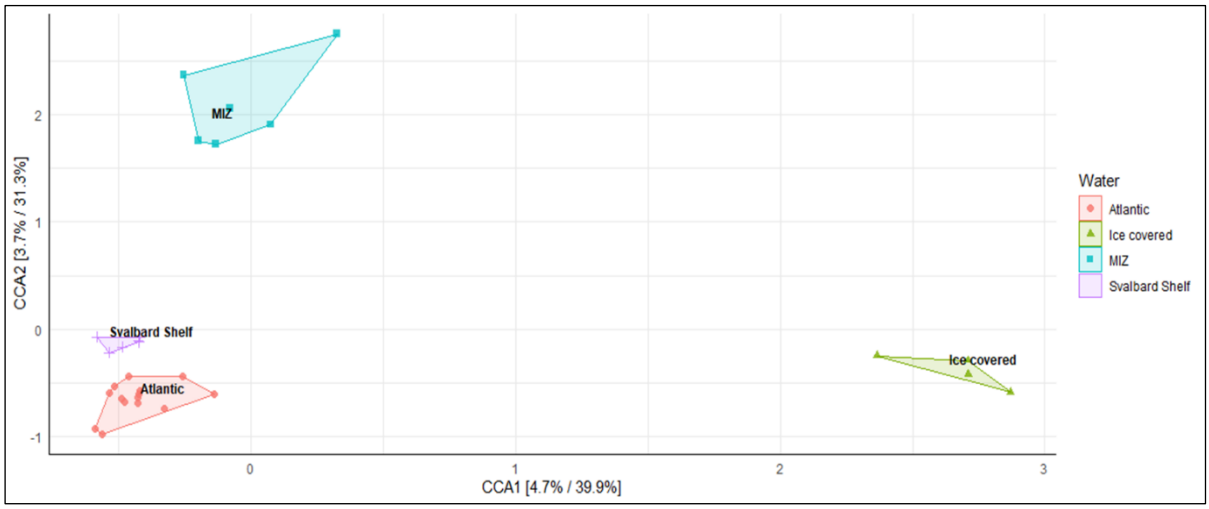

Fig. 5.9: Ordination plot illustrating differences in eukaryotic microbial community composition in different watermasses and with differences in ice-coverage retrieved from 18S metabarcoding sequences. Selected samples were collected at the depth of the Chl a maximum at ice-free stations in Atlantic water (Atlantic), on the Svalbard shelf (Svalbard shelf) and at ice-covered stations in Atlantic water (MIZ) and the East Greenland Current (Ice-covered).

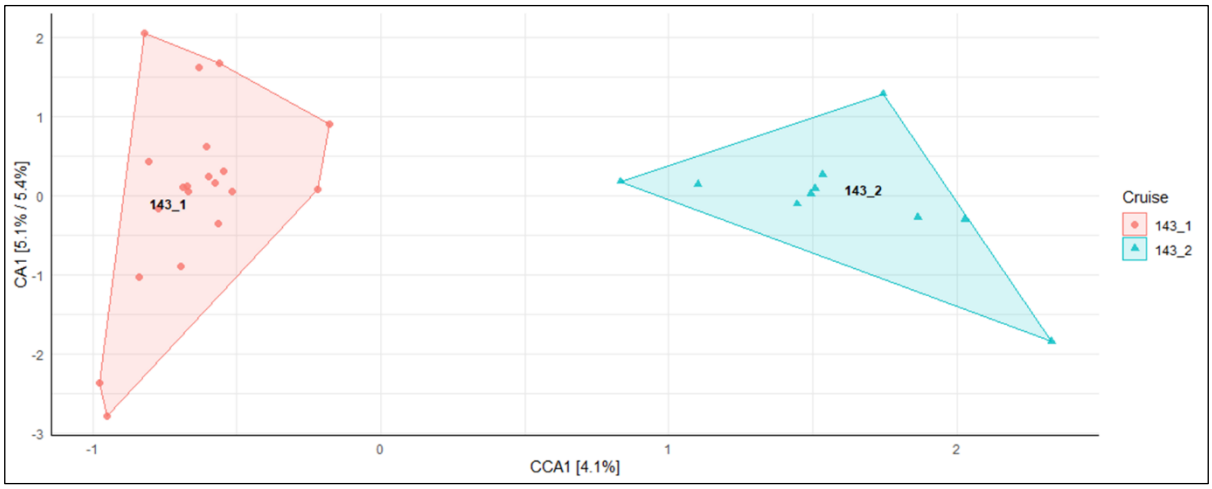

Fig. 5.10: Ordination plot illustrating differences in eukaryotic microbial community composition at the depth of the Chl a max between the two cruise legs of PS143 retrieved from 18S metabarcoding sequences.

Phytoplankton community composition

The net hauls revealed a total of 80 distinct phytoplankton taxa. These were mainly members of centric and pennate diatoms (57 taxa), with some dinoflagellate (14 taxa), ciliate and coccolithophore taxa (2 taxa each) also present. The number of taxa between station varied greatly. In stations N5TE8 and N5TE11 only 12 and 13 taxa were found respectively and were dominated by dinoflagellates. Similarly, Station Svalbard 2 only comprised 15 taxa with a mix of diatoms and dinoflagellates (Fig. 5.11). At station EGI on the other hand, 31 taxa were detected. It has to be noted however, that the data are still very preliminary for all stations and are likely to be revised upwards. Some diatom species, commonly associated with sea ice

were also present. While *M. arctica*, a species that actually grows attached to the ice, appeared to be limited in its distribution to stations in the East Greenland Current and the most northerly stations, others such as Fragilariopsis occurred throughout the sampling area.

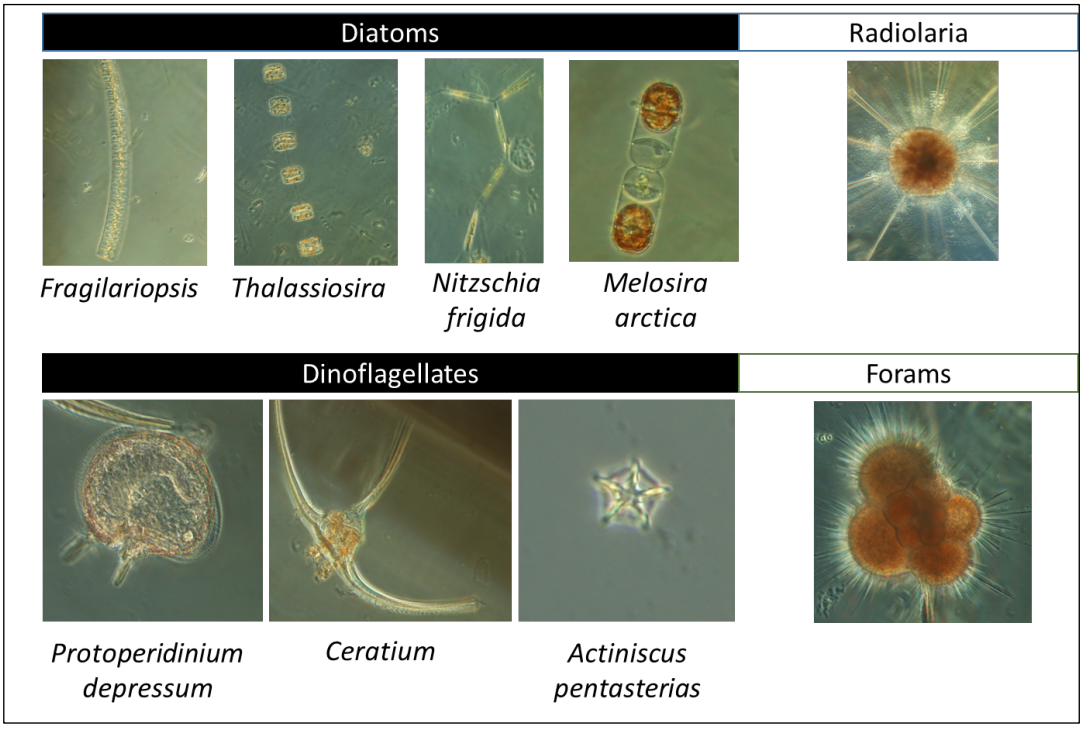

Fig. 5.11: Examples of important phytoplankton (black bars) and Rhizaria (white bars) taxa in the HAUSGARTEN area

One goal of the study was to identify, and bring into culture, parasite host systems (mainly chytrids and oomycetes as well as their hosts and all samples were screened for these taxa. However, parasites appeared to be rare. Only two pennate diatom cells were found to be parasitized, potentially by an oomycete. In addition, several Thalassiosira cells were suspected to contain a parasite. However, this remains to be confirmed in the laboratory (Fig. 5.12).

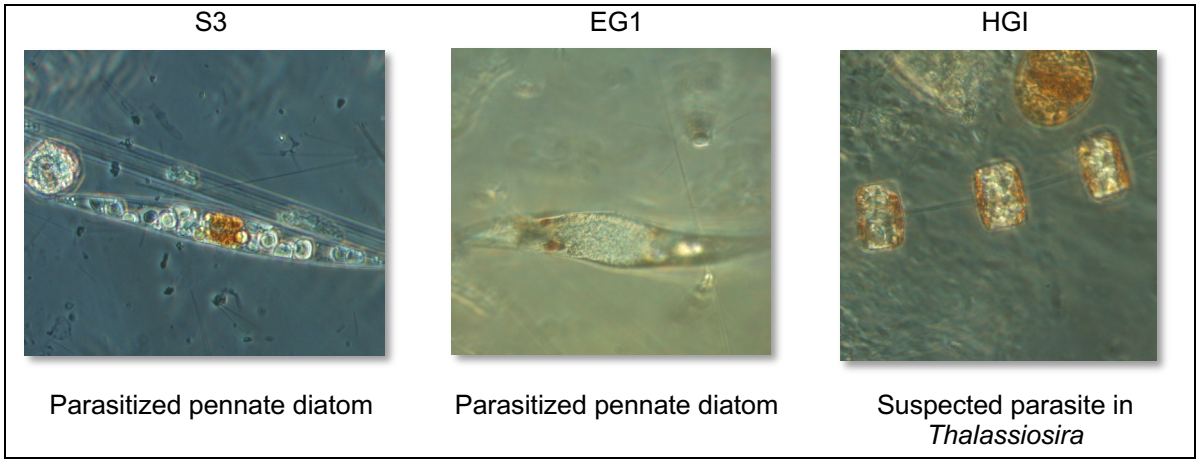

Fig. 5.12: Diatoms confirmed or suspected of harbouring parasites

Zooplankton

The vertical LOKI cast yielded in total 289,983 images and most of those images that presented marine organisms showed copepods, and among these, the cyclopoid family Oncaeidea was the most frequent (Fig. 5.13). In this family, we sometimes observed females carrying egg-sacs, indicating ongoing reproduction. The calanoid copepods were dominated by the large, lipid rich *Calanus* species, mostly *C. finmarchicus*. There were, however, many other taxa that we were also able to identify on the images, for examples representatives of Rhizaria, Pteropoda, Chaetognatha, Euphausiacea, Cnidaria, Polychaeta and Amphipoda (see also Fig. 5.13).

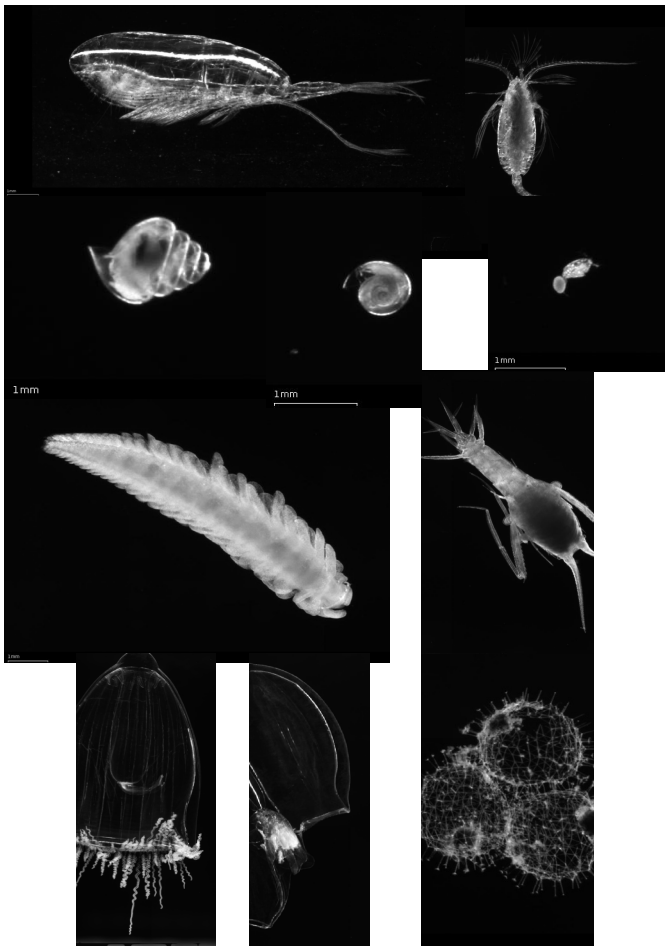

Fig. 5.13: Zooplankton in the Fram Strait on iImages from the optical system LOKI (Lightframe On sight Key species Investigations). Upper row: Calanus hyperboreus, Scaphocalanus major (both calanoid copepods), second row: Limacina helicina, Limacina retroversa (both Gastropoda), Oncaeidae (female with eggs; cyclopoid copepod), third row: Thyphoscolex (Polychaeta), Lanceola clausi (Amphipoda), lower row: Aglantha digitale (Cnidaria), Dimophyes arctica (Cnidaria), Rhizaria.

As to be expected, most organisms were photographed in the upper 50 m of the water column. This finding was supported by the Multinet samples. Here, vials that contained the sample from 50-0m were always the fullest. All samples and image data collected during PS143/2 will be analysed in detail in the laboratories at AWI using semi-automatic image analyses methods to obtain information on biodiversity and distribution of the zooplankton community in relation to environmental conditions (ice cover, depth, temperature, salinity, chlorophyll a concentration).

These data will continue our time series on zooplankton biomass and abundance in the Fram Strait and the Central Arctic Ocean.

Phytooptics (Astrid Bracher, Christian Hohe, Carolin Uhlig)

The continuously measured optical data are used via using semi-analytical techniques to determine the spectrally resolved underwater light attenuation and the concentration of optical constituents, such as Chl *a* concentration of the whole phytoplankton community and the major phytoplankton groups and CDOM absorption. These data are also used together with the data set determined on the discrete water samples regarding pigment concentration and derived phytoplankton group Chl *a* concentration from the HPLC data and the absorption properties, for validating satellite ocean colour retrievals following formerly established procedures for FRAM or other Polarstern cruises (e.g., Cherkasheva et al. 2014; Liu et al. 2018; Soppa et al. 2014; Losa et al. 2017; Xi et al. 2023). We expect this new data set for our long-term measurements to elucidate further changes in the Fram Strait pelagic environment due to Global Change and/or other environmental shifts.

So far, we have obtained the following measurements/data:

- Underway flowthrough measurements:

  25-day (12 July to 5 August 2024) non-stop total and particulate absorption/attenuation measurements of surface water from AC-S. Part of the post-processing completed on bord, processing to particulate absorption, Chl *a* and phytoplankton groups Chl *a* analyzed back at AWI.
- Discrete samples (underway samples see Table 5.11, station samples see Table 5.12):
  a. HPLC pigments: 89 samples from CTDs, 200 samples from Underway. Filters send back to AWI and analyzed in home laboratory.
  b. CDOM absorption: 89 samples from CTDs, 200 samples from Underway. Most measurements were completed and data analysed on board, last 50 samples will be analyzed at AWI.
  c. Particulate, non-alagal and phytoplankton absorption: 89 samples from CTDs, 118 samples from underway. All measurements completed on bord and data processing finalized on bord.
- Station work from light profiler mostly until 100 m (three stations until 120 m, details see Table 5.13):
  d. 19 valid RAMSES underwater hyperspectral radiance and iiradiance profiles. All data have been processed to final AOPs (remote sensing reflectance, diffuse attenuation) on bord.
  e. 19 valid ACS profiles for the total absorption. Processing to total abosorption, Chl *a* and phytoplankton groups Chl *a* will be done back at AWI.
- Triaxus work from hyperspectral sensors:
  f. ~50 valid RAMSES underwater hyperspectral radiance and riradiance profiles.
  g. 19 valid ACS profiles for the total absorption.

On board we finished all measurements, except for the phytoplankton pigment data for which the filters will be analysed in the home laboratory. Additonally, the last 50 CDOM samples could not be measured because of the LWCC system having a broken capillary. From the completed measurements already on bord we analysed the RAMSES station, the LWCC and the QFT particulate, phytoplankton and non-algal absorption data. Further, we processed part of the ACS flowthrough data and the CDOM absorption data.

Tab. 5.11: Positions of underway discrete water samples used for measurements of absorption by phytoplankton, all particles and non-algal particles (PABS) and by CDOM (CDOM) and collected for analysis by High Pressure Liquid Chromatography (HPLC) to determine phytoplankton pigments.

Samp. ID	Date	Time Start	Time End	Latitude [°]	Longitude [°]	no PABS
UW1	2024-07-12	18:00:00	18:03:53	69.83675	19.6242	
UW2	2024-07-12	21:00:00	21:08:17	70.34198	20.5912	
UW3	2024-07-13	00:00:00	00:04:14	70.81882	19.62377	
UW4	2024-07-13	03:01:00	03:03:30	71.2545	18.66165	
UW5	2024-07-13	06:00:00	06:04:00	71.68667	17.68625	
UW6	2024-07-13	09:00:50	09:03:47	72.11832	16.68893	
UW7	2024-07-13	11:59:54	12:03:53	72.54903	15.6704	
UW8	2024-07-13	15:01:18	15:04:22	72.97255	14.60125	
UW9	2024-07-13	18:00:00	18:06:20	73.46165	13.84442	
UW10	2024-07-13	21:00:00	21:05:10	73.97203	13.3144	
UW11	2024-07-14	00:04:11	00:09:56	74.50195	12.74712	
UW12	2024-07-14	03:00:30	03:05:10	74.98368	12.21415	
UW13	2024-07-14	06:02:18	06:07:00	75.49343	11.63227	
UW14	2024-07-14	09:12:03	09:13:55	76.03685	10.98972	
UW15	2024-07-14	12:09:26	12:11:28	76.55983	10.34688	
UW16	2024-07-14	15:00:00	15:01:57	77.03257	9.7449	
UW17	2024-07-14	18:03:00	18:04:55	77.54417	9.06883	
UW18	2024-07-14	21:00:00	21:03:22	78.06358	8.3532	
UW19	2024-07-15	00:00:01	00:01:54	78.57088	7.62403	
UW20	2024-07-15	12:01:00	12:03:00	79.0006	6.90028	
UW21	2024-07-15	22:00:56	22:04:40	79.0027	7.55038	
UW22	2024-07-16	23:59:17	00:01:43	79.0303	7.01043	
UW23	2024-07-16	02:56:14	02:58:00	79.029	7.1142	
UW24	2024-07-16	06:00:00	06:01:45	79.00042	7.01917	
UW25	2024-07-16	10:03:15	10:05:10	79.02315	6.99933	
UW26	2024-07-16	14:30:00	14:31:59	78.70255	5.4976	
UW27	2024-07-17	01:07:18	01:09:10	78.61643	5.03718	
UW28	2024-07-17	02:57:15	02:59:13	78.61725	5.09168	
UW29	2024-07-17	06:08:03	06:09:40	78.91922	6.68623	
UW30	2024-07-17	09:01:40	09:03:20	79.00048	7.0665	
UW31	2024-07-17	12:03:58	12:05:40	79.00037	7.0012	
UW32	2024-07-17	15:23:00	15:24:23	79.0117	7.03408	
UW33	2024-07-17	18:00:00	18:02:30	79.01482	7.86068	
UW34	2024-07-18	02:58:18	03:00:07	79.01578	8.416	
UW35	2024-07-18	06:01:34	06:03:05	79.01683	8.33465	
UW36	2024-07-18	09:04:05	09:05:58	79.0024	8.33637	
UW37	2024-07-18	10:59:28	11:01:30	78.98577	9.21877	
UW38	2024-07-18	21:00:32	21:02:20	78.9816	9.72063	
UW39	2024-07-19	02:59:42	03:01:30	79.01282	9.51415	
UW40	2024-07-19	06:00:00	06:01:30	79.00033	8.33168	
UW41	2024-07-19	10:59:24	11:01:11	79.00353	7.99872	

Samp. ID	Date	Time Start	Time End	Latitude [°]	Longitude [°]	no PABS
UW42	2024-07-19	15:10:26	15:11:11	79.04047	7.44445	
UW43	2024-07-20	03:00:25	03:02:04	78.610885	5.076038	
UW44	2024-07-20	06:05:50	06:07:25	79.135083	6.0062604	
UW45	2024-07-20	09:08:15	09:09:45	79.166585	6.3433224	
UW46	2024-07-20	10:52:00	10:53:00	79.183043	6.2842636	
UW47	2024-07-20	14:00:00	14:01:42	79.011606	6.96848	
UW48	2024-07-20	17:52:50	17:54:20	79.058528	5.014686	
UW49	2024-07-21	05:56:00	05:57:45	79.079069	4.192879	
UW50	2024-07-21	09:12:33	09:14:03	79.048344	4.033213	
UW51	2024-07-22	03:09:10	03:11:17	79.249986	3.324597	
UW52	2024-07-22	05:59:55	06:01:50	79.471436	4.546836	
UW53	2024-07-22	12:14:00	12:17:30	79.572614	5.233125	
UW54	2024-07-22	14:59:00	15:02:05	79.808949	3.985562	
UW55	2024-07-23	03:00:07	03:01:45	79.937842	3.442225	X
UW56	2024-07-23	03:30:00	03:31:26	79.937963	3.721396	X
UW57	2024-07-23	04:00:20	04:01:40	79.940797	3.746659	X
UW58	2024-07-23	04:30:35	04:32:00	79.937614	3.821217	X
UW59	2024-07-23	05:00:00	05:01:20	79.937794	4.126532	
UW60	2024-07-23	05:31:00	05:32:00	79.939823	4.3253	X
UW61	2024-07-23	09:30:10	09:32:00	79.943181	4.362911	X
UW62	2024-07-23	10:08:00	10:11:00	79.940529	4.768636	X
UW63	2024-07-23	10:29:30	10:31:15	79.938767	4.897672	X
UW64	2024-07-23	11:30:00	11:31:15	79.93976	5.17574	X
UW65	2024-07-23	12:00:00	12:01:06	79.937399	5.474358	X
UW66	2024-07-23	13:00:00	13:01:17	79.937244	5.884645	X
UW67	2024-07-23	13:30:00	13:31:40	79.940305	6.043433	
UW68	2024-07-23	14:00:00	14:02:10	79.938398	6.21995	X
UW69	2024-07-23	14:30:20	14:31:54	79.938496	6.615251	X
UW70	2024-07-23	15:30:06	15:31:50	79.941899	6.898072	X
UW71	2024-07-23	16:00:00	16:01:30	79.937751	7.180682	
UW72	2024-07-23	17:00:10	17:01:15	79.938631	7.466858	X
UW73	2024-07-23	21:00:28	21:03:02	79.93783	8.09065	X
UW74	2024-07-23	21:32:23	21:34:39	79.933412	8.278879	
UW75	2024-07-23	22:30:00	22:32:00	79.931556	8.459467	X
UW76	2024-07-23	23:00:00	23:01:58	79.937372	8.751988	X
UW77	2024-07-24	00:00:00	00:01:55	79.92831	8.983915	X
UW78	2024-07-24	00:31:31	00:33:30	79.937212	9.441978	
UW79	2024-07-24	01:30:00	01:32:00	79.939667	9.743277	X
UW80	2024-07-24	02:59:08	03:01:25	79.939089	10.515005	
UW81	2024-07-24	04:00:08	04:02:35	79.966836	10.662938	
UW82	2024-07-24	06:00:00	06:01:30	80.280366	10.236038	
UW83	2024-07-24	09:02:25	09:04:00	80.378391	10.084556	
UW84	2024-07-24	18:04:00	18:05:50	79.938045	9.117595	

Samp. ID	Date	Time Start	Time End	Latitude [°]	Longitude [°]	no PABS
UW85	2024-07-24	21:00:00	21:01:40	79.938108	6.837039	
UW86	2024-07-25	00:00:30	00:02:35	79.938129	4.564392	
UW87	2024-07-25	02:30:00	02:31:30	79.934345	3.188328	
UW88	2024-07-25	03:00:17	03:01:30	79.937606	3.078614	X
UW89	2024-07-25	04:00:18	04:01:28	79.938153	2.765528	X
UW90	2024-07-25	04:30:35	04:31:55	79.937743	2.483025	X
UW91	2024-07-25	05:30:00	05:32:40	79.938134	2.180404	
UW92	2024-07-25	10:00:07	10:01:42	79.937355	1.766237	
UW93	2024-07-25	11:00:05	11:01:46	79.938249	1.316131	
UW94	2024-07-25	12:00:00	12:01:30	79.934693	1.0464	
UW95	2024-07-25	12:30:00	12:32:20	79.934173	0.808969	
UW96	2024-07-25	13:30:00	13:31:40	79.936394	0.879644	
UW97	2024-07-25	14:00:42	14:02:40	79.939916	0.722437	
UW98	2024-07-25	14:30:00	14:31:40	79.935419	0.42838	
UW99	2024-07-25	15:05:45	15:07:40	79.940029	0.150051	X
UW100	2024-07-25	16:00:00	16:01:00	79.930795	-0.119758	X
UW101	2024-07-25	16:30:45	16:31:45	79.909327	-0.412889	X
UW102	2024-07-25	23:00:05	23:01:50	79.958979	-0.887291	
UW103	2024-07-25	23:30:39	23:32:40	79.940132	-1.031247	X
UW104	2024-07-26	00:07:37	00:09:38	79.940112	-1.098498	X
UW105	2024-07-26	00:30:00	00:31:40	79.94824	-1.283897	X
UW106	2024-07-26	01:56:03	01:58:03	79.93924	-1.740152	X
UW107	2024-07-26	02:26:26	02:28:18	79.939824	-2.028818	
UW108	2024-07-26	03:30:00	03:31:35	79.940438	-2.275819	X
UW109	2024-07-26	04:00:00	04:01:00	79.939524	-2.531056	X
UW110	2024-07-26	04:30:30	04:31:30	79.935938	-2.738349	X
UW111	2024-07-26	04:59:10	05:00:10	79.931986	-2.816119	X
UW112	2024-07-26	05:31:00	05:32:30	79.927794	-2.956269	
UW113	2024-07-26	05:59:50	06:00:50	79.926768	-3.218128	X
UW114	2024-07-26	07:00:00	07:01:24	79.920424	-3.146923	X
UW115	2024-07-26	07:32:43	07:33:50	79.94384	-3.347163	X
UW116	2024-07-26	08:00:06	08:01:00	79.940722	-3.41	
UW117	2024-07-26	08:29:30	08:30:00	79.946856	-3.571181	X
UW118	2024-07-26	09:00:00	09:01:17	79.933945	-3.830887	X
UW119	2024-07-26	09:29:16	09:30:16	79.924291	-4.089015	X
UW120	2024-07-26	10:31:30	10:32:30	79.924851	-4.72446	X
UW121	2024-07-26	18:00:00	18:01:20	79.711653	-5.542253	
UW122	2024-07-26	21:00:04	21:01:50	79.480732	-5.093785	
UW123	2024-07-26	00:01:01	00:02:35	79.278069	-4.611563	
UW124	2024-07-27	02:56:20	02:57:28	79.08071	-5.177009	
UW125	2024-07-27	06:00:00	06:01:30	78.979655	-5.433425	
UW126	2024-07-27	09:00:00	09:01:00	78.984343	-5.486555	
UW127	2024-07-27	12:00:20	12:02:25	78.999644	-5.409027	

Samp. ID	Date	Time Start	Time End	Latitude [°]	Longitude [°]	no PABS
UW128	2024-07-27	19:07:20	19:09:17	78.971771	-5.295378	
UW129	2024-07-27	23:56:56	23:59:39	78.976079	-5.349804	
UW130	2024-07-28	03:02:54	03:04:55	78.985532	-5.488049	
UW131	2024-07-28	05:59:25	06:01:20	78.978506	-5.42843	
UW132	2024-07-28	15:00:00	15:01:50	79.010692	-5.17376	
UW133	2024-07-28	17:02:30	17:04:20	79.000337	-6.207681	
UW134	2024-07-28	18:00:00	18:01:40	78.988081	-6.462177	
UW135	2024-07-28	21:00:00	21:01:50	78.98248	-4.882398	
UW136	2024-07-28	00:00:00	00:01:50	78.982744	-3.214976	
UW137	2024-07-29	02:57:53	03:00:00	79.013453	-2.025924	
UW138	2024-07-29	05:59:50	06:01:40	79.055781	-0.130017	
UW139	2024-07-29	09:13:50	09:15:25	79.051937	1.55372	
UW140	2024-07-29	13:09:25	13:11:22	79.080717	4.092454	
UW141	2024-07-29	15:04:50	15:05:45	78.997181	4.353936	
UW142	2024-07-29	21:00:00	21:02:06	79.034098	4.172667	
UW143	2024-07-30	00:00:00	00:01:45	79.040393	4.209894	
UW144	2024-07-30	02:58:37	03:01:00	79.061952	4.292129	
UW145	2024-07-30	06:00:36	06:01:58	79.135138	4.880495	
UW146	2024-07-30	09:18:25	09:19:50	79.104751	5.04597	
UW147	2024-07-30	11:58:45	12:00:30	79.00361	5.662704	
UW148	2024-07-30	15:25:40	15:27:10	79.00003	5.666787	
UW149	2024-07-30	23:59:20	00:01:30	79.012943	7.083503	
UW150	2024-07-31	03:02:43	03:05:08	78.982761	6.939939	
UW151	2024-07-31	11:00:16	11:01:50	78.931867	8.033128	
UW152	2024-07-31	11:55:46	11:57:30	78.932307	8.510489	X
UW153	2024-07-31	13:00:33	13:03:26	78.951385	8.656659	X
UW154	2024-07-31	14:00:00	14:02:46	78.983482	8.339781	
UW155	2024-07-31	15:00:20	15:03:30	78.983792	7.410409	X
UW156	2024-07-31	16:01:00	16:03:30	78.983888	7.009007	X
UW157	2024-07-31	17:00:02	17:01:42	78.983826	6.25654	
UW158	2024-07-31	18:00:00	18:01:30	78.982444	5.441268	X
UW159	2024-07-31	19:00:00	19:03:20	78.983684	5.044423	X
UW160	2024-07-31	20:00:52	20:02:35	78.983587	4.118566	
UW161	2024-07-31	21:02:10	21:04:00	78.983103	3.75005	X
UW162	2024-07-31	22:02:06	22:04:10	78.982245	2.825373	X
UW163	2024-07-31	23:00:04	23:01:58	78.981767	2.316667	
UW164	2024-07-31	23:56:50	23:59:22	78.981559	2.052612	X
UW165	2024-08-01	00:58:08	01:00:29	78.981586	1.439226	X
UW166	2024-08-01	01:57:10	01:59:25	78.981635	0.862476	
UW167	2024-08-01	03:03:42	03:06:02	78.975402	0.739498	X
UW168	2024-08-01	03:59:24	04:01:44	78.981851	0.184048	X
UW169	2024-08-01	05:00:00	05:01:30	78.982241	-0.420943	
UW170	2024-08-01	05:59:35	06:01:12	78.983832	-0.83103	X

Samp. ID	Date	Time Start	Time End	Latitude [°]	Longitude [°]	no PABS
UW171	2024-08-01	07:01:05	07:02:30	78.982244	-1.235206	X
UW172	2024-08-01	07:59:50	08:01:10	78.982264	-1.83359	
UW173	2024-08-01	09:03:20	09:03:45	78.983641	-2.389762	X
UW174	2024-08-01	09:59:45	10:01:20	78.98324	-2.588015	X
UW175	2024-08-01	11:00:13	11:02:25	78.983186	-3.176761	
UW176	2024-08-01	12:00:10	12:02:03	78.980223	-3.83882	X
UW177	2024-08-01	13:01:15	13:02:52	78.982057	-4.502165	X
UW178	2024-08-01	21:00:00	21:01:40	78.887153	-3.844717	
UW179	2024-08-02	14:17:54	14:20:04	78.830515	-2.724763	
UW180	2024-08-02	18:00:00	18:02:00	78.723979	-2.431012	
UW181	2024-08-02	21:00:20	21:02:15	78.538188	-1.755554	
UW182	2024-08-03	00:00:00	00:02:00	78.196378	-0.540467	
UW183	2024-08-03	02:58:38	03:00:00	77.806244	0.808125	
UW184	2024-08-03	06:04:15	06:06:30	77.431152	2.063655	
UW185	2024-08-03	08:58:20	09:00:00	77.1238	3.063566	
UW186	2024-08-03	12:03:28	12:05:30	76.800111	4.092586	
UW187	2024-08-03	15:03:10	15:04:55	76.477055	5.096391	
UW188	2024-08-03	18:00:04	18:01:40	76.164763	6.043328	
UW189	2024-08-03	21:03:00	21:04:25	75.846354	6.988567	
UW190	2024-08-04	00:00:04	00:02:06	75.535639	7.889193	
UW191	2024-08-04	03:02:18	03:04:00	75.215021	8.801076	
UW192	2024-08-04	05:57:20	05:59:00	74.904444	9.664731	
UW193	2024-08-04	09:30:30	09:32:02	74.533211	10.675505	
UW194	2024-08-04	12:00:00	12:01:30	74.275434	11.363352	
UW195	2024-08-04	16:13:22	16:14:48	73.829879	12.52705	
UW196	2024-08-04	18:00:02	18:01:20	73.64193	13.008309	
UW197	2024-08-04	21:00:40	21:02:10	73.318876	13.812805	
UW198	2024-08-04	23:58:58	00:00:35	73.004537	14.566829	
UW199	2024-08-05	02:59:40	03:01:00	72.678755	15.358951	
UW200	2024-08-05	06:07:45	06:09:20	72.352709	16.137615	

Tab. 5.12: List of date, time, sample depth of Phytooptics discrete water samples at CTD Stations including the HAUSGARTEN longterm observation name (LTO-Name) with measurements of absorption by phytoplankton, all particles and non-algal particles (PABS) and by CDOM (CDOM) and collected for analysis by High Pressure Liquid Chromatography (HPLC) to determine phytoplankton pigments.

Station	LTO-Name	Sampled Depths [m]	Latitude [°]	Longitutde [°]	HPLC	CDOM	PABS
PS143/2_1-1	test	10,23,50,100	79.00698	6.94154	X	X	X
PS143/2_2-6	SV4	10,15,21,49,100	79.02916	7.00254	X	X	X
PS143/2_7-6	S3	10,30,40,50,100	78.60916	5.056	X	X	X
PS143/2_11-1	SV3	10,25,30,50,100	79.0169	8.33718	X	X	X
PS143/2_14-1	SV2	10,20,25,50,100	78.98054	9.50676	X	X	X

Station	LTO-Name	Sampled Depths [m]	Latitude [°]	Longitutde [°]	HPLC	CDOM	PABS
PS143/2_15-1	SV1	10,26,35,50,100	79.02362	10.72568	X	X	X
PS143/2_18-7	HG1	10,31,42,50,100	79.13418	6.09122	X	X	X
PS143/2_21-6	HG4	10,18,30,50,100	79.08046	4.0913	X	X	X
PS143/2_23-4	HG9	10,25,35,50,100	79.14306	2.75148	X	X	X
PS143/2_25-7	N5	10,31,38,49,100	79.937717	3.193467	X	X	X
PS143/2_27-1	N5TE3	2,10,19,50,100	79.940501	4.325098	X	X	X
PS143-2_33-1	N5TE8	1,10,30,50,100	79.937619	7.758113	X	X	X
PS143/2_40-1	N5TE11	2,10,28,50,100	79.938918	10.172684	X	X	X
PS143/2_44-1	N5TW3	1,10,15,50,100	79.937691	1.916306	X	X	X
PS143/2_48-2	N5TW7	1.1,9,16,30,100	79.935741	-0.668457	X	X	X
PS143/2_54-1	N5TW14	2,10,20,26,100	79.912332	-5.249412	X	X	X
PS143/2_62-1	F5	10,20,30,50,100	78.990584	5.668927	X	X	X
PS143/2_75-1	EGC-I	10,20,32,50,100	78.983172	-5.290478	X	X	X
PS143/2_76-1	EGC-IV	10,20,31,50,100	78.832849	-2.795114	X	X	X

Tab. 5.13: Station positions and max. depth of profiling for hyperspectral upwelling and downwelling radiation in the water with the RAMSES radiometers and for hyperspectral total absorption and attenuation with the ACS spectrophotomter. At PS143/2-33 (NSTE8) no measurements were taken because the data logger was broken.

Station	LTO-Name	Device	Latitude [°]	Longitutde [°]	Max depth (m)
PS143/2_2-5	SV4	RAMSES, ACS	79.028065	7.002645	100
PS143/2_7-3	S3	RAMSES, ACS	78.607608	5.063504	120
PS143/2_11-3	SV3	RAMSES, ACS	79.016796	8.333137	120
PS143/2_14-3	SV2	RAMSES, ACS	78.980828	9.511345	120
PS143/2_15-2	SV1	RAMSES, ACS	79.02491	10.726819	100
PS143/2_18-4	HG1	RAMSES, ACS	79.13352	6.092405	100
PS143/2_22-4	HG4	RAMSES, ACS	79.080516	4.08591	100
PS143/2_23-3	HG9	RAMSES, ACS	79.143126	2.757244	100
PS143/2_25-4	N5	RAMSES, ACS	79.937725	3.195005	100
PS143/2_27-2	N5TE2	RAMSES, ACS	79.941287	4.317117	100
PS143/2_40-6	N5TE11	RAMSES, ACS	79.939046	10.176841	100
PS143/2_44-3	N5TW3	RAMSES, ACS	79.934785	1.915804	100
PS143/2_48-3	N5TW7	RAMSES, ACS	79.936016	-0.68297	100
PS143/2_54-4	N5TW14	RAMSES, ACS	79.90941	-5.250629	100
PS143/2_56-5	EGC-I	RAMSES, ACS	78.972468	-5.283722	100
PS143/2_62-2	F5	RAMSES, ACS	78.99063	5.667311	100
PS143/2_76-3	EGC-IV	RAMSES, ACS	78.8296	-2.772973	100

From the measurements of the QFT-ICAM we calculated the total particulate, phytoplankton and non-algal absorption and the absorption line height at 676 nm (aLH). From the later we obtained a proxy for the chlorophyll-a concentrations (Chl *a*), following Roesler and Barnard (2013) using the coefficients from Liu et al. (2018) determined for the Fram Strait (Chl *a* proxy

= 57.5 * ($aLH^{0.91}$). Fig. 5.15 shows the results of derived Chl *a* conc. for the underway measurements sampled for the entire PS143/2 transect. Maximum Chl *a* was measured in the Atlantic waters of the Fram Strait at the beginning of the cruise and close to Svalbard Coast. Around the east Greenland Crueent and at the Western side of the transect back to Tromsö Chl *a* is also quite low. The chlorophyll-concentration was also determined for the water samples from the CTD station which is shown in Fig. 5.16. Highest biomass is found around 2 mg/m^3 at 0-30m for SV4 and the test station close to SV4. Compared to former years Chl *a* is rather low and indicates post-bloom conditions. Chl *a* concentration results from the QFT particulate absorption data sampled at the high densly north-transect between 23 to 26 July are shown in Fig. 5.17. It shows highest Chl *a* conc. of 1.9 and 1.7 mg/m^3 at subsurface at 20 and 30 m and lower at surface with 0.5 and 0.9 Chl *a* mg/m^3 in the at stations NSTW7 and NSTE2, respectively.

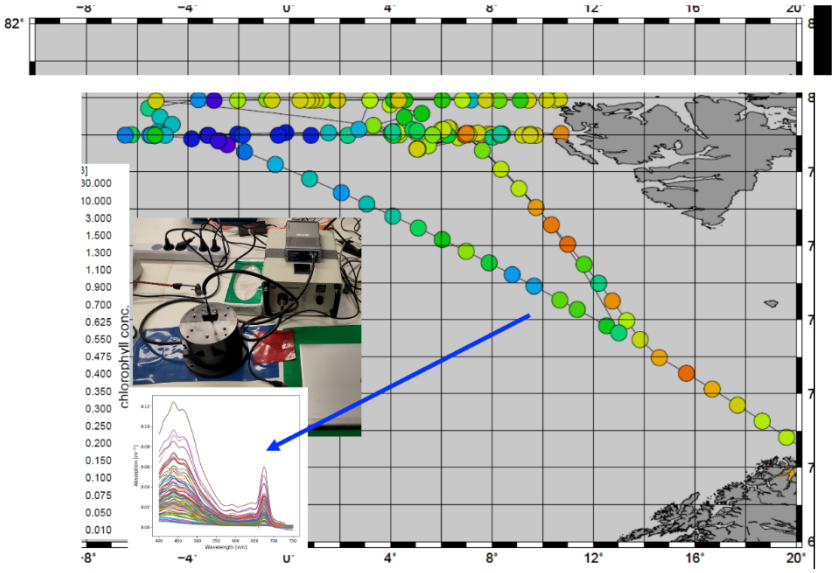

Fig. 5.15: Chl a along the PS143-2 cruise track estimated from particulate absorption, measured with the QFT-ICAM technique, used to determine the absorption line height at 676 nm following Roesler and Barnard (2013 and using vcoefficients from Liu et al. (2018). On the left all particulate absorption spectra and a photograph of the set-up of QFT-ICAM system are shown.

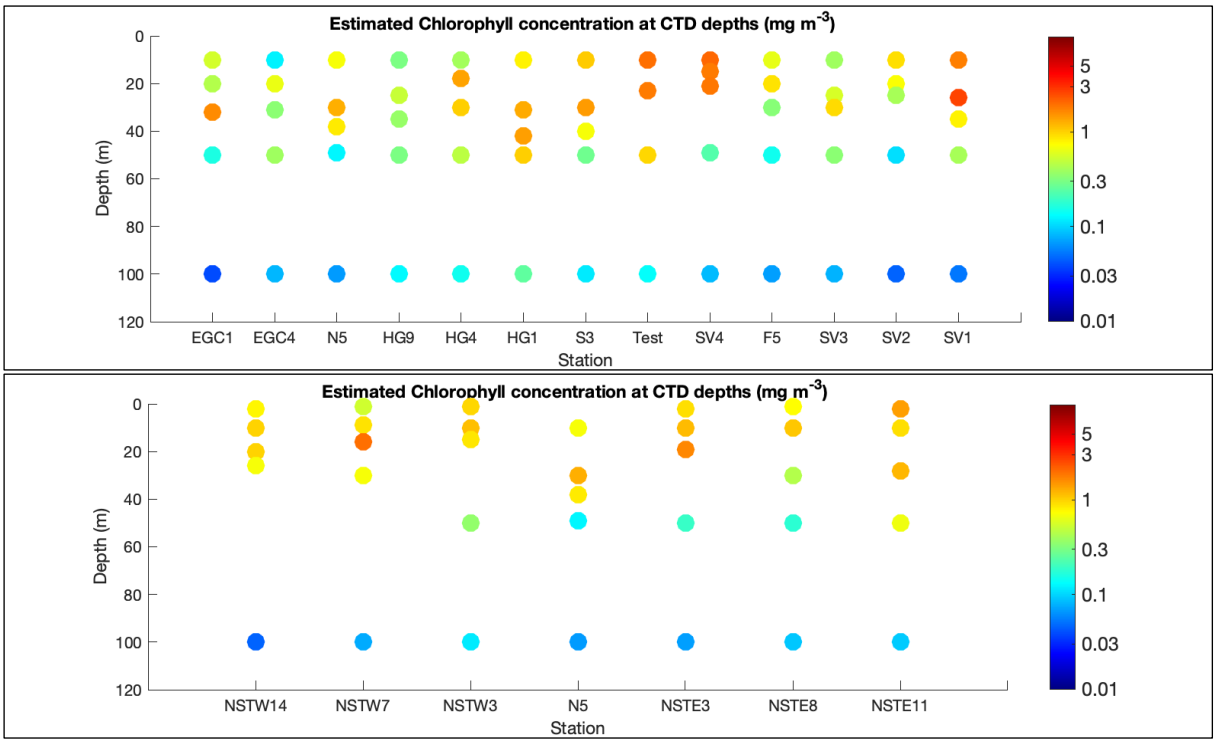

Fig. 5.16: Chl a at the PS143/2 HAUSGARTEN stations and a test station near by (upper panel) and at the high resolution North transect at 79°59' (lower panel) estimated from particulate absorption, measured with the QFT-ICAM technique (Röttgers et al. 2016), used to determine the absorption line height at 676 nm following Roesler and Barnard (2013) using coefficients from Liu et al. (2018).

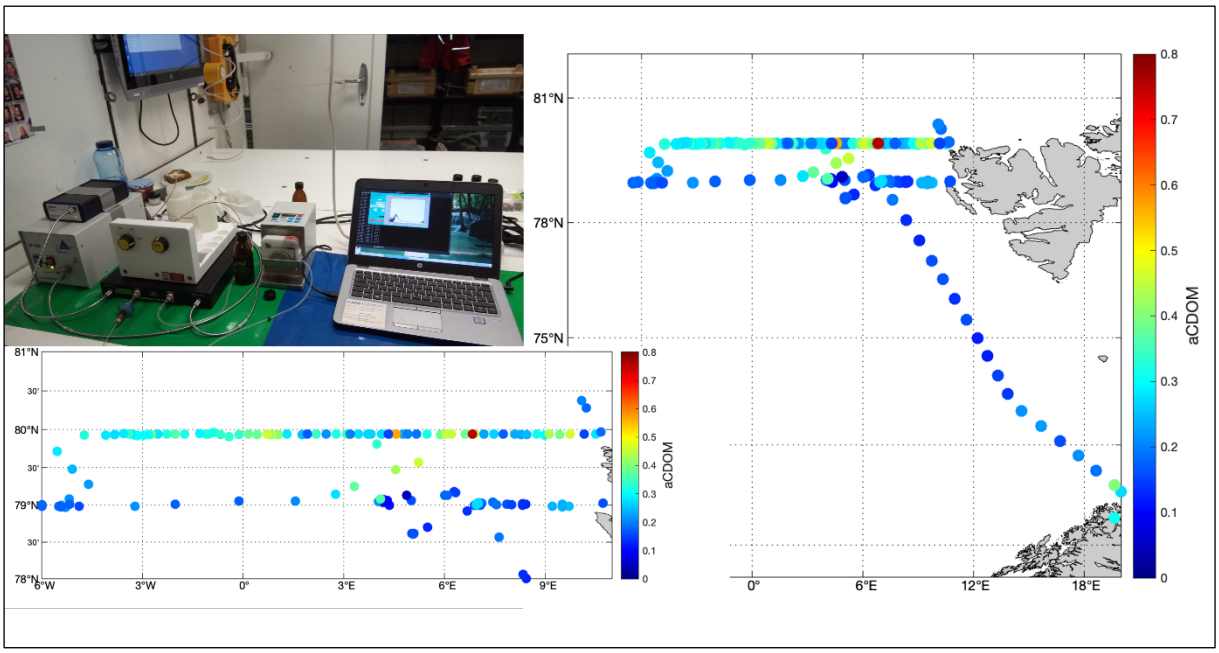

Fig. 5.17: CDOM absorption (uncorrected for salinity) at 440 nm measured with the LWCC technique (following Levering et al. 2017 adapted in Alvarez et al. 2022) along the PS143-2 cruise track.

Finally, preliminary results from the discrete water sample CDOM measurements (uncorrected for salinity) show low CDOM absorption at 440 nm in the Atlantic waters at 10-11m, much higher values at the northern transect at 79°59' where polar waters have reached the surface. The final data set in consideration of the temperature and salinity measurements taken at the CTD stations and from the thermosalinograph will probably enable to identify clearly the different water masses.

Recovery of autonomous sampling devices (Christian Konrad, Katja Metfies, Morten Iversen)

All 40 cups of the BOB system had rotated into their programmed position and all contained material. Thus, the BOP system was able to capture settling particles over one year and at all seasons. Unfortunately, however, the camera system did not capture any images during the deployment. The is reason might be a problem with the timing circuit, and this will be investigated in detail later in the lab after the return of the equipment.

Of the six sediment traps that had been recoverd, five had functioned properly, collecting material over the year (Fig. 5.18). One trap did not collect any material, and we will need to clarify why this trap did not function in the laboratory.

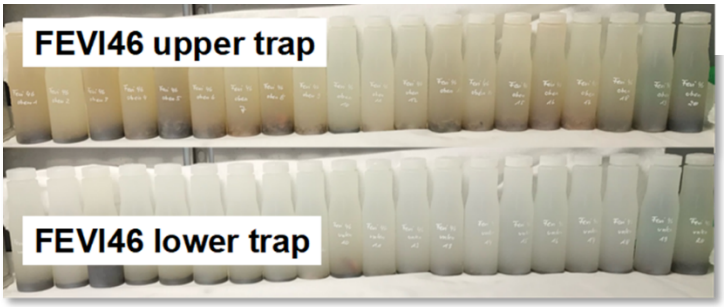

Fig. 5.18: Sediment traps samples collected between 15.06.2023-15-06-2024 by an upper trap moored in 204 m depth and a lower trap moored in 2,318 m depth

Data management

Environmental data will be archived, published and disseminated according to international standards by the World Data Center PANGAEA Data Publisher for Earth & Environmental Science (https://www.pangaea.de) within two years after the end of the cruise at the latest. By default, the CC-BY license will be applied.

Molecular data (DNA and RNA data) will be archived, published and disseminated within one of the repositories of the International Nucleotide Sequence Data Collaboration (INSDC, www.insdc.org) comprising of EMBL-EBI/ENA, GenBank and DDBJ).

Image data will be uploaded to the web-site EcoTaxa (https://ecotaxa.obs-vlfr.fr/) and archived.

Any other data will be submitted to an appropriate long-term archive that provides unique and stable identifiers for the datasets and allows open online access to the data.

This expedition was supported by the Helmholtz Research Programme "Changing Earth – Sustaining our Future" Topic 6, Subtopics 6.1, 6.2, and 6.3.

In all publications based on this expedition, the **Grant No. AWI_PS143/2_04** will be quoted and the following publication will be cited:

Alfred-Wegener-Institut Helmholtz-Zentrum für Polar- und Meeresforschung (2017) Polar

References

Artigas F, Créach V, Houliez E; Karlson B, Lizon F, Seppälä J, Wacquet G (2019) Novel methods for automated in situ observations of phytoplankton diversity and productivity: synthesis of exploration, inter comparisons and improvements. WP 3 - D3.2. https://www.jerico-ri.eu/previous-project/jerico-next/deliverables/, checked on 3/11/2024

Aksenov Y, Popova EE, Yool A, Nurser AJG, Williams TD, Bertino L, Bergh J (2017) On the future navigability of Arctic sea routes: High-resolution projections of the Arctic Ocean and sea ice. Mar Pol, 75:300–317

Bachy C, Sudek L, Choi CF, Eckmann CA, Nöthig EM, Metfies K, Worden AZ (2022) Phytoplankton Surveys in the Arctic Fram Strait Demonstrate the Tiny Eukaryotic Alga Micromonas and Other Picoprasinophytes Contribute to Deep Sea Export. In Microorganisms 10. https://10.3390/microorganisms10050961

Bracher A, Vountas M, Dinter T, Burrows JP, Röttgers R, Peeken I (2009) Quantitative observation of cyanobacteria and diatoms from space using PhytoDOAS on SCIAMACHY data. Biogeosciences 6: 751-764, https://doi.org/10.5194/bg-6-751-2009

Buaya A, Kraberg A, Thines M (2019) Dual culture of the oomycete *Lagenisma coscinodisci* Drebes and Coscinodiscus diatoms as a model for plankton/parasite interactions. Helgoland Mar Res 73:2. https://doi.org/10.1186/s10152-019-0523-0

Cherkasheva A, Nöthig E-M., Bauerfeind E, Melsheimer C, Bracher A (2013) From the chlorophyll-a in the surface layer to its vertical profile: a Greenland Sea relationship for satellite applications. Ocean Sci 9: 431-445

Cherkasheva A, Bracher A, Melsheimer C, Köberle C, Gerdes R, Nöthig E-M, Bauerfeind E, Boetius A (2014) Influence of the physical environment on phytoplankton blooms: a case study in the Fram Strait. Journal of Marine Systems 132: 196-207. https://10.1016/j.jmarsys.2013.11.008

Cornils A, Thomisch K, Hase J, Hildebrandt N, Auel H, Niehoff B (2022) Testing the usefulness of optical data for zooplankton long-term monitoring: Taxonomic composition, abundance, biomass, and size spectra from ZooScan image analysis. Limnol Oceanogr: Methods 20(7):428–450. https://doi.org/10.1002/lom3.10495

Engel A, Bracher A, Dinter T, Endres S, Grosse J, Metfies K, Peeken I, Piontek J, Salter I, Nöthig E.-M (2019) Inter-annual variability of organic carbon concentrations across the Fram Strait (Arctic Ocean) during summer 2009 -2017. Frontiers Mar Sci 6:187.

Fadeev E, Rogge A, Ramondenc S, Nöthig E-M, Wekerle C, Bienhold C, Salter I, Waite A, Hehemann L, Boetius A, Iversen M (2021) Sea ice presence is linked to higher carbon export and vertical microbial connectivity in the Eurasian Arctic Ocean, Communications Biol 4:1255. https://doi.org/10.1038/s42003-021-02776-w

Gonçalves-Araujo R, Granskog M A, Bracher A, Azetsu-Scott K, Dodd PA, Stedmon CA (2016) Using fluorescent dissolved organic matter to trace and distinguish the origin of Arctic surface waters. Sci Rep 6:33978. https//doi.org/10.1038/srep33978

Hardge K, Peeken I, Neuhaus S, Krumpen T, Stoeck T, Metfies K (2017) Sea ice origin and sea ice retreat as possible drivers of variability in Arctic marine protist composition. Mar Ecol Prog Ser 571:43–57.

Hassett BT, Borrego EJ, Vonnahme TR, et al (2019a) Arctic marine fungi: biomass, functional genes, and putative ecological roles. ISME J 13:1484–1496. https://doi.org/10.1038/s41396-019-0368-1

Hassett BT, Thines M, Buaya A, et al. (2019b) A glimpse into the biogeography, seasonality, and ecological functions of arctic marine Oomycota. IMA Fungus 10:6. https://doi.org/10.1186/s43008-019-0006-6

Heinrichs ME, Piedade GJ, Popa O, Sommers P, Tubl G, Weissenbach J, Rhalff J (2024) Breaking the Ice: A Review of Phages in Polar Ecosystems. Methods in Molecular Biology 2738:31--71. https://doi.org/10.1007/978-1-0716-3549-03/TABLES/1

Houliez E, Lizon F, Thyssen M, Artigas L F, Schmitt FG (2012) Spectral fluorometric characterization of Haptophyte dynamics using the FluoroProbe: an application in the eastern English Channel for monitoring Phaeocystis globosa. J Plankton Res 34:136–151. https://doi.org/10.1093/plankt/fbr091

Gradinger RR, Baumann MEM (1991) Distribution of phytoplankton communities in relation to the large-scale hydrographical regime in the Fram Strait. Mar Biol, 111:311–321.

Kraft A, Nöthig EM, Bauerfeind E, Wildish DJ, Pohle GW, Bathmann UV, Beszczynska-Möller A, Klages M (2013) First evidence of reproductive success in a southern invader indicates possible community shifts among Arctic zooplankton. Mar Ecol Prog Ser, 493:291–296.

Krumpen T, Belter HJ, Boetius A, Damm E, Haas C, Hendricks S, Nicolaus M. Nöthig EM, Paul S, Peeken I, Ricker R, Stein R (2019) Arctic warming interrupts the Transpolar Drift and affects long-range transport of sea ice and ice-rafted matter. Sci Rep-Uk, 9. https://doi.org/10.1038/s41598-019-41456-y

Lalande C, Nöthig EM, Fortier L (2019) Algal Export in the Arctic Ocean in Times of Global Warming. Geophys Res Let, 46:5959–5967.

Liu Y, Roettgers R, Ramírez-Pérez M, Dinter T, Steinmetz F, Noethig EM, Hellmann S, Wiegmann S, Bracher A (2018) Underway spectrophotometry in the Fram Strait (European Arctic Ocean): a highly resolved chlorophyll *a* data source for complementing satellite ocean color. Optics Express 26:A678–A698.

Liu Y, Boss E, Chase AP, Xi H, Zhang X, Röttgers R, Pan Y, Bracher A (2019) Retrieval of phytoplankton pigments from underway spectrophotometry in the Fram Strait. Remote Sensing 11:318.

Losa S, Soppa MA, Dinter T, Wolanin A, Brewin RJW, Bricaud A, Oelker J, Peeken I, Gentili B, Rozanov VV, Bracher A (2017) Synergistic exploitation of hyper- and multispectral precursor Sentinel measurements to determine Phytoplankton Functional Types at best spatial and temporal resolution (SynSenPFT). Frontiers in Mar Sci 4:203.

Massicotte P, Peeken I, Katlein C, Flores H, Huot Y, Castellani G, Arndt S, Lange BA; TremblayJE, Babin M (2019) Sensitivity of Phytoplankton Primary Production Estimates to Available Irradiance Under Heterogeneous Sea Ice Conditions. J Geophys Res-Oceans 124:5436–5450.

Metfies K, von Appen WJ, Kilias E, Nicolaus A, Nöthig EM (2016) Biogeography and photosynthetic biomass of Arctic marine pico-eukaryotes during summer of the record sea ice minimum 2012. PLoS ONE 11.

Nöthig EM, Bracher A., Engel A, Metfies K, Niehoff B, Peeken I. et al. (2015) Summertime plankton ecology in Fram Strait - a compilation of long- and short-term observations. Polar Research 34. https://10.3402/polar.v34.23349

Nöthig E-M, Ramondenc S, Haas A, Hehemann L, Walter A, Bracher A, Lalande C, Metfies K, Peeken I, Bauerfeind E and Boetius A (2020) Summertime Chlorophyll a and Particulate Organic Carbon Standing Stocks in Surface Waters of the Fram Strait and the Arctic Ocean (1991–2015). Front Mar Sci 7:35.

Oelker J, Losa SN, Richter A, Bracher A (2022) TROPOMI-retrieved underwater light attenuation in three spectral regions in the ultraviolet to blue. Front Mar Sci 9:787992. https://10.3389/fmars.2022.787992

Oldenburg E, Popa O, Wietz M, von Appen WJ, Torres-Valdes S, Bienhold C, Ebenhöh O, Metfies K (2024) Sea-ice melt determines seasonal phytoplankton dynamics and delimits the habitat of temperate Atlantic taxa as the Arctic Ocean atlantifies, ISME communications, ycae027. https://doi.org/10.1101/2023.05.04.539293

Röttgers R, Doxaran D, Dupouy D (2016), Quantitative filter technique measurements of spectral light absorption by aquatic particles using a portable integrating cavity absorption meter (QFT-ICAM), Opt. Express 24(2):A1–A20.

Schoemann V, Becquevort S, Stefels J, Rousseau V, Lancelot C (2005) *Phaeocystis* blooms in the global ocean and their controlling mechanisms: a review. J Sea Res 53 (1-2):43–66. https://10.1016/j.seares.2004.01.008

Schröter F, Havermans C, Kraft A, Knüppel N, Beszczynska-Möller A, Bauerfeind E and Nöthig E-M (2019) Pelagic Amphipods in the Eastern Fram Strait With Continuing Presence of *Themisto compressa* Based on Sediment Trap Time Series. Front Mar Sci 6:11.

Soltwedel T (2023) The Expedition PS136 of the Research Vessel POLARSTERN to the Fram Strait in 2023. In Berichte zur Polar- und Meeresforschung = Reports on polar and marine research 780. https://10.57738/BzPM_0780_2023

Soppa M A, Hirata T, Silva B, Dinter T, Peeken I, Wiegmann S, Bracher A (2014) Global retrieval of diatoms abundance based on phytoplankton pigments and satellite. Remote Sensing 6:10089–10106.

Strong C, Rigor IG (2013) Arctic marginal ice zone trending wider in summer and narrower in winter, Geophys Res Lett 40:4864–4868.

Suttle CA (2007) Marine viruses—major players in the global ecosystem. Nature Reviews Microbiology, 5:801–812. https://doi.org/10.1038/nrmicro1750

Xi H, Losa SN, Mangin A, Soppa MA, Garnesson P, Demaria J, Liu Y, Fanton d'Andon O, Bracher A (2020) Global retrieval of phytoplankton functional types based on empirical orthogonal functions using CMEMS GlobColour merged products and further extension to OLCI data. Remote Sensing of Environment 240:111704.

Xi H, Losa SN, Mangin A, Garnesson P, Bretagnon M, Demaria J, Soppa MA, Fanton d'Andon O, Bracher A (2021) Global orophyll a concentrations of phytoplankton functional types with detailed uncertainty assessment using multisensor ocean color and sea surface temperature satellite products. J Geophysical Res: Oceans 126:e2020JC017127.

Xi H, Bretagnon M, Losa SN, Brotas V, Gomes M, Peeken I, Alvarado LMA, Mangin A, Bracher A (2023) Two-decade satellite monitoring of surface phytoplankton functional types in the Atlantic Ocean, State of the Planet 1-osr7:5. https://doi.org/10.5194/sp-1-osr7-5-2023.

Von Appen WJ, Waite AM, Bergmann M, Bienhold C, Boebel O, Bracher A, Cisewski B, Hagemann J, Hoppema M, Iversen MH, Konrad C, Krumpen T, Lochthofen N, Metfies K, Niehoff B, Nöthig EM, Purser A, Salter I, Schaber M, Scholz D, Soltwedel T, Torres-Valdes S, Wekerle C, Wenzhöfer F, Wietz M, Boetius A (2021) Sea-ice derived meltwater stratification slows the biological carbon pump: results from continuous observation. Nature Comm, 12:7309.

Weiss J, von Appen WJ, Niehoff B, Hildebrand N, Graeve M, Neuhaus S, Bracher A, Nöthig EM, Metfies K (2024) Unprecedented insights into extents of biological responses to physical forcing in an Arctic sub-mesoscale filament by combining high-resolution measurement approaches, Sci Rep 14:8192. https://doi.org/10.1038/s41598-024-58511-y

6. NEW INTEGRATED EXPERIMENTAL AND MODELLING TOOLS FOR GEOREFERENCED SOURCE APPORTIONMENT OF AEROSOL CLIMATE-RELEVANT PARAMETERS FROM MID-LATITUDES TILL THE ARCTIC ON POLARSTERN (GAIA-PS)

Fabio Giardi[1];

not on board: Giulia Calzolai[1], Vera Bernardoni[2], Alessandro Bracci[3], Federica Crova[2], Luca Di Liberto[3], Luca Ferrero[4], Niccolò Losi[4], Angelo Lupi[5], Ferdinando Pasqualini[3], Marco Potenza[2]

[1]IT.INFN
[2]IT.UNIMI
[3]IT.CNR-ISAC
[4]IT.UNIMIB
[5]IT.CNR-ISP

Grant-No. AWI_PS143/2_05

Outline

Arctic warming is the result of complex global feedbacks acting at different spatial and temporal scales; our comprehension of these mechanisms is still limited and debated as related to the results obtained using modelling simulations. Among the causes of the Arctic Amplification, the role played by atmospheric aerosol is one of the most uncertain, due to difficulties in the characterization of its physical-chemical properties, their space and time variability, and uncertainties in the quantification of the contribution from its emission sources within and outside the Arctic itself. Increasing scientific interest is focused on “emerging aerosol sources” related to Arctic warming as their contribution is increasing (e.g. high-latitude dust, sea spray, biomass burning, as well as increasing contribution from anthropogenic activities in the Arctic as ship emissions or gas flaring). Some Arctic monitoring stations provide long-term series of data on ground-based aerosol properties, lidar profiles, radiometric and meteorological data. Nevertheless, it has been recently demonstrated (Losi et al. 2023; Ferrero et al. 2019a,b) that the aerosol sources identified at on-land stations can differ from those measured on a larger spatial scale, both horizontally and vertically. Thus, the possibility to use research vessels (RV) as a privileged platform for wide spatial investigations becomes crucial considering the Arctic surface covered by seawater and some RVs have already been exploited for atmospheric studies (e.g., MOSAiC (Shupe et al. 2022) and AREX (Ferrero et al. 2019a) expeditions). Apart from some simulation studies (Shindell and Faluvegi 2009; Sand et al. 2016) no rigorous quantification of the role of aerosol sources and related aerosol-radiation climate forcing at different latitudes and over a large synergic temporal- spatial scale has been carried out via experimental activity. Receptor modelling can support this investigation. Multi-time Positive Matrix Factorization (PMF) using Multi-linear Engine (ME-2) with both chemical and optical variables (Forello et al. 2019) already proved to be a valuable tool for source apportionment (SA) of optical variables and rolling PMF (Parworth et al. 2015) has been developed and used to capture source profile temporal variabilities. Integration of these approaches has not been performed yet, but it has the potential to be a SA tool to be used on complex datasets collected at moving receptors to also provide spatial- temporal variability of source profiles. Further, a novel HR experimental quantification method (Ferrero et al. 2018; Ferrero et al. 2021a) to determine the atmospheric warming in all sky conditions (in function of cloud type and cloudiness) (Ferrero et al. 2021b) has recently been developed and has the potential to be coupled with the SA approach.

Moving in this frame, the European Union – Next Generation EU, under the Italian call PRIN, funded the GAIA project (ongoing, project 20229JLCRZ). Within GAIA, the have set up a mobile lab (GAInfrA), consisting of a half-container equipped with all the instruments needed to allow a complete aerosol investigation. Further, they are implementing multi-time rolling PMF to be integrated to HR estimates: this will allow exploiting measurements obtainable using GAInfrA to reach multi-time source apportionment of HR and columnar aerosol forcing.

Targeting to high time resolution measurements is a key-aspect in this expedition to guarantee the possibility to identify temporally-limited source contribution, spatial resolution, and to provide a number of samples suitable for receptor modelling based on statistical analysis.

Objectives

GAIA-PS aims at using the mobile lab GAInfrA developed in the overarching GAIA project on the 2024 PS summer cruise, to collect geo-referenced data on aerosol chemical, physical, and optical properties, broadband and spectrally-resolved radiation budgets, and vertical structure of the atmosphere from Mid-latitudes to the Arctic. The main objective of GAIA-PS is getting a comprehensive, coordinated and simultaneous data-set of all the physical-chemical quantities that are needed as input to the modelling tools, newly implemented by the proponents in the GAIA project, that will allow to gain information on georeferenced climatic impact of different aerosol sources and types in all sky conditions on a large latitude range.

In detail, GAIA-PS will measure the following quantities along all the path of the already planned 2024 *Polarstern* summer cruises:

Aerosol Physical Properties:

- Number size distribution data (with 8-800 nm SMPS size range and optical particle
- counters OPC 300-30000 nm)
- Multi-wavelength Absorption (Aethalometer) and Scattering Coefficients (Nephelometer) - Vertical Profiling (Ceilometer)
- Aerosol Chemical Composition:
- Gravimetric aerosol mass (on collected samples)
- Aerosol chemical composition (ions, elements) on samples collected with a low volume sampler (every 12-24h) and with a high-time-resolution sampler (6h)
- On-line Total Carbon measurements (6h)

Radiation and Meteorological data:

- Broadband (300-3000 nm) global, diffuse and reflected irradiance and Sky Camera
- Spectral measurements (300-1000 nm) of global, diffuse and reflected irradiance
- 3D wind, temperature, humidity, pressure

Regarding sample collection, sampling strategies are modulated to fit the analytical detection limits and to capture time-spatial variations. Time and spatial data resolution is crucial for the use of the data-set with the implemented modelling tools.

Besides the environmental scientific field, this expedition is expected to have impact on Metrology: space- and wavelength-dependent multiple-scattering enhancement parameters for Aethalometer data will be assessed. Aethalometers are widely used around the globe, but open issues concerning the corrections to be applied to the collected data still exist, preventing suitable measurement accuracy and data harmonisation.

Work at sea

A new mobile lab (GAInfrA) has been set up to be mounted on board a Research Vessel. GAInfrA instruments are placed in a half-container with power connections and lifting inlets for the instrumentation. The temperature of the container is controlled by an Air Conditioning inverter. The shelter and inlets have been designed to best follow the observational requirements of the main international networks for aerosol sampling (e.g. ACTRIS). PM10 (particles with diameter below 10 μm) inlets will be used in GAIA-PS for all the instruments as this is the most used metric and thus ensures the comparability of the acquired data withthe ones available in literature and in on-land observatories (e.g, Ny-Alesund). Further, focusing on PM10, GAIA-PS data will allow GAIA to be also sensitive to those emerging natural sources that are expected to mostly contribute to the coarse mode, such as high latitude dust (dust resuspended from high latitude lands left ice-uncovered) and marine aerosol.

GAInfrA includes: 2 low-volume sequential samplers for aerosol, Aethalometer, Total carbon analyzer, Nephelometer, pyranometers (global, direct and diffuse radiation), hyperspectral radiometers (global, direct, diffuse and reflected radiation), Scanning Mobility Particle Sizer, Aerodynamic particle sizer, optical particle sizer. Meteorological sensors and radiometer will be installed on the roof of GAInfrA with a dedicated platform. A ceilometer will be also installed on board to get information on the atmospheric profiles of aerosol optical properties along the vessel cruise.

Data will be acquired and samples will be collected en-route during the already planned expeditions (aiming at having a latitude range as large as possible).

Preliminary (expected) results

The high number of samples and the detailed characterisation carried out (including markers for different sources) will guarantee high-quality results for receptor modelling. Indeed, these models require a high number of input data (to be able to catch all the possible sources) and the presence of source markers in the dataset (i.e., the model cannot catch sources for which no marker is available). As an example, the assessment of crustal elements (Al, Si, Ti, Fe), as guaranteed by the use of the analytical techinque PIXE (Particle Induced X-ray Emission), will be fundamental for mineral dust study. Sources such as high-latitude dust and long-range transported one have similar tracers, but can be distinguished on the basis of slightly different ratios among them, due to differences in soil composition and particle size. The availability of high-time resolved samples will increase the possibility of having samples in which one of these sources (e.g. transported for a few-hour periods) is dominating, enhancing model ability to identify it. Further, the use of both chemical and optical data in the modelling process has already been shown as advantageous 1) to strengthen the source identification especially when relevant chemical tracers (e.g. levoglucosan for biomass burning) are not available; 2) to give estimates for source-specific atmospheric parameters which are typically assumed a priori in other types of SA approaches (i.e. optical SA) based on optical data; 3) to provide information on source- dependent mass absorption cross-section (MAC) values at different wavelengths for absorbing species (e.g. black carbon) (Forello et al. 2019). Indeed, the MAC depends not only on the emitted absorbing species, and it represents one of the important sources of uncertainty in models for radiative forcing estimates.

Data management

Environmental data will be archived, published and disseminated according to international standards by the World Data Center PANGAEA Data Publisher for Earth & Environmental Science (https://www.pangaea.de) within two years after the end of the expedition at the latest. By default, the CC-BY license will be applied. Further, all datasets will be stored and made available trough the CNR (http://iadc.cnr.it/cnr/) data center, which is First Level Node of the new Italian Arctic Data Center (IADC).

Any other data will be submitted to an appropriate long-term archive that provides unique and stable identifiers for the datasets and allows open online access to the data.

This expedition was supported by the European Union – Next Generation EU.

In all publications based on this expedition, the **Grant No. AWI_PS143/2_05** will be quoted and the following publication will be cited:

Alfred-Wegener-Institut Helmholtz-Zentrum für Polar- und Meeresforschung (2017) Polar Research and Supply Vessel POLARSTERN Operated by the Alfred-Wegener-Institute. Journal of large-scale research facilities, 3, A119. http://dx.doi.org/10.17815/jlsrf-3-163.

References

Ferrero L, Močnik G, Cogliati S, Gregorič A. Colombo R, Bolzacchini E (2018) Heating Rate of Light Absorbing Aerosols: Time-Resolved Measurements, the Role of Clouds, and Source Identification. Environmental Science and Technology 52:3546–3555. https://doi.org/10.1021/acs.est.7b04320

Ferrero L, Sangiorgi G, Perrone MG, Rizzi C, Cataldi M, Markuszewski P, Pakszys P, Makuch P, Petelski T, Becagli S, Traversi R, Bolzacchini E, Zielinski T (2019) Chemical Composition of Aerosol over the Arctic Ocean from Summer ARctic EXpedition (AREX) 2011–2012 Cruises: Ions, Amines, Elemental Carbon, Organic Matter, Polycyclic Aromatic Hydrocarbons, n-Alkanes, Metals, and Rare Earth Elements. Atmosphere 10:54. https://doi.org/10.3390/atmos10020054 (a)

Ferrero L, Ritter C, Cappelletti D, Moroni B, Močnik G, Mazzola M, Lupi A, Becagli S, Traversi R, Cataldi M, Neuber R, Vitale V, Bolzacchini E (2019b) Aerosol optical properties in the Arctic: The role of aerosol chemistry and dust composition in a closure experiment between Lidar and tethered balloon vertical profiles. Science of the Total Environment 686:452–467. https://doi.org/10.1016/j.scitotenv.2019.05.399

Ferrero L, Bernardoni V, Santagostini L, Cogliati S, Soldan F, Valentini S, Massabò D, Močnik G, Gregorič A, Rigler M, Prati P, Bigogno A, Losi N, Valli G, Vecchi R, Bolzacchini E (2021a) Consistent determination of the heating rate of light-absorbing aerosol using wavelength- and time-dependent Aethalometer multiple-scattering correction. Science of the Total Environment 791:148277. https://doi.org/10.1016/j.scitotenv.2021.148277

Ferrero L, Gregorič A, Močnik G, Rigler M, Cogliati S, Barnaba F, Di Liberto L, Gobbi GP, Losi N, Bolzacchini E (2021) The impact of cloudiness and cloud type on the atmospheric heating rate of black and brown carbon in the Po Valley. Atmospheric Chemistry and Physics 21:4869–4897, https://doi.org/10.5194/acp-21-4869-2021

Forello AC, Bernardoni V, Calzolai G, Lucarelli F, Massabò D, Nava S, Pileci RE, Prati P, Valentini S, Valli G, Vecchi R (2019) Exploiting multi-wavelength aerosol absorption coefficients in a multi-time resolution source apportionment study to retrieve source-dependent absorption parameters. Atmospheric Chemistry and Physics 19:11235–11252. https://doi.org/10.5194/acp-19-11235-2019

Losi N, Markuszewski P, Rigler M, Gregorič A, Močnik G, Drozdowska V, Makuch P, Zielinski T, Pakszys P, Kitowska M, Manuel A, Gini I, Doldi A, Cerri S, Maroni P, Bolzacchini E, Ferrero (2023) Anthropic Settlements' Impact on the Light-Absorbing Aerosol Concentrations and Heating Rate in the Arctic. Atmosphere 14:1768. https://doi.org/10.3390/atmos14121768

Parworth C, Fast J, Mei F, Shippert T, Sivaraman C, Tilp A, Watson T, Zhang Q (2015) Long-term measurements of submicrometer aerosol chemistry at the Southern Great Plains (SGP) using an Aerosol Chemical Speciation Monitor (ACSM). Atmospheric Environment 106:43–55. https://doi.org/10.1016/j.atmosenv.2015.01.060

Sand M, Berntsen TK, von Salzen K, Flanner MG, Langner J, Victor DG (2016) Response of Arctic temperature to changes in emissions of short-lived climate forcers. Nature Climate Change 6:286–289. https://doi.org/10.1038/NCLIMATE2880

Shindell D, Faluvegi G (2009) Climate response to regional radiative forcing during the twentieth century. Nature Geoscience 2:294–300. https://doi.org/10.1038/ngeo473

Shupe MD, Rex M, Blomquist B, Persson POG, Schmale J, Uttal T, Althausen D, Angot H, Archer S, Bariteau L, Beck I, Bilberry J, Bucci S, Buck C, Boyer M, Brasseur Z, Brooks IM, Calmer R, Cassano J, Castro V, Chu D, Costa D, Cox CJ, Creamean J, Crewell S, Dahlke S, Damm E, de Boer G, Deckelmann H., Dethloff K, Dütsch M, Ebell K, Ehrlich A, Ellis J, Engelmann R, Fong AA, Frey MM,

Gallagher MR, Ganzeveld ., Gradinger R, Graeser J, Greenamyer V, Griesche H, Griffiths S, Hamilton J, Heinemann G, Helmig D, Herber A, Heuzé C, Hofer J, Houchens T, Howard D, Inoue J, Jacobi H-W, Jaiser R, Jokinen T, Jourdan O, Jozef O, King W, Kirchgaessner A, Klingebiel M, Krassovski M, Krumpen T, Lampert A, Landing W, Laurila T, Lawrence D, Lonardi M, Loose B, Lüpkes C, Maahn M, Macke A, Maslowski W, Marsay C, Maturilli M, Mech M, Morris S, Moser M, Nicolaus M, Ortega P, Osborn J, Pätzold F, Perovich DK, Petäjä T, Pilz C, Pirazzini R, Posman K, Powers H, Pratt KA, Preußer A, Quéléver L, Radenz M, Rabe B, Rinke A, Sachs T, Schulz A, Siebert H, Silva T, Solomon A, Sommerfeld A, Spreen G, Stephens M, Stohl A, Svensson G, Uin J, Viegas J, Voigt C, von der Gathen P, Wehner B, Welker JM, Wendisch M, Werner M, Xie Z, Yue F (2022) Overview of the MOSAiC expedition: Atmosphere. Elementa: Science of the Anthropocene 10. https://doi.org/10.1525/elementa.2021.00060

APPENDIX

A.1 TEILNEHMENDE INSTITUTE / PARTICIPATING INSTITUTES

A.2 FAHRTTEILNEHMER:INNEN / CRUISE PARTICIPANTS

A.3 SCHIFFSBESATZUNG / SHIP‘S CREW

A.4. STATIONSLISTE / STATION LIST

A.1 TEILNEHMENDE INSTITUTE / PARTICIPATING INSTITUTES

Affiliation	Address
DE.AWI	Alfred-Wegener-Institut Helmholtz-Zentrum für Polar- und Meeresforschung Postfach 120161 27515 Bremerhaven Germany
DE.BMBF/PtJ	Projektträger Jülich Nachhaltige Entwicklung und Innovation/Marine und maritime Forschung Godesberger Allee 105-107 53175 Bonn Germany
DE.UniHB	Universität Bremen Bibliothekstrasse 1 28359 Bremen Germany
DE.HSBHV	Hochschule Bremerhaven An der Karlstadt 8 27568 Bremerhaven Germany
DE.UniD	Universität Düsseldorf Universitätsstrasse 1 40225 Düsseldorf Germany
DE.DWD	Deutscher Wetterdienst Seewetteramt Bernhard Nocht Str. 76 20359 Hamburg Germany
DE.GEOMAR	GEOMAR Helmholtz-Zentrum für Ozeanforschung Kiel Wischhofstrasse 1-3 24148 Kiel Germany
DE.UniHH	Universität Hamburg Mittelweg 177 20148 Hamburg Germany
DE.UniHRO	Universität Rostock Universitätsplatz 1 18051 Rostock Germany
IT.INFN	National Institute for Nuclear Physics Florence Division Via G. Sansone 1 50019 Sesto Fiorentino (FI) Italy

Affiliation	Address
IT.UNIMI	Università degli Studi di Milano Department of Physics Via Celoria 16 20133 Milan Italy
IT.CNR-ISAC	National Research Council (CNR) Institute of Atmospheric Sciences and Climate (ISAC) Via Fosso del Cavaliere 100 00133 Rome Italy
IT.UNIMIB	University of Milano Bicocca Department of Environmental and Earth Sciences Piazza della Scienza 1 20126 Milan Italy
IT.CNR-ISP	National Research Council (CNR) Institute of Polar Sciences (ISP) Via P. Gobetti 101 40129 Bologna Italy
DE.UniOl	Carl von Ossietzky Universtät Oldenburg Ammerländer Heerstrasse 114-118 26129 Oldenburg Germany
NL.NIOZ	Royal Netherlands Institute for Sea Research (NIOZ) Landsdiep 4 SZ `t Horntje (Texel) Netherlands
FR.CNRS-LOG ULGO	Laboratory of Oceanology and Geosciences (CNRS) MREN-ULCO and SMW 32 Avenue du Maréchal Foch Wimereux France
UK.NOC	National Oceanographic Centre European Way SO143ZH Southampton United Kingdom

A.2 FAHRTTEILNEHMER:INNEN / CRUISE PARTICIPANTS

Name/ Last name	Vorname/ First name	Institut/ Institute	Beruf/ Profession	Fachrichtung/ Discipline
Becker	Hauke	DE.AWI	Engineer	Physics
Behrendt	Celina	DE.AWI	Technician	Biology
Böhringer	Lilian	DE.AWI	PhD Student	Biology
Bracher	Astrid	DE.AWI	Scientist	Meteorology
Busack	Michael	DE.AWI	Engineer	Biology
Detsch	Christian	DE.AWI	Student	Biology
Dolinkiewicz	Magdalena	DE.AWI	PhD Student	Biology
Duong	Buu Lik	DE.UniOldenburg	Student	Physics
Engicht	Carina	DE.AWI	Techician	Physics
Fuchs	Daniel	DE.Northern_Heli	Technician	
Galonska	Tabea	DE.AWI	Technician	Biology
Giardi	Fabio	IT.INFN	Scientist	Meterology
Günther	Babett	DE.GEOMAR	Scientist	Biology
Hagemann	Jonas	DE.AWI	Engineer	Biology
Handelmann	Nils	DE.AWI	Engineer	Biology
Harding	Jack	DE.Northern_Heli	Pilot	
Hirschmann	Sophia	DE.GEOMAR	PhD Student	Biology
Hohe	Christian	DE.AWI	Scientist	Biology
Klüver	Tanja	DE.GEOMAR	Technician	Biology
Konrad	Christian	DE.AWI	Scientist	Biology
Korte	Kerstin	DE.AWI	Technician	Biology
Lehmenhecker	Sascha	DE.AWI	Engineer	Biology
Lochthofen	Normen	DE.AWI	Engineer	Biology
Ludzuweit	Janine	DE.AWI	Technician	Biology
McPherson	Rebecca	DE.AWI	Scientist	Physics
Meister	Marlene	DE.AWI	PhD Student	Physics
Metfies	Katja	DE.AWI	Scientist	Biology
Niehoff	Barbara	DE.AWI	Scientist	Biology
Oldenburg	Ellen	DE.UniDüsseldorf	PhD Student	Biology
Otte	Frank	DE.DWD	Scientist	Meteorology
Pontiller	Benjamin	DE.GEOMAR	Scientist	Biology
Popa	Ovidiu	DE.UniDüsseldorf	Scientist	Biology
Purser	Autun	DE.AWI	Scientist	Biology
Reich	Marlis	DE.UniBremen	Scientist	Biology
Reifenberg	Simon	DE.AWI	PhD Student	Physics
Rohling	Clemens	DE.HH	Student	Physics
Schaubensteiner	Stefan	DE.Northern_Heli	Pilot	
Schmidt	Ina	DE.UniRostock	Student	Biology
Schnell	Vincent	DE.BMBF/PtJ		Biology
Scholz	Daniel	DE.AWI	Engineer	Chemistry
Schroeder	Sebastian	DE.	Journalist	

Name/ Last name	Vorname/ First name	Institut/ Institute	Beruf/ Profession	Fachrichtung/ Discipline
Seifert	Michael	DE.Northern_Heli	Technician	
Uhlir	Carolin	DE.AWI	Technician	Biology
von Appen	Wilken-Jon	DE.AWI	Scientist	Physics
Wenzel	Julia	DE.DWD	Scientist	Meteorology
Westphal	Matthias	DE.HSBHV	Student	Chemistry

A.3 SCHIFFSBESATZUNG / SHIP‘S CREW

No	Dienstgrad	Rank	Nachname / Last name	Vorname / First name
1	Kapitän	Master	Schwarze	Stefan
2	1. Offizier	Chief Mate	Strauß	Erik
3	1. Offizier Ladung	Chief Mate Cargo	Eckenfels	Hannes
4	2. Offizier	2nd Mate	Weiß	Daniel
5	2. Offizier	2nd Mate	Peine	Lutz Gerhard
6	Schiffsarzt	Doctor	Guba	Klaus
7	Leitender Ingenieur	Chief Engineer	Ziemann	Olaf Hermann August
8	2. Ingenieur	2nd Engineer	Ehrke	Tom
9	2. Ingenieur	2nd Engineer	Krinfeld	Oleksandr
10	2. Ingenieurin	2nd Engineer	Rusch	Torben
11	Schiffselektrotechniker Maschine	Ship Electrotechnical Officer Engine	Pommerencke	Bernd
12	Elektroniker Winden	Electrotechnical Engineer Winches	Krüger	Lars
13	Elektroniker Netzwerk	Electrotechnical Engineer Network/Bridge	Müller	Andreas
14	Elektroniker Labor	Electrotechnical Engineer Labor	Zivanov	Stefan
15	Elektroniker System	Electrotechnical Engineer System	Winter	Andreas
16	Bootsmann	Bosun	Meier	Jan
17	Zimmermann	Carpenter	Keller	Eugen Jürgen
18	Schiffsmechaniker Deck	Multi Purpose Rating Deck	Buchholz	Joscha
19	Schiffsmechaniker Deck	Multi Purpose Rating Deck	Burzan	Gerd-Ekkehard
20	Schiffsmechaniker Deck	Multi Purpose Rating Deck	Mahlmann	Oliver Karl-Heinz
21	Schiffsmechaniker Deck	Multi Purpose Rating Deck	Münzenberger	Börge
22	Schiffsmechaniker Deck	Multi Purpose Rating Deck	Decker	Jens
23	Schiffsmechaniker Deck	Multi Purpose Rating Deck	Fisahn	Paul

No	Dienstgrad	Rank	Nachname / Last name	Vorname / First name
24	Schiffsmechaniker Deck	Multi Purpose Rating Deck	Siemon	Leon Anton
25	Schiffsmechaniker Deck	Multi Purpose Rating Deck	Ellner	Leopold
26	Decksmann/Matrose	Able Seaman	Niebuhr	Tim
27	Lagerhalter	Storekeeper	Plehn	Marco Markus
28	Schiffsmechaniker Maschine	Multi Purpose Rating Engine	Loew	Caspar
29	Schiffsmechaniker Maschine	Multi Purpose Rating Engine	Probst	Lorenz
30	Schiffsmechanikerin Maschine	Multi Purpose Rating Engine	Hansen	Jan Nils
31	Schiffsmechaniker Maschine	Multi Purpose Rating Engine	Buchholz	Karl Erik
32	Schiffsmechaniker Maschine	Multi Purpose Rating Engine	Juszczyk	Michal Stanislaw
33	1. Koch	1st Cook	Skrzipale	Mitja
34	2. Köchin	2nd Cook	Fehrenbach	Martina
35	2. Koch	2nd Cook	Loibl	Patrick
36	1. Stewardess	1st Steward	Witusch	Petra Gertrud Ramona
37	2. Stewardess	2nd Stewardess	Stocker	Eileen Sigourney
38	2. Steward	2nd Steward	Golla	Gerald
39	2. Stewardess	2nd Stewardess	Holl	Claudia
40	2. Stewardess / Krankenschwester	2nd Stewardess / Nurse	Ilk	Romy
41	2. Steward / Wäscherei	2nd Steward / Laundry	Shi	Wubo
42	2. Steward / Wäscherei	2nd Steward / Laundry	Chen	Jirong
43	2. Steward / Wäscherei	2nd Steward / Laundry	Chen	Quanlun
44	Auszubildende Schiffsmechanikerin	Apprentice Ship Mechanic	Schneider	Denise

A.4 STATIONSLISTE / STATION LIST PS143/2

Station list of expedition PS143/2 from Tromsø – Tromsø; the list details the action log for all stations along the cruise track.
See https://www.pangaea.de/expeditions/events/PS143/2 to display the station (event) list for expedition PS143/2.
This version contains Uniform Resource Identifiers for all sensors listed under https://sensor.awi.de. See https://www.awi.de/en/about-us/service/computing-centre/data-flow-framework.html for further information about AWI's data flow framework from sensor observations to archives (O2A).

Event label	Optional label	Date/Time	Latitude	Longitude	Depth [m]	Gear	Action	Comment *
PS143/2-track		2024-07-12T00:00:00	69.67800	18.98980		CT	Station start	Tromsø - Tromsø
PS143/2-track		2024-08-06T00:00:00	69.67800	18.98980		CT	Station end	Tromsø - Tromsø
PS143/2_0_Underway-3		2024-07-12T18:15:13	69.85229	19.75249	151.6	FBOX	Station start	
PS143/2_0_Underway-3		2024-08-05T13:54:33	71.52152	18.06169	270.8	FBOX	Station end	
PS143/2_0_Underway-5		2024-07-12T18:17:36	69.85498	19.77054	119.3	MAG	Station start	
PS143/2_0_Underway-5		2024-08-05T13:55:35	71.51976	18.06583	267.1	MAG	Station end	
PS143/2_0_Underway-6		2024-07-12T18:18:53	69.85694	19.77927	155.2	GRAV	Station start	
PS143/2_0_Underway-6		2024-08-05T13:56:12	71.51869	18.06827	265.1	GRAV	Station end	

Event label	Optional label	Date/Time	Latitude	Longitude	Depth [m]	Gear	Action	Comment *
PS143/2_0_Underway-16		2024-07-12T17:56:30	69.83313	19.59174	164.2	TSG	Station start	
PS143/2_0_Underway-16		2024-08-05T13:53:30	71.52331	18.05737	268.9	TSG	Station end	
PS143/2_0_Underway-17		2024-07-12T17:56:57	69.83363	19.59591	163.1	TSG	Station start	
PS143/2_0_Underway-17		2024-08-05T13:54:02	71.52240	18.05955	269.8	TSG	Station end	
PS143/2_0_Underway-19		2024-07-12T07:37:34	69.74727	19.14254	12.7	SWEAS	Station start	
PS143/2_0_Underway-19		2024-08-06T05:57:22	69.74733	19.14241	12.2	SWEAS	Station end	
PS143/2_0_Underway-20		2024-07-12T18:03:01	69.84000	19.65087	172.5	ADCP	Station start	
PS143/2_0_Underway-20		2024-08-05T13:52:24	71.52519	18.05294	272.9	ADCP	Station end	
PS143/2_0_Underway-21		2024-07-12T18:00:00	69.83675	19.62420		UWS	Station start	not logged in D-Ship
PS143/2_0_Underway-21		2024-08-05T06:07:45	72.35271	16.13762		UWS	Station end	not logged in D-Ship
PS143/2_1-1		2024-07-15T03:16:19	79.00682	6.94262	1201.8	CTD-RO	max depth	
PS143/2_1-2		2024-07-15T04:07:39	79.00737	6.94275	1203.4	AUV_Iab	Station start	
PS143/2_1-2		2024-07-15T04:55:29	79.00865	6.94216	1207.0	AUV_Iab	Station end	

Event label	Optional label	Date/Time	Latitude	Longitude	Depth [m]	Gear	Action	Comment *
PS143/2_1-3	F4-S-7	2024-07-15T05:30:20	79.01656	6.98092	1238.3	MOOR	Station start	recovery
PS143/2_1-3	F4-S-7	2024-07-15T07:27:16	79.01742	6.96626	1235.9	MOOR	Station end	recovery
PS143/2_1-4		2024-07-15T08:29:17	79.01215	6.96328	1222.8	AUV_Iab	Station start	
PS143/2_1-4		2024-07-15T13:00:30	78.99519	6.91888	1195.5	AUV_Iab	Station end	
PS143/2_2-2		2024-07-15T13:43:22	79.03020	6.99640	1262.4	HN	Station start	
PS143/2_2-2		2024-07-15T13:58:44	79.03040	6.99907	1263.0	HN	Station end	
PS143/2_2-1		2024-07-15T14:10:31	79.03033	6.99936	1262.8	CTD-RO	max depth	
PS143/2_2-3		2024-07-15T14:52:42	79.03001	7.00037	1262.4	LOKI	Station start	
PS143/2_2-3		2024-07-15T16:29:20	79.02945	6.99916	1261.3	LOKI	Station end	
PS143/2_2-4		2024-07-15T16:29:49	79.02946	6.99923	1261.5	MSN	Station start	
PS143/2_2-4		2024-07-15T18:39:28	79.02795	7.00106	1259.2	MSN	Station end	
PS143/2_2-5		2024-07-15T18:45:06	79.02806	7.00265	1259.4	LIGHT	Station start	
PS143/2_2-5		2024-07-15T19:37:55	79.02917	7.00790	1262.2	LIGHT	Station end	

Event label	Optional label	Date/Time	Latitude	Longitude	Depth [m]	Gear	Action	Comment *
PS143/2_2-6		2024-07-15T20:30:00	79.02927	7.00380	1261.8	CTD-RO	max depth	
PS143/2_3-1		2024-07-15T21:40:07	79.00012	7.55413	1198.2	AUV_lab	Station start	
PS143/2_3-1		2024-07-16T05:00:51	79.00270	7.52688	1207.4	AUV_lab	Station end	
PS143/2_4-1		2024-07-15T23:41:19	79.02981	6.99873	1261.8	OFOBS	Station start	
PS143/2_4-1		2024-07-16T02:23:36	79.02957	7.11282	1277.3	OFOBS	Station end	
PS143/2_5-1	F4-21	2024-07-16T05:47:37	78.99974	7.02028	1213.0	MOOR	Station start	recovery
PS143/2_5-1	F4-21	2024-07-16T08:14:10	79.00683	6.98019	1216.7	MOOR	Station end	recovery
PS143/2_5-2		2024-07-16T08:56:27	79.02314	6.99900	1251.8	TOPR	Station start	
PS143/2_5-2		2024-07-16T09:30:47	79.02341	6.99777	1252.0	TOPR	Station end	
PS143/2_6-1	F4W-5-ST	2024-07-16T10:30:39	79.02349	6.99742	1252.2	MOOR	Station start	deployment
PS143/2_6-1	F4W-5-ST	2024-07-16T11:51:02	79.02275	6.99629	1251.1	MOOR	Station end	deployment
PS143/2_7-2		2024-07-16T15:34:23	78.60864	5.06859	2276.4	HN	Station start	
PS143/2_7-2		2024-07-16T15:43:10	78.60797	5.06524	2276.8	HN	Station end	

Event label	Optional label	Date/Time	Latitude	Longitude	Depth [m]	Gear	Action	Comment *
PS143/2_7-1		2024-07-16T16:15:09	78.60769	5.06204	2277.6	CTD-RO	max depth	
PS143/2_7-3		2024-07-16T17:35:59	78.60763	5.06375	2277.4	LIGHT	Station start	
PS143/2_7-3		2024-07-16T18:21:03	78.60776	5.06384	2277.5	LIGHT	Station end	
PS143/2_7-4		2024-07-16T18:30:13	78.60811	5.06450	2277.5	MSN	Station start	
PS143/2_7-4		2024-07-16T20:44:54	78.60770	5.06345	2277.6	MSN	Station end	
PS143/2_7-5		2024-07-16T20:47:46	78.60785	5.06410	2277.5	LOKI	Station start	
PS143/2_7-5		2024-07-16T22:21:33	78.60841	5.06153	2278.3	LOKI	Station end	
PS143/2_7-6		2024-07-16T22:50:56	78.60929	5.05645	2279.9	CTD-RO	max depth	
PS143/2_7-7		2024-07-17T00:33:33	78.61659	5.00819	2300.1	OFOBS	Station start	
PS143/2_7-7		2024-07-17T02:33:10	78.61722	5.08911	2277.1	OFOBS	Station end	
PS143/2_8-1	F4-H-1	2024-07-17T07:01:52	79.00029	7.06718	1223.6	MOOR	Station start	deployment
PS143/2_8-1	F4-H-1	2024-07-17T09:42:39	79.00053	7.06785	1224.2	MOOR	Station end	deployment
PS143/2_9-1	F4-22	2024-07-17T10:42:11	79.00054	6.99549	1205.1	MOOR	Station start	deployment

Event label	Optional label	Date/Time	Latitude	Longitude	Depth [m]	Gear	Action	Comment *
PS143/2_9-1	F4-22	2024-07-17T13:41:59	79.00054	7.00095	1207.2	MOOR	Station end	deployment
PS143/2_10-1	F4-S-8	2024-07-17T14:17:19	79.01134	7.03859	1237.4	MOOR	Station start	deployment
PS143/2_10-1	F4-S-8	2024-07-17T17:00:03	79.01202	7.03428	1237.9	MOOR	Station end	deployment
PS143/2_11-2		2024-07-17T18:51:49	79.01686	8.33557	788.2	HN	Station start	
PS143/2_11-2		2024-07-17T19:03:06	79.01682	8.33480	789.3	HN	Station end	
PS143/2_11-1		2024-07-17T19:06:13	79.01676	8.33512	788.6	CTD-RO	max depth	
PS143/2_11-3		2024-07-17T20:03:43	79.01682	8.33307	791.7	LIGHT	Station start	
PS143/2_11-3		2024-07-17T20:48:02	79.01726	8.33368	791.0	LIGHT	Station end	
PS143/2_11-4		2024-07-17T20:51:37	79.01725	8.33312	791.8	MSN	Station start	
PS143/2_11-4		2024-07-17T22:23:51	79.01699	8.32805	797.7	MSN	Station end	
PS143/2_11-5		2024-07-17T22:25:57	79.01740	8.32803	797.9	LOKI	Station start	
PS143/2_11-5		2024-07-17T23:45:39	79.01762	8.33643	788.2	LOKI	Station end	
PS143/2_11-6		2024-07-18T00:06:02	79.01746	8.33240	792.3	CTD-RO	max depth	

Event label	Optional label	Date/Time	Latitude	Longitude	Depth [m]	Gear	Action	Comment *
PS143/2_11-7		2024-07-18T01:03:02	79.01659	8.33117	793.8	OFOBS	Station start	
PS143/2_11-7		2024-07-18T04:45:57	79.01588	8.50430	482.4	OFOBS	Station end	
PS143/2_12-1		2024-07-18T05:50:26	79.01653	8.33654	786.1	AUV_Iab	Station start	
PS143/2_12-1		2024-07-18T15:00:29	78.98043	9.51239	213.6	AUV_Iab	Station end	
PS143/2_13-1	F2-21	2024-07-18T08:30:25	79.00152	8.34631	754.7	MOOR	Station start	recovery
PS143/2_13-1	F2-21	2024-07-18T09:56:56	79.00739	8.36406	737.7	MOOR	Station end	recovery
PS143/2_14-1		2024-07-18T11:46:48	78.98097	9.50704	213.1	CTD-RO	max depth	
PS143/2_14-2		2024-07-18T12:03:34	78.98046	9.50659	213.1	OOSS	Station start	
PS143/2_14-2		2024-07-18T12:34:27	78.98043	9.50919	213.4	OOSS	Station end	
PS143/2_14-3		2024-07-18T12:57:25	78.98083	9.51123	214.3	LIGHT	Station start	
PS143/2_14-3		2024-07-18T13:41:50	78.98077	9.51586	214.6	LIGHT	Station end	
PS143/2_14-4		2024-07-18T15:07:00	78.98040	9.51377	214.1	MSN	Station start	
PS143/2_14-4		2024-07-18T15:43:16	78.98024	9.51584	214.8	MSN	Station end	

Event label	Optional label	Date/Time	Latitude	Longitude	Depth [m]	Gear	Action	Comment *
PS143/2_14-5		2024-07-18T15:43:50	78.98024	9.51582	214.7	MSN	Station start	
PS143/2_14-5		2024-07-18T16:26:07	78.98018	9.51584	214.7	MSN	Station end	
PS143/2_14-6		2024-07-18T16:39:34	78.98001	9.51566	214.6	LOKI	Station start	
PS143/2_14-6		2024-07-18T17:16:36	78.98044	9.51588	214.7	LOKI	Station end	
PS143/2_14-7		2024-07-18T17:44:06	78.98065	9.51532	214.5	OFOBS	Station start	
PS143/2_14-7		2024-07-18T20:35:47	78.98084	9.64022	237.2	OFOBS	Station end	
PS143/2_15-1		2024-07-18T22:29:38	79.02286	10.72389	316.2	CTD-RO	max depth	
PS143/2_15-2		2024-07-18T23:12:18	79.02491	10.72682	315.5	LIGHT	Station start	
PS143/2_15-2		2024-07-18T23:43:02	79.02463	10.72875	315.3	LIGHT	Station end	
PS143/2_15-3		2024-07-18T23:54:51	79.02517	10.73136	315.1	MSN	Station start	
PS143/2_15-3		2024-07-19T00:30:42	79.02533	10.73578	315.0	MSN	Station end	
PS143/2_15-4		2024-07-19T00:42:13	79.02562	10.73668	314.9	LOKI	Station start	
PS143/2_15-4		2024-07-19T01:18:14	79.02510	10.74085	314.4	LOKI	Station end	

Event label	Optional label	Date/Time	Latitude	Longitude	Depth [m]	Gear	Action	Comment *
PS143/2_16-1	F2-22	2024-07-19T04:49:02	79.00023	8.33299	772.1	MOOR	Station start	deployment
PS143/2_16-1	F2-22	2024-07-19T08:20:03	79.00015	8.25324	865.5	MOOR	Station end	deployment
PS143/2_17-1	F3-20	2024-07-19T08:45:31	79.00388	8.01054	1062.4	MOOR	Station start	recovery
PS143/2_17-1	F3-20	2024-07-19T10:05:51	79.00247	8.01137	1060.8	MOOR	Station end	recovery
PS143/2_17-2	F3-21	2024-07-19T13:03:58	79.00215	7.99622	1067.8	MOOR	Station start	deployment
PS143/2_17-2	F3-21	2024-07-19T14:25:59	79.00204	7.99468	1067.9	MOOR	Station end	deployment
PS143/2_18-2		2024-07-19T17:24:02	79.13388	6.09210	1239.9	HN	Station start	
PS143/2_18-2		2024-07-19T17:40:58	79.13404	6.09230	1240.2	HN	Station end	
PS143/2_18-1		2024-07-19T17:25:04	79.13389	6.09216	1240.0	CTD-RO	max depth	
PS143/2_18-3		2024-07-19T17:54:52	79.13396	6.09314	1240.4	OOSS	Station start	
PS143/2_18-3		2024-07-19T18:40:41	79.13356	6.09345	1240.0	OOSS	Station end	
PS143/2_18-4		2024-07-19T18:12:22	79.13361	6.09267	1239.7	LIGHT	Station start	
PS143/2_18-4		2024-07-19T18:56:41	79.13343	6.09335	1239.7	LIGHT	Station end	

Event label	Optional label	Date/Time	Latitude	Longitude	Depth [m]	Gear	Action	Comment *
PS143/2_18-5		2024-07-19T18:57:34	79.13344	6.09344	1239.7	MSN	Station start	
PS143/2_18-5		2024-07-19T20:53:47	79.13351	6.09421	1240.5	MSN	Station end	
PS143/2_18-6		2024-07-19T20:56:35	79.13348	6.09421	1240.4	LOKI	Station start	
PS143/2_18-6		2024-07-19T22:33:22	79.13362	6.09250	1240.7	LOKI	Station end	
PS143/2_18-7		2024-07-19T23:37:40	79.13342	6.09027	1240.8	CTD-RO	max depth	
PS143/2_18-8		2024-07-20T01:03:01	79.13437	6.09333	1241.7	OFOBS	Station start	
PS143/2_18-8		2024-07-20T04:43:38	79.13463	5.93358	1256.9	OFOBS	Station end	
PS143/2_19-1		2024-07-20T06:00:04	79.13419	6.09398	1242.1	AUV_lab	Station start	
PS143/2_19-1		2024-07-20T15:39:29	79.01489	6.91527		AUV_lab	Station end	
PS143/2_19-2		2024-07-20T07:28:41	79.13552	6.07649	1242.9	TVMUC	max depth	
PS143/2_20-1	F4-OZA-3	2024-07-20T08:41:32	79.16740	6.30816	1396.9	MOOR	Station start	recovery
PS143/2_20-1	F4-OZA-3	2024-07-20T10:09:49	79.18057	6.29266	1419.9	MOOR	Station end	recovery
PS143/2_20-2		2024-07-20T10:41:04	79.18283	6.28441	1421.0	OOSS	Station start	

Event label	Optional label	Date/Time	Latitude	Longitude	Depth [m]	Gear	Action	Comment *
PS143/2_20-2		2024-07-20T11:02:30	79.18369	6.27834	1419.9	OOSS	Station end	
PS143/2_21-1	F4W-5	2024-07-20T12:42:12	79.01163	6.96643	1222.5	MOOR	Station start	deployment
PS143/2_21-1	F4W-5	2024-07-20T14:26:14	79.01167	6.96781		MOOR	Station end	deployment
PS143/2_22-3		2024-07-20T19:15:43	79.08059	4.08685	2450.3	OOSS	Station start	
PS143/2_22-3		2024-07-20T19:46:43	79.08057	4.08874	2449.1	OOSS	Station end	
PS143/2_22-2		2024-07-20T19:34:37	79.08056	4.08822	2449.2	HN	Station start	
PS143/2_22-2		2024-07-20T19:45:32	79.08057	4.08876	2448.9	HN	Station end	
PS143/2_22-1		2024-07-20T19:55:04	79.08052	4.08857	2449.4	CTD-RO	max depth	
PS143/2_22-4		2024-07-20T21:16:20	79.08073	4.08911	2449.4	LIGHT	Station start	
PS143/2_22-4		2024-07-20T22:04:11	79.07994	4.09134	2450.0	LIGHT	Station end	
PS143/2_22-5		2024-07-20T22:16:17	79.07968	4.09074	2450.8	MSN	Station start	
PS143/2_22-5		2024-07-21T00:13:37	79.08075	4.08997	2447.8	MSN	Station end	
PS143/2_22-6		2024-07-21T00:25:56	79.08073	4.08981	2448.8	LOKI	Station start	

Event label	Optional label	Date/Time	Latitude	Longitude	Depth [m]	Gear	Action	Comment *
PS143/2_22-6		2024-07-21T01:46:38	79.08103	4.09108	2447.7	LOKI	Station end	
PS143/2_22-7		2024-07-21T02:24:01	79.08030	4.09104	2449.0	CTD-RO	max depth	
PS143/2_22-8		2024-07-21T04:48:43	79.07827	4.16602	2390.4	TVMUC	max depth	
PS143/2_22-9		2024-07-21T07:35:00	79.03046	4.25463	2527.8	MOOR	Station start	Lander, recovery
PS143/2_22-9		2024-07-21T08:47:28	79.03088	4.23346	2531.1	MOOR	Station end	Lander, recovery
PS143/2_23-1		2024-07-21T12:57:53	79.14474	2.74813	5538.6	CTD-RO	max depth	
PS143/2_23-2		2024-07-21T13:36:15	79.14417	2.74991	5541.7	OOSS	Station start	
PS143/2_23-2		2024-07-21T13:57:59	79.14424	2.74904	5540.4	OOSS	Station end	
PS143/2_23-3		2024-07-21T16:11:48	79.14340	2.75697	5545.7	LIGHT	Station start	
PS143/2_23-3		2024-07-21T16:57:09	79.14264	2.75908	5545.9	LIGHT	Station end	
PS143/2_23-5		2024-07-21T17:29:02	79.14277	2.76052	5546.4	HN	Station start	
PS143/2_23-5		2024-07-21T17:38:31	79.14290	2.76036	5545.6	HN	Station end	
PS143/2_23-4		2024-07-21T18:23:30	79.14317	2.75881	5545.9	CTD-RO	max depth	

Event label	Optional label	Date/Time	Latitude	Longitude	Depth [m]	Gear	Action	Comment *
PS143/2_23-6		2024-07-21T20:13:53	79.14199	2.75145	5540.8	MSN	Station start	
PS143/2_23-6		2024-07-21T23:09:29	79.14340	2.76085	5546.8	MSN	Station end	
PS143/2_23-7		2024-07-21T23:11:59	79.14350	2.76070	5545.9	MSN	Station start	
PS143/2_23-7		2024-07-22T01:18:02	79.14189	2.75865	5546.1	MSN	Station end	
PS143/2_24-1		2024-07-22T07:57:20	79.58342	5.21386	2657.3	OFOBS	Station start	
PS143/2_24-1		2024-07-22T11:01:25	79.57250	5.26849	2583.6	OFOBS	Station end	
PS143/2_25-2		2024-07-22T17:06:28	79.93812	3.19618	2476.4	HN	Station start	
PS143/2_25-2		2024-07-22T17:14:44	79.93816	3.19530	2476.7	HN	Station end	
PS143/2_25-1		2024-07-22T17:23:25	79.93810	3.19629	2476.5	CTD-RO	max depth	
PS143/2_25-3		2024-07-22T17:46:50	79.93810	3.19669	2476.2	OOSS	Station start	
PS143/2_25-3		2024-07-22T18:06:08	79.93807	3.19512	2476.9	OOSS	Station end	
PS143/2_25-4		2024-07-22T18:33:37	79.93819	3.19456	2476.7	LIGHT	Station start	
PS143/2_25-4		2024-07-22T19:19:26	79.93780	3.19209	2478.3	LIGHT	Station end	

Event label	Optional label	Date/Time	Latitude	Longitude	Depth [m]	Gear	Action	Comment *
PS143/2_25-5		2024-07-22T19:21:11	79.93781	3.19227	2478.2	MSN	Station start	
PS143/2_25-5		2024-07-22T21:32:46	79.93795	3.19298	2477.7	MSN	Station end	
PS143/2_25-6		2024-07-22T21:33:38	79.93793	3.19305	2477.7	LOKI	Station start	
PS143/2_25-6		2024-07-22T23:01:20	79.94084	3.19173	2474.8	LOKI	Station end	
PS143/2_25-7		2024-07-22T23:42:22	79.93772	3.19347	2478.8	CTD-RO	max depth	
PS143/2_25-8		2024-07-23T01:09:46	79.93787	3.19281	2479.3	TVMUC	Station start	
PS143/2_25-8		2024-07-23T01:10:12	79.93788	3.19277	2479.3	TVMUC	Station end	
PS143/2_26-1		2024-07-23T03:59:42	79.94086	3.74749	2365.2	CTD-RO	max depth	
PS143/2_27-1		2024-07-23T05:42:45	79.94035	4.32504	2209.4	CTD-RO	max depth	
PS143/2_27-2		2024-07-23T06:24:28	79.94130	4.31674	2164.1	LIGHT	Station start	
PS143/2_27-2		2024-07-23T07:05:41	79.94789	4.32145	1681.8	LIGHT	Station end	
PS143/2_27-3		2024-07-23T07:20:55	79.94803	4.32707		MSN	Station start	
PS143/2_27-3		2024-07-23T08:18:03	79.94414	4.30806		MSN	Station end	

Event label	Optional label	Date/Time	Latitude	Longitude	Depth [m]	Gear	Action	Comment *
PS143/2_27-4		2024-07-23T08:19:28	79.94358	4.30656	1875.1	LOKI	Station start	
PS143/2_27-4		2024-07-23T09:17:48	79.94883	4.28768	1703.0	LOKI	Station end	
PS143/2_28-1		2024-07-23T10:44:27	79.93982	4.90126	1278.3	CTD-RO	max depth	
PS143/2_29-1		2024-07-23T12:10:02	79.93760	5.47798	1047.6	CTD-RO	max depth	
PS143/2_30-1		2024-07-23T13:31:30	79.94046	6.04451	905.5	CTD-RO	max depth	
PS143/2_31-1		2024-07-23T14:48:55	79.93871	6.61730	809.3	CTD-RO	max depth	
PS143/2_32-1		2024-07-23T16:12:22	79.93798	7.18125	714.8	CTD-RO	max depth	
PS143/2_33-2		2024-07-23T17:51:23	79.93775	7.75848	567.3	HN	Station start	
PS143/2_33-2		2024-07-23T17:59:27	79.93746	7.75749	568.0	HN	Station end	
PS143/2_33-1		2024-07-23T17:52:58	79.93770	7.75833	567.4	CTD-RO	max depth	
PS143/2_33-3		2024-07-23T18:43:47	79.92715	7.73019	578.5	MSN	Station start	
PS143/2_33-3		2024-07-23T19:35:55	79.93258	7.74298	573.5	MSN	Station end	
PS143/2_33-4		2024-07-23T19:42:03	79.93320	7.74371	573.3	LOKI	Station start	

Event label	Optional label	Date/Time	Latitude	Longitude	Depth [m]	Gear	Action	Comment *
PS143/2_33-4		2024-07-23T20:27:46	79.93345	7.74710	572.7	LOKI	Station end	
PS143/2_34-1		2024-07-23T21:52:19	79.93225	8.29593	487.5	CTD-RO	max depth	
PS143/2_35-1		2024-07-23T23:33:55	79.94027	8.88950	462.6	CTD-RO	max depth	
PS143/2_36-1		2024-07-24T00:55:03	79.93676	9.45974	462.1	CTD-RO	max depth	
PS143/2_37-1		2024-07-24T02:20:56	79.94008	10.17164	439.9	CTD-RO	max depth	
PS143/2_38-1		2024-07-24T03:31:19	79.93866	10.69742	300.4	CTD-RO	max depth	
PS143/2_39-1	Y2-1	2024-07-24T07:17:23	80.41977	10.06025	679.0	MOOR	Station start	recovery
PS143/2_39-1	Y2-1	2024-07-24T08:48:49	80.41175	10.08033	685.9	MOOR	Station end	recovery
PS143/2_40-1		2024-07-24T12:25:48	79.93886	10.17374	437.9	CTD-RO	max depth	
PS143/2_40-2		2024-07-24T12:29:28	79.93903	10.17114	439.1	HN	Station start	
PS143/2_40-2		2024-07-24T12:34:57	79.93896	10.16983	439.7	HN	Station end	
PS143/2_40-3		2024-07-24T13:42:08	79.93951	10.17077	440.1	MSN	Station start	
PS143/2_40-3		2024-07-24T14:30:18	79.93859	10.17390	438.4	MSN	Station end	

Event label	Optional label	Date/Time	Latitude	Longitude	Depth [m]	Gear	Action	Comment *
PS143/2_40-4		2024-07-24T14:36:34	79.93805	10.16986	439.5	LOKI	Station start	
PS143/2_40-4		2024-07-24T15:27:41	79.93876	10.17364	438.4	LOKI	Station end	
PS143/2_40-5		2024-07-24T14:51:24	79.93826	10.17043	439.6	OOSS	Station start	
PS143/2_40-5		2024-07-24T15:18:28	79.93844	10.17552	438.8	OOSS	Station end	
PS143/2_40-6		2024-07-24T15:28:39	79.93877	10.17304	438.7	LIGHT	Station start	
PS143/2_40-6		2024-07-24T16:19:42	79.93905	10.18537	438.7	LIGHT	Station end	
PS143/2_41-1		2024-07-25T02:29:04	79.93447	3.18908	2488.2	CTD-RO	max depth	
PS143/2_42-1		2024-07-25T03:20:01	79.93718	3.07680	2522.5	CTD-RO	max depth	
PS143/2_43-1		2024-07-25T04:43:08	79.93778	2.48313	2687.2	CTD-RO	max depth	
PS143/2_44-2		2024-07-25T06:09:34	79.93827	1.91604	3349.2	HN	Station start	
PS143/2_44-2		2024-07-25T06:18:22	79.93800	1.91715	4259.9	HN	Station end	
PS143/2_44-1		2024-07-25T06:25:14	79.93770	1.91624	3293.3	CTD-RO	max depth	
PS143/2_44-3		2024-07-25T07:02:16	79.93503	1.91587	3734.1	LIGHT	Station start	

Event label	Optional label	Date/Time	Latitude	Longitude	Depth [m]	Gear	Action	Comment *
PS143/2_44-3		2024-07-25T07:47:46	79.93624	1.91876	3352.1	LIGHT	Station end	
PS143/2_44-4		2024-07-25T07:50:37	79.93643	1.91914		MSN	Station start	
PS143/2_44-4		2024-07-25T08:52:19	79.93551	1.91883	3365.3	MSN	Station end	
PS143/2_44-5		2024-07-25T08:56:13	79.93552	1.91857	3366.5	LOKI	Station start	
PS143/2_44-5		2024-07-25T09:42:43	79.93715	1.91681	3337.3	LOKI	Station end	
PS143/2_45-1		2024-07-25T11:10:54	79.93790	1.31986	3007.7	CTD-RO	max depth	
PS143/2_46-1		2024-07-25T12:56:57	79.93149	0.81760	2617.9	CTD-RO	max depth	
PS143/2_47-1		2024-07-25T15:15:20	79.94058	0.14646	2533.7	CTD-RO	max depth	
PS143/2_48-2		2024-07-25T17:13:02	79.93544	-0.66856	2679.8	HN	Station start	
PS143/2_48-2		2024-07-25T17:22:21	79.93565	-0.66750	2680.0	HN	Station end	
PS143/2_48-1		2024-07-25T17:23:52	79.93571	-0.66801	2680.1	CTD-RO	max depth	
PS143/2_48-3		2024-07-25T17:49:34	79.93592	-0.67885	2678.3	LIGHT	Station start	
PS143/2_48-3		2024-07-25T18:36:26	79.93520	-0.70263	2672.1	LIGHT	Station end	

Event label	Optional label	Date/Time	Latitude	Longitude	Depth [m]	Gear	Action	Comment *
PS143/2_48-4		2024-07-25T18:44:09	79.93533	-0.70766	2671.0	MSN	Station start	
PS143/2_48-4		2024-07-25T19:39:42	79.94355	-0.75908	2653.3	MSN	Station end	
PS143/2_48-5		2024-07-25T19:40:46	79.94408	-0.75953	2652.9	LOKI	Station start	
PS143/2_48-5		2024-07-25T20:34:38	79.95601	-0.78749	2616.7	LOKI	Station end	
PS143/2_48-6		2024-07-25T21:44:29	79.96500	-0.82058	2628.5	TVMUC	max depth	
PS143/2_49-1		2024-07-25T23:48:18	79.93999	-1.03535	2713.7	CTD-RO	max depth	
PS143/2_50-1		2024-07-26T01:24:52	79.93640	-1.59772	2757.2	CTD-RO	max depth	
PS143/2_51-1		2024-07-26T03:07:44	79.94214	-2.23044	2687.5	CTD-RO	max depth	
PS143/2_52-1		2024-07-26T05:02:20	79.93162	-2.81725	2526.1	CTD-RO	max depth	
PS143/2_53-1		2024-07-26T08:00:04	79.94092	-3.40949	2335.0	CTD-RO	max depth	
PS143/2_54-2		2024-07-26T11:25:55	79.91383	-5.24926	965.6	HN	Station start	
PS143/2_54-2		2024-07-26T11:31:48	79.91279	-5.24925	963.9	HN	Station end	
PS143/2_54-3		2024-07-26T11:34:00	79.91249	-5.24943	962.9	OOSS	Station start	

Event label	Optional label	Date/Time	Latitude	Longitude	Depth [m]	Gear	Action	Comment *
PS143/2_54-3		2024-07-26T12:02:34	79.91050	-5.24962	960.3	OOSS	Station end	
PS143/2_54-1		2024-07-26T11:39:52	79.91229	-5.24941	962.6	CTD-RO	max depth	
PS143/2_54-4		2024-07-26T12:30:32	79.90957	-5.25048	958.8	LIGHT	Station start	
PS143/2_54-4		2024-07-26T12:55:40	79.90878	-5.24998	959.3	LIGHT	Station end	
PS143/2_54-5		2024-07-26T13:11:20	79.90842	-5.24921	961.1	MSN	Station start	
PS143/2_54-5		2024-07-26T14:12:02	79.90821	-5.24222	969.0	MSN	Station end	
PS143/2_54-6		2024-07-26T15:19:43	79.90816	-5.23978	971.9	TVMUC	max depth	
PS143/2_55-1	EGC-9	2024-07-27T07:38:35	78.98229	-5.42106	961.3	MOOR	Station start	recovery
PS143/2_55-1	EGC-9	2024-07-27T09:46:58	78.99145	-5.51786	908.1	MOOR	Station end	recovery
PS143/2_56-1	EGC-8	2024-07-27T10:38:57	78.99845	-5.41048	995.9	MOOR	Station start	recovery
PS143/2_56-1	EGC-8	2024-07-27T12:21:19	79.00124	-5.41117	1001.8	MOOR	Station end	recovery
PS143/2_56-2		2024-07-27T13:19:41	78.97178	-5.29104	1050.5	CTD-RO	max depth	
PS143/2_56-3		2024-07-27T13:21:43	78.97179	-5.29080	1050.9	HN	Station start	

Event label	Optional label	Date/Time	Latitude	Longitude	Depth [m]	Gear	Action	Comment *
PS143/2_56-3		2024-07-27T13:26:56	78.97188	-5.29015	1051.6	HN	Station end	
PS143/2_56-5		2024-07-27T14:03:43	78.97224	-5.28532	1056.7	LIGHT	Station start	
PS143/2_56-5		2024-07-27T14:41:35	78.97226	-5.28377	1058.3	LIGHT	Station end	
PS143/2_56-4		2024-07-27T14:10:46	78.97248	-5.28648	1056.4	OOSS	Station start	
PS143/2_56-4		2024-07-27T14:26:30	78.97231	-5.28488	1057.6	OOSS	Station end	
PS143/2_56-6		2024-07-27T14:42:15	78.97223	-5.28387	1058.0	MSN	Station start	
PS143/2_56-6		2024-07-27T20:04:43	78.97384	-5.30126	1045.7	MSN	Station end	
PS143/2_56-7		2024-07-27T21:13:04	78.97553	-5.29832	1049.1	TVMUC	max depth	
PS143/2_56-8		2024-07-27T22:45:28	78.97754	-5.31142	1039.0	OFOBS	Station start	
PS143/2_56-8		2024-07-28T04:55:48	78.99265	-5.58875	862.4	OFOBS	Station end	
PS143/2_57-1		2024-07-28T06:00:04	78.97863	-5.42911	951.8	MOOR	Station start	deployment?
PS143/2_57-1		2024-07-28T08:29:29	78.99629	-5.39723	999.5	MOOR	Station end	deployment?
PS143/2_58-1		2024-07-28T12:57:24	79.14421	-5.42289	1177.9	TOPR	Station start	

Event label	Optional label	Date/Time	Latitude	Longitude	Depth [m]	Gear	Action	Comment *
PS143/2_58-1		2024-07-28T20:27:09	78.98255	-5.21641	1117.2	TOPR	Station end	
PS143/2_59-1	HG-IV-FEVI-46	2024-07-29T14:40:36	79.00327	4.33150	2540.2	MOOR	Station start	recovery
PS143/2_59-1	HG-IV-FEVI-46	2024-07-29T16:25:28	78.99533	4.40620	2525.4	MOOR	Station end	recovery
PS143/2_59-2	HG IV-FEVI-48	2024-07-29T16:53:08	78.99945	4.33672	2544.8	MOOR	Station start	deployment
PS143/2_59-2	HG IV-FEVI-48	2024-07-29T19:43:32	78.99990	4.33192	2545.7	MOOR	Station end	deployment
PS143/2_59-3		2024-07-29T20:19:18	79.03163	4.22255	2525.1	MOOR	Station start	
PS143/2_59-3		2024-07-29T20:37:20	79.02961	4.22194	2530.0	MOOR	Station end	
PS143/2_59-4		2024-07-29T21:03:11	79.03401	4.17264	2553.8	OFOBS	Station start	
PS143/2_59-4		2024-07-30T03:16:41	79.06423	4.29788	2340.4	OFOBS	Station end	
PS143/2_60-1		2024-07-30T05:50:00	79.13592	4.88218	1489.7	AUV_lab	Station start	
PS143/2_60-1		2024-07-30T17:11:52	78.99760	5.65290	2098.9	AUV_lab	Station end	
PS143/2_60-2	ArcFoce	2024-07-30T07:21:21	79.13814	4.88742	1473.1	MOOR	Station start	recovery
PS143/2_60-2	ArcFoce	2024-07-30T08:47:55	79.13689	4.88903	1478.9	MOOR	Station end	recovery

Event label	Optional label	Date/Time	Latitude	Longitude	Depth [m]	Gear	Action	Comment *
PS143/2_61-1	F5-20	2024-07-30T10:27:24	79.00496	5.67056	2033.3	MOOR	Station start	recovery
PS143/2_61-1	F5-20	2024-07-30T12:58:44	79.00287	5.66886	2048.1	MOOR	Station end	recovery
PS143/2_61-2	F5-21	2024-07-30T13:28:17	79.00289	5.66036	2058.0	MOOR	Station start	deployment
PS143/2_61-2	F5-21	2024-07-30T15:50:00	79.00028	5.66703	2068.6	MOOR	Station end	deployment
PS143/2_62-1		2024-07-30T18:35:05	78.99059	5.66885	2121.7	CTD-RO	max depth	
PS143/2_62-2		2024-07-30T20:01:28	78.99059	5.66915	2121.7	LIGHT	Station start	
PS143/2_62-2		2024-07-30T20:47:54	78.99065	5.66755	2122.4	LIGHT	Station end	
PS143/2_62-3		2024-07-30T21:41:38	78.99044	5.67015	2121.8	TVMUC	max depth	
PS143/2_63-1		2024-07-31T00:39:31	79.01184	7.10472	1245.2	CTD-RO	max depth	
PS143/2_64-1		2024-07-31T02:02:52	78.98295	6.89838	1231.4	OFOBS	Station start	
PS143/2_64-1		2024-07-31T04:31:41	78.98188	7.01196	1185.5	OFOBS	Station end	
PS143/2_65-1	F4-W-5-ST	2024-07-31T05:48:12	79.02641	7.00161	1256.4	MOOR	Station start	recovery
PS143/2_65-1	F4-W-5-ST	2024-07-31T08:29:56	79.03442	7.05533	1278.7	MOOR	Station end	recovery

Event label	Optional label	Date/Time	Latitude	Longitude	Depth [m]	Gear	Action	Comment *
PS143/2_66-1		2024-07-31T09:34:22	79.00398	7.81583	1146.8	TOPR	Station start	
PS143/2_66-1		2024-07-31T12:36:05	78.89182	8.64321	238.9	TOPR	Station end	
PS143/2_67-1		2024-07-31T13:35:02	78.98444	8.56992	261.1	CTD-RO	max depth	
PS143/2_68-1		2024-07-31T15:53:00	78.98408	7.00997	1183.3	CTD-RO	max depth	
PS143/2_69-1		2024-07-31T18:18:44	78.98305	5.43827	2320.3	CTD-RO	max depth	
PS143/2_70-1		2024-07-31T20:40:24	78.98410	3.87236	2730.7	CTD-RO	max depth	
PS143/2_71-1		2024-07-31T23:14:03	78.98329	2.32330	2360.5	CTD-RO	max depth	
PS143/2_72-1		2024-08-01T02:33:04	78.97932	0.78736	2506.6	CTD-RO	max depth	
PS143/2_73-1		2024-08-01T06:05:30	78.98446	-0.83073	2566.4	CTD-RO	max depth	
PS143/2_74-1		2024-08-01T09:23:24	78.98301	-2.38476	2531.2	CTD-RO	max depth	
PS143/2_75-1		2024-08-01T14:00:31	78.98367	-5.27814	1071.1	CTD-RO	max depth	
PS143/2_75-2		2024-08-01T14:10:08	78.98353	-5.28135	1068.3	HN	Station start	
PS143/2_75-2		2024-08-01T14:18:44	78.98361	-5.28630	1064.5	HN	Station end	

Event label	Optional label	Date/Time	Latitude	Longitude	Depth [m]	Gear	Action	Comment *
PS143/2_75-3		2024-08-01T14:30:35	78.98353	-5.28940	1061.9	OOSS	Station start	
PS143/2_75-3		2024-08-01T15:22:38	78.98299	-5.29090	1059.9	OOSS	Station end	
PS143/2_75-4		2024-08-01T15:11:10	78.98311	-5.29029	1060.4	MSN	Station start	
PS143/2_75-4		2024-08-01T16:41:15	78.98312	-5.29034	1060.3	MSN	Station end	
PS143/2_75-5		2024-08-01T16:42:10	78.98312	-5.29031	1060.3	LOKI	Station start	
PS143/2_75-5		2024-08-01T18:12:02	78.97370	-5.30772	1036.7	LOKI	Station end	
PS143/2_76-2		2024-08-01T23:06:00	78.83289	-2.79585	2525.6	HN	Station start	
PS143/2_76-2		2024-08-01T23:32:32	78.83076	-2.78261	2529.0	HN	Station end	
PS143/2_76-1		2024-08-01T23:06:29	78.83286	-2.79540	2526.0	CTD-RO	max depth	
PS143/2_76-3		2024-08-01T23:33:40	78.83073	-2.78168	2529.3	LIGHT	Station start	
PS143/2_76-3		2024-08-02T00:22:47	78.82773	-2.74738	2536.9	LIGHT	Station end	
PS143/2_76-4		2024-08-01T23:40:29	78.83033	-2.77838	2530.2	OOSS	Station start	
PS143/2_76-4		2024-08-01T23:57:52	78.82910	-2.76737	2531.8	OOSS	Station end	

Event label	Optional label	Date/Time	Latitude	Longitude	Depth [m]	Gear	Action	Comment *
PS143/2_76-5		2024-08-02T00:35:25	78.83544	-2.80497	2522.9	MSN	Station start	
PS143/2_76-5		2024-08-02T02:37:52	78.83193	-2.75807	2533.4	MSN	Station end	
PS143/2_76-6		2024-08-02T02:38:15	78.83189	-2.75792	2533.4	MSN	Station start	
PS143/2_76-6		2024-08-02T04:58:07	78.83364	-2.79764	2524.3	MSN	Station end	
PS143/2_76-7		2024-08-02T04:58:38	78.83365	-2.79764	2524.3	LOKI	Station start	
PS143/2_76-7		2024-08-02T06:41:49	78.83405	-2.79374	2525.3	LOKI	Station end	
PS143/2_76-8		2024-08-02T07:57:50	78.83416	-2.79414	2525.4	CTD-RO	max depth	
PS143/2_76-10		2024-08-02T10:06:35	78.83422	-2.79310	2525.7	OOSS	Station start	
PS143/2_76-10		2024-08-02T10:28:38	78.83463	-2.79742	2524.8	OOSS	Station end	
PS143/2_76-9		2024-08-02T10:24:53	78.83453	-2.79650	2525.0	TVMUC	max depth	
PS143/2_76-11		2024-08-02T12:22:36	78.83453	-2.79672	2525.0	OFOBS	Station start	
PS143/2_76-11		2024-08-02T15:31:07	78.82830	-2.66642	2550.3	OFOBS	Station end	
PS143/2_77-1		2024-08-02T16:53:17	78.82281	-2.60878	2563.4	CTD-RO	max depth	

Event label	Optional label	Date/Time	Latitude	Longitude	Depth [m]	Gear	Action	Comment *
PS143/2_78-1		2024-08-02T18:50:47	78.66621	-2.21540	2638.2	ICE	Station start	
PS143/2_78-1		2024-08-02T19:30:54	78.65756	-2.23416	2634.1	ICE	Station end	

**Comments are limited to 130 characters. See https://www.pangaea.de/expeditions/events/PS143/2 to show full comments in conjunction with the station (event) list for expedition PS143/2.*

Abbreviation	Method/Device
ADCP	Acoustic Doppler Current Profiler
AUV_lab	Autonomous underwater vehicle Polar Autonomous Underwater Laboratory
CT	Underway cruise track measurements
CTD-RO	CTD/Rosette
FBOX	FerryBox
GRAV	Gravimetry
HN	Hand net
ICE	Ice station
LIGHT	Light profiler
LOKI	Light frame on-sight keyspecies investigation
MAG	Magnetometer
MOOR	Mooring
MSN	Multiple opening/closing net
OFOBS	Ocean Floor Observation and Bathymetry System
OOSS	Ocean optics spectrometer system
SWEAS	Ship Weather Station
TOPR	Towed Ocean Profiler
TSG	Thermosalinograph
TVMUC	Multicorer with television
UWS	Underway water sampling

Die **Berichte zur Polar- und Meeresforschung** (ISSN 1866-3192) werden beginnend mit dem Band 569 (2008) als Open-Access-Publikation herausgegeben. Ein Verzeichnis aller Bände einschließlich der Druckausgaben (ISSN 1618-3193, Band 377-568, von 2000 bis 2008) sowie der früheren **Berichte zur Polarforschung** (ISSN 0176-5027, Band 1–376, von 1981 bis 2000) befindet sich im electronic Publication Information Center **(ePIC)** des Alfred-Wegener-Instituts, Helmholtz-Zentrum für Polar- und Meeresforschung (AWI); see https://epic.awi.de. Durch Auswahl “Reports on Polar- and Marine Research“ (via “browse”/”type”) wird eine Liste der Publikationen, sortiert nach Bandnummer, innerhalb der absteigenden chronologischen Reihenfolge der Jahrgänge mit Verweis auf das jeweilige pdf-Symbol zum Herunterladen angezeigt.

The **Reports on Polar and Marine Research** (ISSN 1866-3192) are available as open access publications since 2008. A table of all volumes including the printed issues (ISSN 1618-3193, Vol. 377-568, from 2000 until 2008), as well as the earlier **Reports on Polar Research** (ISSN 0176-5027, Vol. 1–376, from 1981 until 2000) is provided by the electronic Publication Information Center **(ePIC)** of the Alfred Wegener Institute, Helmholtz Centre for Polar and Marine Research (AWI); see URL https://epic.awi.de. To generate a list of all Reports, use the URL http://epic.awi.de and select “browse”/”type” to browse ”Reports on Polar and Marine Research”. A chronological list in declining order will be presented, and pdf-icons displayed for downloading.

Zuletzt erschienene Ausgaben:

Recently published issues:

801 (2025) The Expedition PS143/2 of the Research Vessel POLARSTERN to the Arctic Ocean in 2024. Edited by Katja Metfies with contributions of the participants.

800 (2025) The Expedition PS143/1 of the Research Vessel POLARSTERN to the Arctic Ocean in 2024. Edited by Frank Wenzhöfer with contributions of the participants.

799 (2025) The Expeditions PS147/1 and PS147/2 of the Research Vessel POLARSTERN to the Atlantic Ocean in 2025. Edited by Yvonne Schulze Tenberge and Björn Fiedler with contributions of the participants.

798 (2025) The Expedition PS146 of the Research Vessel POLARSTERN to the Weddell Sea in 2024/2025. Edited by Olaf Boebel with contributions of the participants.

797 (2025) Arctic Land Expeditions in Permafrost Research in 2023. Edited by Anne Morgenstern and Milena Gottschalk with contributions of the participants.

796 (2025) Expeditions to Antarctica: ANT-Land 2023/24 NEUMAYER STATION III, Kohnen Station and Field Campaigns. Edited by Julia Regnery, Tim Heitland and Christine Wesche with contributions of the participants.

795 (2025) The Expeditions PS145/1 and PS145/2 of the Research Vessel POLARSTERN to the Atlantic Ocean in 2024, edited by Claudia Hanfland and Natalie Cornish with contributions of the participants.

794 (2025) The Expedition PS144 of the Research Vessel POLARSTERN to the Arctic Ocean in 2024, edited by Benjamin Rabe and Walter Geibert with contributions of the participants.

793 (2025) The Expedition PS141 of the Research Vessel POLARSTERN to the Davis Sea and Mawson Sea in 2024, edited by Sebastian Krastel with contributions of the participants.

ALFRED-WEGENER-INSTITUT
HELMHOLTZ-ZENTRUM FÜR POLAR-
UND MEERESFORSCHUNG

BREMERHAVEN

Am Handelshafen 12
27570 Bremerhaven
Telefon 0471 4831-0
Telefax 0471 4831-1149
www.awi.de

HELMHOLTZ